BODY-WORN ACCELEROMETER-BASED HEALTH ASSESSMENT ALGORITHMS FOR INDEPENDENT LIVING OLDER ADULTS

A Thesis presented to

the Faculty of the Graduate School

University of Missouri-Columbia

In Partial Fulfillment

of the Requirements for the Degree

Master of Science

By

LIA HOWE

Dr. Marjorie Skubic, Thesis Supervisor

December 2020

The undersigned, appointed by the dean of the Graduate School, have examined the thesis entitled

BODY-WORN ACCELEROMETER-BASED HEALTH ASSESSMENT ALGORITHMS FOR INDEPENDENT LIVING OLDER ADULTS

Presented by Lia Howe,

A candidate for the degree of

Master of Science in Computer Engineering,

And hereby certify that, in their opinion, it is worth of acceptance.

Professor Marjorie Skubic, PhD.,

Professor Dominic Ho, PhD.,

Professor Carmen Abbott, PT, PhD.

ACKNOWLEDGMENTS

This research and my transition to the Electrical Engineering and Computer Science Department would not have been possible without the support of many people. First, I am grateful to my advisor, Dr. Marjorie Skubic, for allowing me to work at the Center for Eldercare and Rehabilitation Technology lab. Her expertise, constant support, and feedback were valuable while conducting my research. Also, I appreciated her patience, positivity, and encouragement each week. Dr. Skubic's enthusiasm and inspirational stories continued to drive my excitement for research.

I also want to express my gratitude to Dr. Ferris Pfeiffer my undergraduate research advisor, Dr. Steve Borgelt, and Dave Grant for their mentoring, advice and motivated me to continue my education. These individuals, along with Dr. Skubic and Sami Kurkowski a colleague, helped with my late transition to graduate school a couple of weeks before a new semester.

Also, many thanks to my thesis committee Dr. Carmen Abbott for her professional advice as an expert in physical therapy, and Dr. Dominic Ho for his teachings of digital signal processing. Dr. Ho specifically helped me keep a positive outlook during my studies and challenged me to understand my work at a deeper level.

I would like to thank my peers and the staff at the Center of Eldercare and Rehabilitation Technology lab for their guidance, help, and support.

Also, this research would not have been possible without the assistance of the staff and residents at TigerPlace Independent Living and other assisted living facilities around Columbia, MO.

Finally, I would like to thank all the students, friends, and professors at the University of Missouri who have helped and supported me along the way.

Table of Contents

List of Figures

List of Tables

ABSTRACT

The mainstream smart wearable products used for activity trackers have experienced significant growth recently. Among the older population, collecting long periods of activity data in a real-life setting is challenging even with wearable devices. Studies have found inconsistent and lower accuracies when older adults use these smart devices [1], [2],[2],[3]. As a person ages, many have lower daily levels of activity and their dynamic functional patterns, such as gaits and sit-to-stand transitional movements vary throughout the day. This thesis explores wearable health-tracking applications by evaluating daytime and nighttime pattern metrics calculated from continuous accelerometer signals. These signals were collected externally from the upper trunk of the body in an independent-living environment of 30 elderly volunteers. Our gold standard to validate the metrics from the accelerometer signals were similar metrics calculated from an in-home sensor network [4]. This thesis first developed an algorithm to count steps and another algorithm to detect stand-to-sit and sit-to-stand (STS) to demonstrate the importance of considering differences in daily functional health patterns when creating algorithms. Next, this thesis validates that accelerometer data can show similar motion density results as motion sensor data. And thirdly, this thesis proposes an updated vacancy algorithm using a new motion sensor system that detects when no one is in the living space, compared against the current algorithm.

1 INTRODUCTION

1.2 Motivation

At the beginning of the year 2030, all the baby boomers born between 1946-1964 will be older than 65, which accounts for 73.1 million Americans and they make up 21 percent of the United States population [5]. The rapid aging population versus the slow-growing population is causing healthcare system challenges. This is where using technology to monitor health changes over time to learn aging-related health patterns can proactively intervene to help mitigate or decrease the typical decline of aging. The goal is to increase the quality of life and maintain independence [4], [6]. Within the last decade, the popularity of wearable devices has emerged. These devices monitor activity, as well as log biometric health metrics like heart rate, respiration, and much more. It is important to accurately measure health and understand the information obtained because inaccurate results can lead to irreversible consequences.

The in-home network systems installed in several apartments around Columbia, MO captures senior resident's daily patterns representing their health and identifies when activity patterns start to deviate from the norm [7]. The motivation for this research was to perform metric validations for independent living applications and analyze the effects of daily activity and functional health patterns from elderly adults.

1.3 Problem Statement

The research and development of these current activity tracking devices lack the understanding of older adult daily activity levels and conditions in a real-living environment using these devices. As a person ages, their gait patterns and daily activity fluctuates depending on how they feel, the time of day, and their medications [8]. Also,

slower movement and the use of assistive devices reduce the accuracy of these current activity monitoring systems. Continuous monitoring of older adult health using wearable devices has been a challenge due to several factors including battery life, device comfortability, and ineffective long-term methods to validate the results from these wearables. For example, relying on self-reports for this age group is risky due to memory loss [9] and people with cognitive disabilities may remove the recording device early. This occurred a few times during the data collection phase for this study and their data had to be excluded. Fortunately, this study had the resources to use an in-home sensor network system consisting of multiple ambient sensors installed in independent and assistive living homes at the same time using an externally fixed-worn accelerometer.

1.4 Contributions

It is important to test algorithms in environments where they are intended to be used. This thesis provides an analysis of a few different algorithms that were developed to monitor activity levels and individual transitional body movements using data collected from older adults over a 24-hour or 48-hour period in a real living environment. The data was collected from a research-based accelerometer fixed to the upper trunk and validated against an in-home sensor network system. The goal of this study was to take a more technical approach and analyze how older adults fluctuating daily living patterns and functional health differences affect these algorithms. Based on the broad range of differences, can we find an algorithm that works well for this population?

As mentioned before, this thesis developed a step detection algorithm and a sit-to-stand (STS) algorithm to look at the effects of various functional mobility differences within the older adult population. The next algorithm computes motion density based on

the ActiGraph accelerometer signals and compares it to existing motion sensor data. And lastly, a current vacancy detection algorithm is compared to a proposed vacancy algorithm using a new system. These accelerometer-based algorithms are potentially intended to be used in a single low powered device in the future. Some technical specifics, such as the filter design and details about the algorithm development for proprietary reasons. This research is a continuum of monitoring health long-term to detect changes from the norm.

1.5 Thesis Structure

The structure of this thesis first explains the types of sensors used in this study, the placement of the accelerometer, and information about the subjects and how they are split into two datasets. Dataset 1 subjects were used individually for algorithm development and dataset 2 was used as validation and testing. The main body of this thesis is organized into four different algorithms; step detection, sit-to-stand, motion density, and vacancy detection algorithm. Each section discusses the background, methods, and conclusion related to the algorithm. At the end, the conclusion summarizes this study and suggests areas for future work. Lastly, the appendix provides additional results about the algorithms and more in-depth detail about the participants, their living spaces, and individual results.

2 Sensors and Dataset

2.1 Environmental Sensors

The in-home network system used in this study was developed by years of work from researchers and graduate students from the University of Missouri. They were installed in assistive living and independent living apartments around Columbia, MO like TigerPlace, an aging in place facility [4],[10]. The sensors include Zigbee PIR motion sensors, depth sensors, and a bed sensor. The combination of these sensors collects important biometrics and information to assess a person's health over time. Currently, there are four Zigbee motion sensors strategically placed in the living room, bedroom, bathroom, and above the front door. These motion sensors simulate the old x10 motion sensor system that fires every 7 seconds if there is motion near. Also, to active the Zigbee motion sensors a large gross movement must be detected, such as walking by or someone continuously waving their arms. Small movements like turning pages in a book rarely are detected.

The bed sensor monitors heart rate, respiration, and restlessness. The depth sensor has a low average frame rate of 5 Hz to protect people's identity within the apartment. It only captures data when detected motion is within the view range of the sensor. For this study, the main use of the depth sensor was to validate activities while the participant was in view, such as counting the number of steps or walking times between different rooms. The database stores and applies algorithms, in which the results are displayed on an interface for evaluation.

2.2 Wearable Sensors

There are many types of wearable sensors, such as watches, rings, belts, clothes, and/or shoes. These wearable devices have some type of pressure sensor, optical sensor, accelerometer, or gyroscope sensor. Accelerometers, which are widely used for assessing physical activity and health monitoring. This study used the research-grade accelerometer device called ActiGraph GT9X Link (3.5 mm x 3.5 mm x 1 mm), a lightweight (20 g) triaxial accelerometer device. One unit was attached to the upper trunk to collect raw 3-axis acceleration signals. All the ActiGraph units were calibrated in all 6-orthogonal x-axis, y-axis, z-axis positions as shown in Figure 2.2-1. The data was sampled at 100 Hz, except for 01BLO1L, 02BCO1L, and 03BHO1L were sampled at 50 Hz due to change in protocols. The raw (unfiltered) 3-axis accelerometer signals were recorded simultaneously with an in-home sensor network.

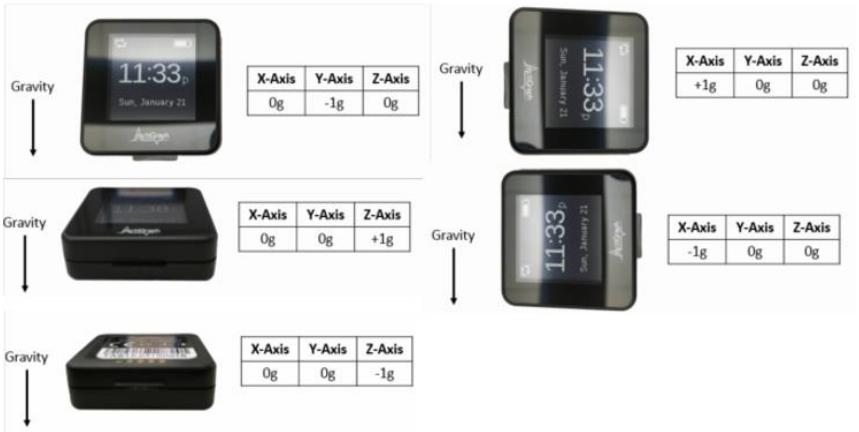

Figure 2.2-1 ActiGraph GT9X Link device orientation with respect to the X-axis, Y-axis, and Z-axis.

2.3 Accelerometer Placement

The placement of the accelerometer is important for activity recognition because it determines the classification accuracy. The wrist, hip, and lower back are popular placements for these monitoring devices, but may not be the most ideal places for older

adults. The wrist is difficult because of the multiple degrees of freedom at the wrist. Also, older adults may forget to wear a wrist-worn device or remove it before taking a shower. According to research, the most optimal placement for accelerometers is near the center of gravity and a place with stability, such as around the hip region [11]. But the placements at the hip or lower back tend to be uncomfortable.

The latest recording from 2011, published in the Journal of American Geriatrics Society reported mobility device usage was 24% or 8.5 million adults age 65 and older in the U.S. Assistive devices, includes canes, walkers, and wheelchairs, which affects the accuracy of monitoring health and 74% of the participants within this study used some form. There is evidence of improper use of assistive device [12], which was also observed amongst the participants in this study. These participants tended to lean forward more than without an assistive device. The angle at which the participant was leaning forward could be seen in the accelerometer signal in this location.

For this study, the ActiGraph GT9X Link device was placed externally on the upper trunk region, as seen in Figure 2.3-1. Before attaching the ActiGraph to the body, an initial Tegaderm patch was placed over the device making sure to cover the backside. Then a piece of medical tape was placed over the back of the device to cover the electrodes. This added an extra layer of protection between the participant's skin and the device. A second adhesive Tegaderm patch was used to attached the ActiGraph device to the body. These patches were particularly selected by nursing staff because they were gentler on the skin. This was important because older adult skin is typically easier to tear and more sensitive.

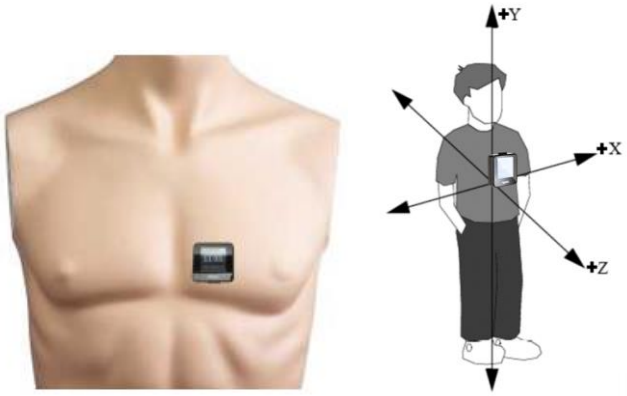

Figure 2.3-1: Placement and orientation of the ActiGraph GT9X Link devices on the participants.

2.4 Dataset

This study was approved by the University of Missouri Institutional Review Board (MUIRB) and all volunteers signed consent forms before collecting data. Data were collected at TigerPlace and other independent or assistive living facilities around Columbia, MO between November 2018 and September 2019. Thirty elderly volunteers who were at least 60 years old, lived on their own with an in-home sensor network and were ambulatory when recruited. They took part in this study over a 24 or 48 period. There were 22 females and 8 males aged 66-96 years old. Table 2.4-1 proves average biometric information for the volunteers. More details and additional information for each subject are shown in Appx. Table D-1.

Table 2.4-1 Average biometric data for 30 volunteers.

	GENDER (F:M)	**AGE (years)**	**HEIGHT (in)**	**WEIGHT (lbs.)**	**BUILD (E:M:EN)**
Volunteers	22:8	84.97 ± 15	64.13 ± 10.5	154.73 ± 78.5	5:10:15
Females	22	84.95 ± 15	61.82 ± 8.5	141.82 ± 55	4:6:12
Males	8	85 ± 12.5	70.5 ± 3	190.25 ± 39	1:4:3

During the data collection, specific procedures were followed:

- Documented when the participant had visitors in the apartment.
- Recording day(s) were selected when the fewest visitors and the least time out of the apartment were expected. Such as not on days with regularly scheduled house cleaners or family visitors.
- Ask participants and document if they changed the position (e.g. removed) of the ActiGraph.

This validation study used participants 1-3 and 5-11 for dataset 1 for algorithm development. And participants 12-13, 15-20, 22-25, and 27-34 for dataset 2 for validation and testing. Participants 4, 14, 21, and 26 were unable to complete the data collection and were excluded from the study. Lastly, participant 13 had two data collection sessions due to the ActiGraph falling off while sleeping. The first data collection 13JAO1L and second data collection 13JAO2L. The full list of the participants (along with complete participant identifiers) is referenced in Appendix C, along with additional information about the participant and their living space in Appendix E.

3 Step Detection Algorithm

3.1 Background

Count steps is a common way to assess physical activity in clinical settings and real-life environments. Accelerometers have been proven to be a reliable device. Compared to other measuring methods, they are low cost and portable due to their small size. However, lower accuracies have been reported for low walking speeds and with older adults. Based on previous step detection algorithm studies, a large number of data collections were performed in controlled experimental settings using treadmills or short walking periods a few meters long. Also, few datasets include a reasonable amount of data from older adults and people with gait impairments [11]. Collecting data in a controlled environment does not represent the subject's natural behaviors.

3.1.1 Step Counting Devices

There are various step counting devices using cameras, mechanical pedometers, electronic accelerometers, and cell phones with both accelerometers and gyroscopes embedded. Pedometers were one of the earliest inventions that originally used a mechanical spring system with a balancing arm attached to a gear counting mechanism [13]. The electronic accelerometers used today are more accurate and use piezoelectric ceramic plates that register electrical charges to determine the acceleration changes in different directions.

3.1.2 Gait Patterns

There is a lot that involves a person's gait pattern. Elderly adult walks are typically slower, increase in variability, have a lower step length, and often use an assistive walking device (i.e. cane, walker) [14]. Gait patterns are especially important

with this age group when considering step detecting devices because of the significant number of older adults that experience uneven gait patterns. Their gaits are strongly influenced by physical ability, personality, and mood [8]. It can vary throughout the day due to medications, pain, or the time of day (i.e. morning, night).

When analyzing a gait, a physical therapist may consider a person's base of support (BOS), walking speed, the dynamic range of motion (i.e. leg swing, arm swing), and gait cycle. The base of support has been defined as the horizontal stride width during the double-support phase when both feet are in contract with the ground and the whole-body center of gravity remains within the BOS [15]. One gait cycle (stride) is from the heel strike of one leg to the next heel strike of the same leg. Heel strike is when one of the heels touches the ground and toe-off is the moment the toe takes off the ground. These are usually described together as heel-strike and toe-off phases and are evaluated to see if the right and left side foot placements are symmetric.

This study also correlated the heel-strike and toe-off with whether a person shuffled their feet or not. Someone who barely had a distinct heel-strike and toe-off, where the foot lifts off the ground might be considered as a shuffle. According to the book Clinical Neuroscience, shuffling is dragging the person's feet and might have a shorter stride length with a reduced arm swing [16]. Next, a person's posture was observed. A forward posture often causes a flat-foot gait reducing heel-strike and toe-off phases. A normal posture for this study is considered a straight upright position measured perpendicular to the ground at 90 degrees. The posture angle was measured from the hip to the head like in Figure 3.1-1.

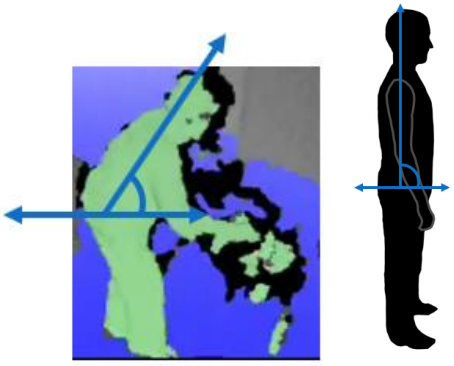

Figure 3.1-1 Measuring posture angle. The left shows a forward-leaning posture and the right shows a straight posture at 90 degrees.

3.2 Dataset Gait Patterns

Below in Table 3.2-2 and Table 3.2-3, shows dataset 1 and dataset 2 gait patterns for each subject. The posture angle was the only gait pattern measured quantitatively from the depth sensor videos. All the other gait patterns were measured qualitatively relative to all the subjects in this study by watching the depth sensor videos. For example, the walking speed, most subjects walked about the same moderate pace. Subject 06DHO1L significantly walked faster and subjects like 33BEO1L walked extremely slower than the others. For dataset 1, no one walked with a shuffle. There were only four people from dataset 2 that periodically shuffled while walking. People that used a walker or an assistive walking device did not have an arm swing due to the nature of the devices restricting arm movement. Some individuals occasionally used their assistive device and some used multiple devices throughout the day like a walker, cane, or pushing a wheelchair.

Also, listed in the tables below are the walking speeds calculated from the depth sensor [17],[18]. These were compared to the observed gait speeds that were qualitatively measured. The average gait speed from the 30 subjects was 40 cm/s. Several calculated

gaits speeds were different from the observed gaits. The differences are notated in the fourth column and indicate what the observed gait speeds should have been. For example, the step detection algorithm categorized subject 03BHO1L as a slow walker (S) based on the observed gait speeds, but based on the depth sensor calculated gait speed of 46 cm/s, he should have been considered a moderate-paced walker. Most of the differences were boarder lined in the next category as seen with subject 19VBO1L. Subject 20JJO1L gait speed calculated by the depth sensor was the only one that seems on the higher side. Based on observation, his gait speed seemed more comparable to subject 06DHO1L. Overall, the subjects observed gait speeds were similar to the ones calculated from the depth sensor.

Table 3.2-1 Gait speeds calculated from the depth sensor. And gait speed ranges relative to the subjects.

Depth Sensor Estimated Gait Speed (cm/s)	
max	68
min	25
average	40
median	38

Gait Description	Speed (cm/s)
Fast	> 55
Moderate	40 - 55
Slow	30 - 39
Very Slow	< 30

*Table 3.2-2 Dataset 1 showing 10 subject gait patterns and other categories that affect gaits. **significantly different reported gait speed from the database due to tracking visitors. ***estimated gait speed from walk data scatter plot models. Fast = F, Moderate = M, Slow = S, Very Slow = VS*

Subject	Assistive Devices	Depth Sensor Est. Gait Speed (cm/s)	Differences (F,M,S,VS)	Qualitative Gait Speed	Shuffle	Leg Swing	Arm Swing	Heel Strike & Toe-off	Gait Symmetry	Posture	Posture Angle (degrees)	Base-of-Support
01BLO1L	none	54		moderate	no	full	full	full	symmetric	normal	90	normal
02BCO1L	none	42		moderate	no	full	full	full	symmetric	normal	90	normal
03BHO1L	walker infrequent	46	S -> M	moderate / slow	no	medium	Full (no walker), none (walker)	Medium (no walker), minimal (walker)	symmetric	normal	90	normal
05LBO1L	walker	34		slow	no	medium	none	medium/ minimal	symmetric	forward	40	narrow
06DHO1L	none	58	F -> M	fast/ moderate	no	full	full	full	symmetric	normal	90	normal
07HRO1L	walker	***30		slow	no	minimal/ none	Full (no walker), none (walker)	medium/ minimal	asymmetric, right dominate	forward	30	narrow

08DWO1L	none	31	S	moderate / slow	no	full	medium	full/ medium	asymmetric, left dominate	slightly forward, head,	90	normal
09HSO1L	walker	26	S -> VS	moderate / slow	no	full	none	medium	symmetric	forward	55	narrow
10JBO1L	walker infrequent	51		moderate	no	full	full	full	symmetric	normal	90	normal
11ASO1L	walker	**29		very slow	no	minimal	none	minimal	asymmetric	forward	50	narrow

*Table 3.2-3 Dataset 2 showing 20 different subject gait patterns and other categories that affect gaits.*13JAO1L and 13JAO2L is the same person, but two separate data collection periods. **significantly different reported gait speed from the database due to tracking visitors. ***estimated gait speed from walk data scatter plot models. Fast = F, Moderate = M, Slow = S, Very Slow = VS*

Subject	Assistive Devices	Depth Sensor Est. Gait Speed (cm/s)	Differences (F,M,S,VS)	Qualitative Gait Speed	Shuffle	Leg Swing	Arm Swing	Heel Strike & Toe-off	Gait Symmetry	Posture	Posture Angle (degrees)	Base-of-Support
12ALO1L	walker	40	S -> M	moderate / slow	no	minimal	none	minimal	symmetric	forward	50	narrow
*13JAO1L	walker	41	S -> M	slow	no	medium	Full (no walker), none (walker)	full	fairly symmetric	normal, head slightly forward	45	normal
*13JAO2L	walker	41	S -> M	slow	no	medium	Full (no walker), none (walker)	full	fairly symmetric	normal, head slightly forward	45	normal
15LOO1L	walker & cane	29		very slow	yes	minimal	full	minimal	asymmetric	forward	40	wide
16NDO1L	cane rarely	38	S	moderate / slow	no	full	full	full	symmetric	normal	90	normal
17LPO1L	walker	36		slow	yes	minimal	none	minimal	symmetric	head slightly forward (looks down)	65	normal
18RCO1L	wheelchair infrequent	55		moderate	no	full	minimal/ none	full	fairly symmetric	normal	90	normal
19VBO1L	walker	***31	VS -> S	slow / very slow	no	full	none	full	symmetric	normal	90	normal
20JJO1L	walker	68	M -> F	moderate	no	full	none	full	symmetric	forward	60	normal
22NDO1L	walker	40		moderate	no	full	none	full	fairly symmetric	forward	60	narrow
23JWO1L	none	***50		moderate	no	full	full	full	asymmetric	backward , head slightly forward	93	narrow
24SPO1L	walker	**30		slow	no	full	none	full	symmetric	forward	65	normal
25EHO1L	Cane infrequent	50		moderate	no	full	full	full	asymmetric	straight posture	90	wide
27CHO1L	none	50		moderate	no	full	full	full	asymmetric	straight posture	90	wide
28JBO1L	none	**50		moderate	no	full	full	full	symmetric	normal	90	normal
29SSO1L	cane, walker	32		slow	no	full	none	full	symmetric	forward	65	normal
30WBO1L	walker	***33		slow	no	full	none	full	symmetric	normal	90	normal
31FSO1L	cane, wheelchair , walker	*** 38	VS -> S	slow / very slow	no	medium	none	minimal/ none	asymmetric	forward	80	normal
32PKO1L	walker	29	S -> VS	slow	yes	none	none	minimal/ none	asymmetric	forward	65	wide
33BEO1L	walker & wheelchair	**25		very slow	yes	minimal/ none	none	none	asymmetric	very forward	50	narrow
34REO1L	walker, wheelchair infrequent	***29	S -> M	very slow	no	full	none	medium	fairly symmetric	forward	55	very narrow

3.3 Method

3.3.1 Step Detection Algorithm Development

The main goal for this section was to develop a step detection algorithm and to see how the different gait patterns affect the results. This algorithm assumed there was a prior walking detection algorithm that found walking periods as the input then it used a peak detection method to count the individual steps. The algorithm developed for this study is comparable to several published step counting algorithms, but not limited to these listed [19],[20],[11]. The main difference for this algorithm was the placement of the accelerometer, a moving average filter, and then using a selection method to determine a single axis instead of the acceleration magnitude (vector magnitude). The filter that was used averaged the neighboring data points within the span of the signal, which is equivalent to lowpass filtering [21]. This smooths the noisy data from the sampled signal, as seen below.

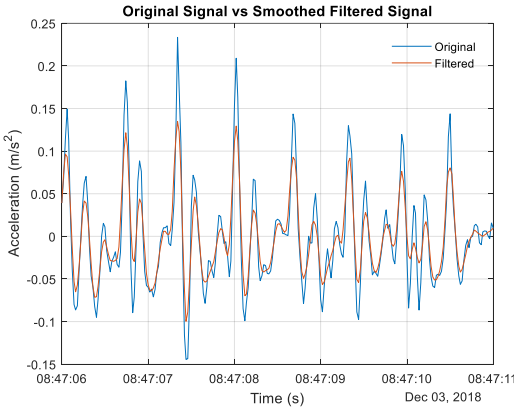

Figure 3.3-1 The original and filtered vector magnitude of acceleration.

Originally, both the vector magnitude method and a single axis was observed to compare the performance. The equation shows the acceleration vector magnitude calculation.

Equation 3.3-1

$$\|S\| = \sqrt{S_x^2 + S_y^2 + S_z^2}$$

The first method used the vector magnitude. The vector magnitude of acceleration removed the directional components of the signal leaving only the intensity of the acceleration. Several values were calculated to determine the local maxima peaks from the filtered signal, including the minimum peak height, minimum peak width, and minimum peak prominence. The minimum peak prominence reflects the relative importance of a peak based on the height and location of other peaks [21].

For the axis selection method, it used a dynamic approach to find the best axis to detect peaks. First, the minimum peak height was determined. The axis with the largest minimum peak height was selected as the best axis. Also, it was used to calculate the minimum peak height, distance, and prominence to determine an appropriate threshold to count steps.

Figure 3.3-2, shows two individual walking periods from 01BLO1L and 11ASO1L, using the acceleration vector magnitude signal. 01BLO1L did not use an assistive device and generally had a normal gait. Full gait cycles with the heel-strike, toe-off, and swing phases can be easily seen in the left figure. On the right, 11ASO1L used a walker and walked slower. For people with a slower walk and shuffling, the amplitude difference between the heel strikes and toe-off phases was reduced with additional noise. The false positives were caused by the additional noise, which are shown below by the red circles. This made it difficult to accurately detect steps.

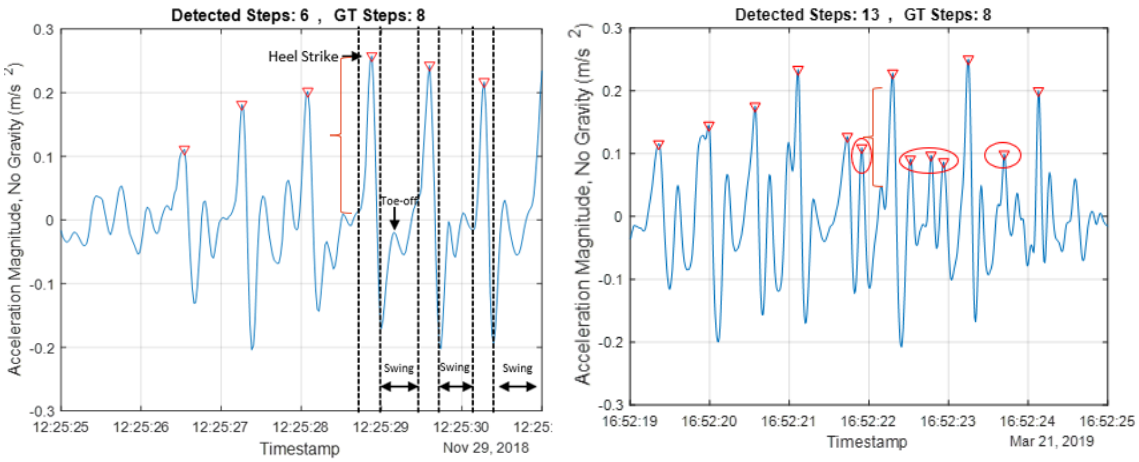

Figure 3.3-2 shows the vector magnitude signal for two subjects. 01BLO1L walked normal, used no assistive walking device, and had a normal gait (left). 11ASO1L walked very slow with a walker and had minimal heel-strike and toe-off phases (right). The amplitude of signal decreased when using a walker. The false-positive step counts are indicated by the red circles.

3.4 Results

The depth sensor was used to label the ground truth step counts while the subject was in view of the depth sensor. The average relative error of the difference in step counts was used to measure the proposed algorithm performance and the effects of the different gait patterns[19]. It is common to measure the reliability of step counts and activity time by looking at the underestimation or overestimation of a cumulative total of steps [1].

Below in Figure 3.4-1, compares 01BLO1L ground truth number of steps shown in the top figures and the number of steps detected from the algorithm on the bottom in red. The main goal was to compare the representation of the results rather than focusing on single errors in the step count difference. The overall representation of the detected results matched the ground truth, even though the algorithm undercounted steps.

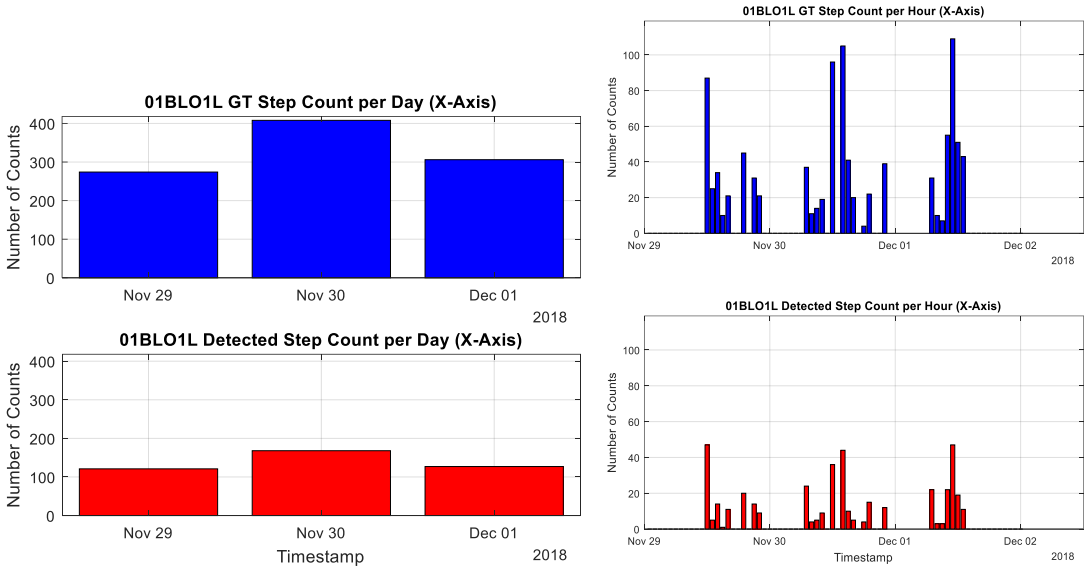

Figure 3.4-1 Subject 01BLO1L step count per day (left) and step count per hour (right).

The results below show averages based on the errors from the two datasets. Figure 3.4-2, shows the difference in performance between the vector magnitude versus individual axes. The acceleration in the x-axis (frontal/mediolateral axis) resulted in the least amount of error for both dataset 1 and dataset 2. The analysis from here on will focus on the algorithm using only the x-axis. Looking at dataset 1 for the x-axis, the step count algorithm underperformed and counted fewer steps than the ground truth. In Dataset 2 the algorithm detected slightly more steps. The remaining figures will help explain the reason for the negative results in dataset 1 in comparison to dataset 2.

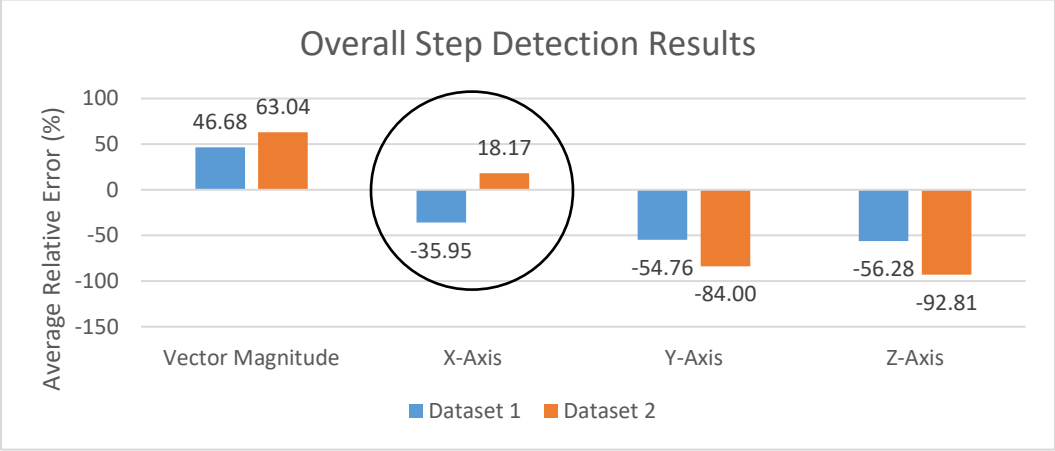

Figure 3.4-2 Overall step detection results comparing the algorithm using the acceleration vector magnitude or a single axis for both dataset 1 and dataset 2. The x-axis resulted in the lowest errors.

Now, we can look closer at how the different gait patterns affect the results. Figure 3.4-3, shows a broad overview of the different gait pattern categories. The top three categories that resulted in the largest error included the assistive device, walking pace, and posture. People using assistive walking devices typically slower with either a reduced or minimal heel-strike and toe-off phases. The participants in this study with an assistive device leaned forward more, mostly due to using the walker improperly. Also, the assistive device limits the horizontal trunk movement (side-to-side), which is seen when a person walks without assistance.

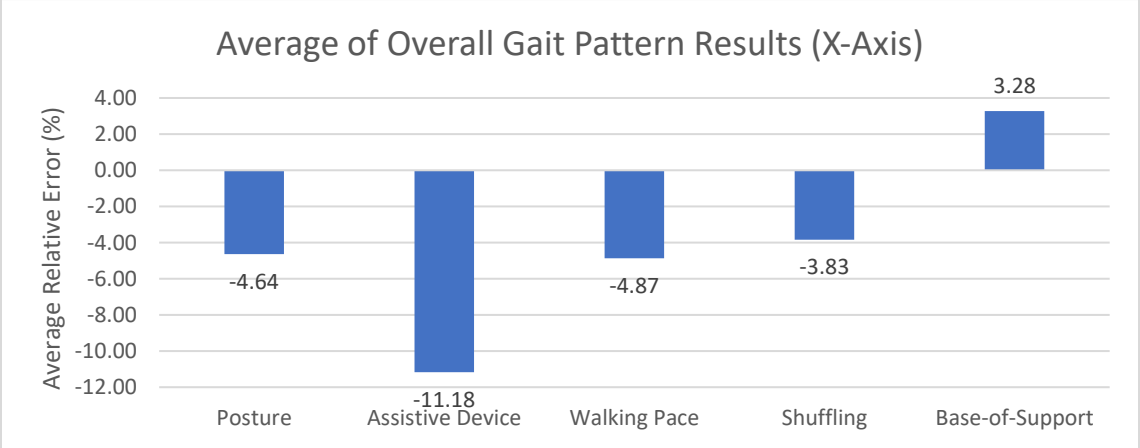

Figure 3.4-3 Different gait pattern categories showing overall average results for the x-axis signal combining both datasets.

Below in Figure 3.4-4, shows a similar overview of all the gait pattern results, but separated into subcategories per dataset. This also helped to see the relationship between the different gait patterns. To point out, there were no individuals for dataset 1 with a wide base-of-support (BOS). And for dataset 2, there were no individuals who walked at a fast pace.

Looking closer at the postural relationships and different assistive device usage, people with a normal posture showed similar results to those that did not use a walker or

infrequently used an assistive device. Oppositely, the people with a forward posture showed similar results to those that did use a walker or multiple devices. It was common to see the people that used an assistive walking device to have an improved gait when they did not use their walker or cane. The individuals walked with a straighter posture and their gait symmetry, base-of-support, leg swing drastically improved.

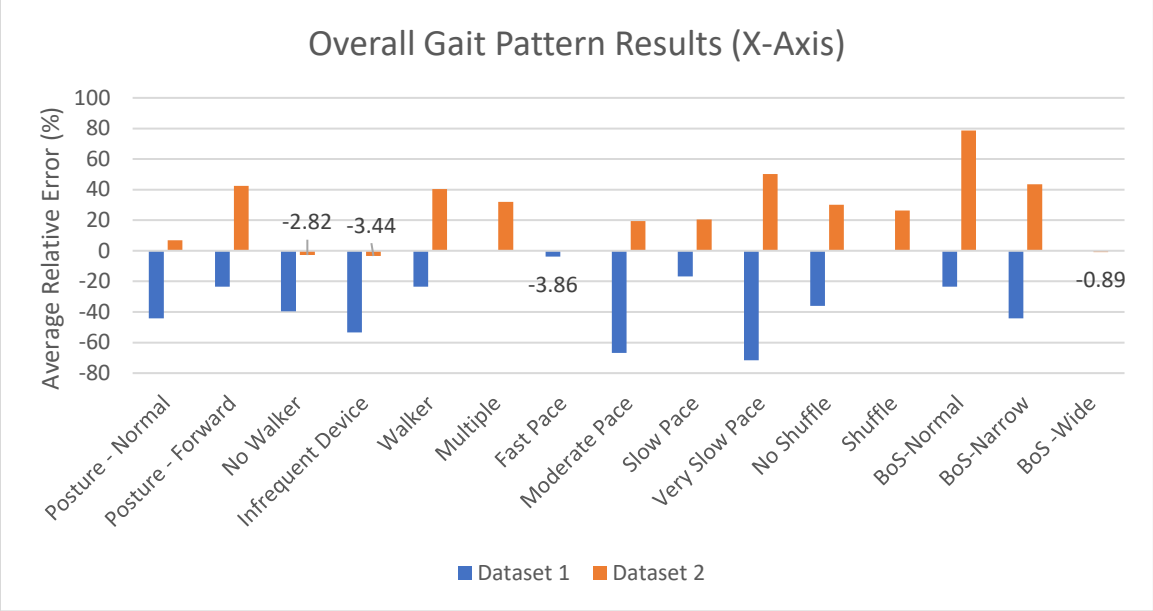

Figure 3.4-4 Overall gait pattern metric results in the x-axis direction for both dataset 1 and dataset 2.

Figure 3.4-5, shows two individual walking periods from the same subjects 01BLO1L and 11ASO1L as in Figure 3.3-2, but using only the x-axis. It is more difficult to visually determine a step looking at a single axis than with the acceleration vector magnitude signal. It is dependent on the orientation of the accelerometer.

Subject 01BLO1L signal on the left represent people without an assistive walking device, normal posture, and moderate speed. Only half the steps were detected compared to the ground truth. On the right, subject 11ASO1L represents subjects that use a walker, forward posture, slower walk, and might occasionally shuffle. Almost all the steps were

detected compared to the ground truth. Also, the signal appears noisier with additional peaks that are mistaken for steps.

Now, comparing the two datasets and reviewing Figure 3.4-4, we can get a better understanding of why dataset 1 resulted in negative errors, underperforming. From dataset 1, 60% of the subjects walked with a normal posture, walked slower, and used some type of assistive walking device. But 42.9% of dataset 2 had a normal posture and 66.7% walked slow. With more than 80% of dataset 2 that uses some type of assistive walking device, this was a big reason why dataset 2 has had negative results. Also, out of the total 30 subjects, only four subjects from dataset 2 walked with a shuffle; barely picking their feet up. These details are also shown in Appx. Table F-1.

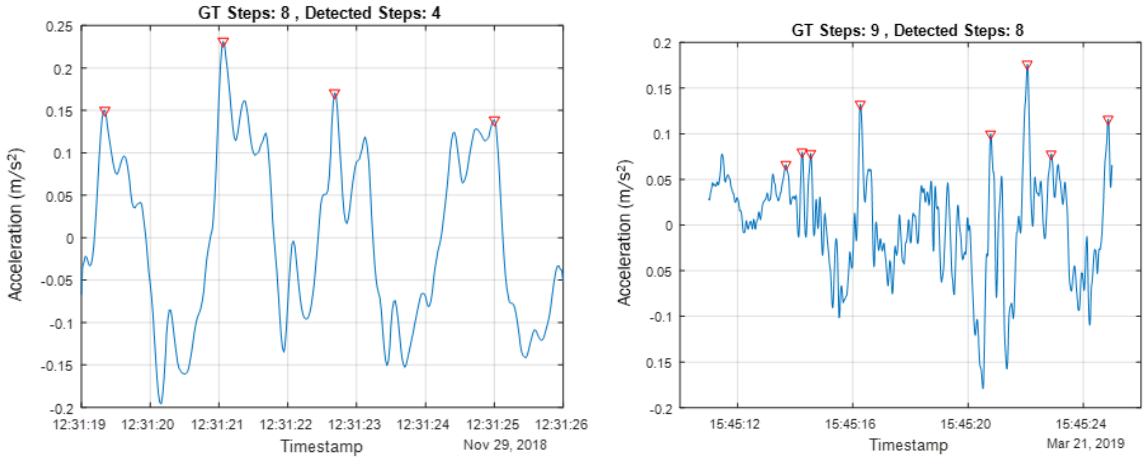

Figure 3.4-5 Shows the x-axis signals for the same subjects as above in Figure 3.3-2. Subject 01BLO1L had no assistive walking device (left) and subject 11ASO1L used a walker (right)

The next two figures show the overall results from dataset 1 and dataset 2. Figure 3.4-6, compares acceleration results in the x, y, and z-direction for each subject from dataset 1. Starting with the acceleration in the z-direction in green, subjects 02BCO1L and 06DHO1L were the only ones that had positive errors. Their gaits were significantly

different from the others. They walked with a more exaggerated heel-strike and had a larger vertical foot displacement.

Next, the acceleration in the y-direction in orange, subjects 05LBO1L, 07HRO1L, and 11ASO1L walked slower, postures less than 50 degrees, and least amount of heel-strike. These individuals periodically shuffled their feet.

And, the acceleration in the x-direction in blue, all dataset 1 subjects had negative values except for subjects 07HRO1L and 08DWO1L. Subject 07HRO1L had the lowest posture angle of 30 degrees. Comparing the two subjects to the rest of dataset 1, there was not a lot that stood out. They did limp slightly with a more lateral side-to-side motion.

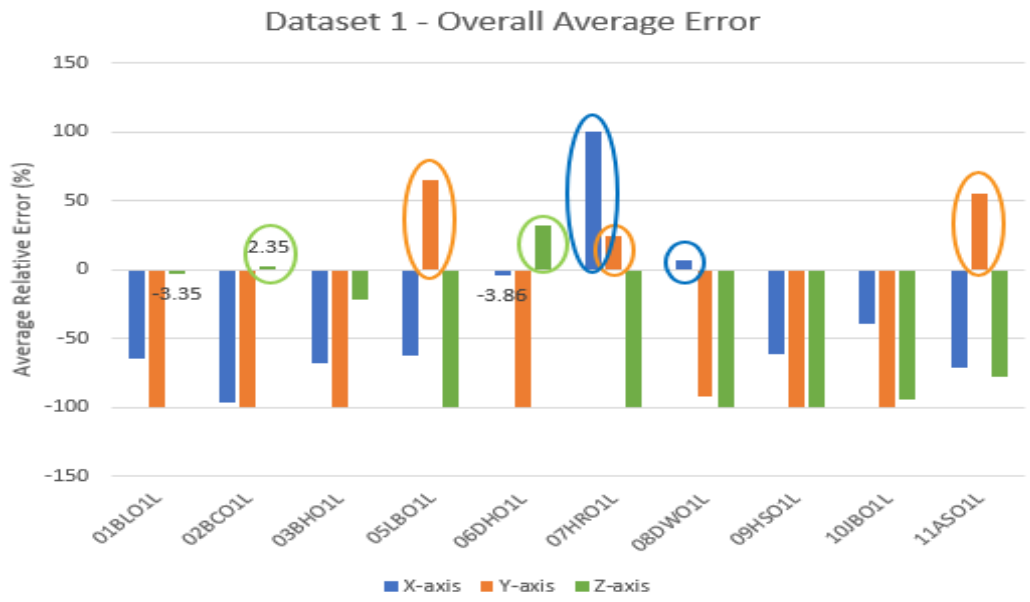

Figure 3.4-6 Comparison of the average errors from dataset 1 using the x, y, and z acceleration.

Figure 3.4-7, shows the standard deviation of the step count errors, which indicates the amount of variance. The x-axis had the largest variance shown by all the blue and the y-axis had the least variance. Only subject 05LBO1L, 07HRO1L,

08DWO1L, and 11ASO1L step count errors varied the most in the y-direction. These subjects had the least amount of average error shown above in Figure 3.4-6. As stated before, they walked slowly with a forward posture.

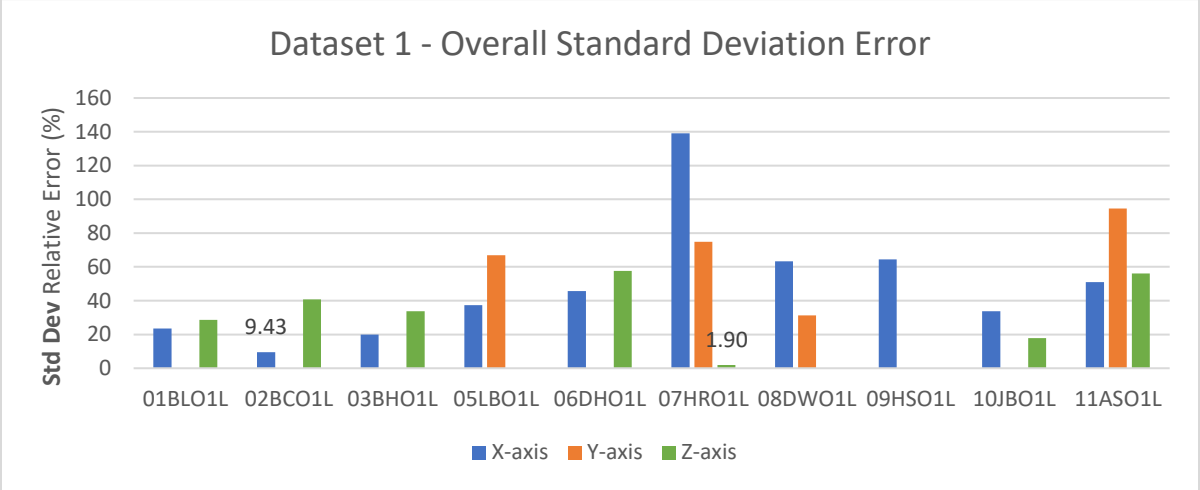

Figure 3.4-7 Dataset 1 overall standard deviation error.

Figure 3.4-8 shows dataset 1 average errors like the results shown previously in Figure 3.4-6. The graphs shown below include the error bars that indicate the minimum and maximum errors. Looking at subject 07HRO1L in the middle in the x-direction and y-direction, her results had the largest range of error. There was a lot of walking periods, which the step detection algorithm was not able to find peaks to count as steps. This resulted in a lot of negative errors. The subjects with positive errors shown previously had the largest range of errors indicated below. Overall, the x-axis had the least amount of variance compared to the y-axis and z-axis.

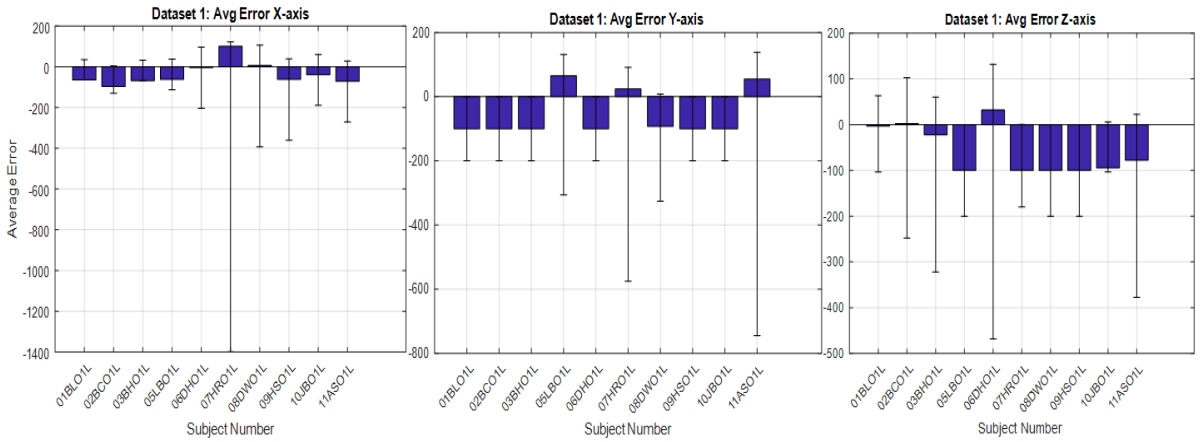

Figure 3.4-8 Dataset 1 average error with error bars showing the minimum and maximum errors.

Figure 3.4-9 shows similar explanations as above, but for dataset 2. Starting with the acceleration in the z-direction in green, only subject 23JWO1L showed positive errors. Same as in dataset 1, she had a more exaggerated heel-strike and had a larger vertical foot displacement. Her walk especially resembled more of a marching style and she slightly leaned back with her legs more out front than any other subject.

Looking at the acceleration in the y-direction in orange, only subject 29SSO1L showed positive errors. She walked with a straight poster, slow and usually with a cane. She had a full leg swing and executed a full heel-strike toe-off cycle. Occasionally, she would hold on to the wall or kitchen counter while walking.

And lastly, the acceleration in the x-direction in blue, all the subjects showed positive results except for subjects 13JAO1L/13JAO2L, 18RCO1L, 25EHO1L, 27CHO1L, and 31FSO1L. For all three axes, their results were negative. Comparing 13JAO1L to 13JAO2L, his second data collection had less error using the x-axis signal.

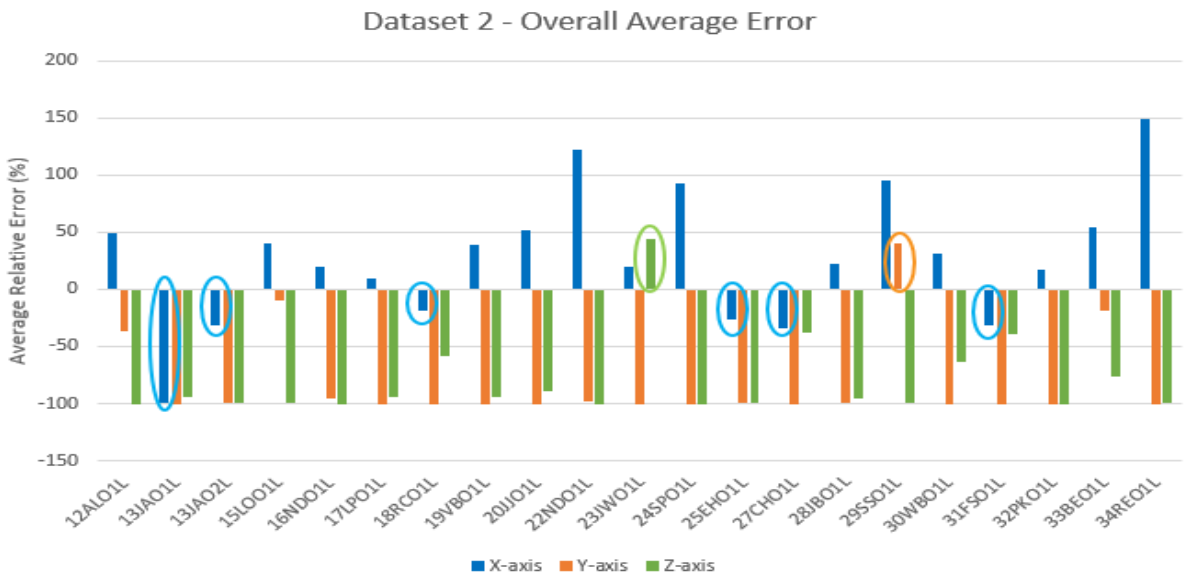

Figure 3.4-9 Comparison of overall average errors from dataset 2 using the x, y, and z acceleration signal.

Figure 3.4-10 shows an example of the filtered ActiGraph accelerometer signal in the x, y, and z-direction. It demonstrates the y-axis had the most defined signal compared to the acceleration in the z-direction and x-direction used in this study. However, in other published work, the y-axis (vertical) is used for step and activity detection [20], [21]. For younger healthy people, the y-axis shows significant vertical displacements while walking. In other adults, the vertical displacement is possibly reduced due to shuffling and smaller steps. People walk in the mediolateral axis (x-axis) and sagittal plane, which shows more flexion and extension motion [23]. Healthy adults walk with a straight posture with their shoulders and truck moving at the same level. As seen in this study, older adults tend to have an increase in forward flexion of the truck around the mediolateral axis. Also, an increase in lateral motion leaning side-to-side. But a decrease in vertical displacement, due to shuffling and slower walks.

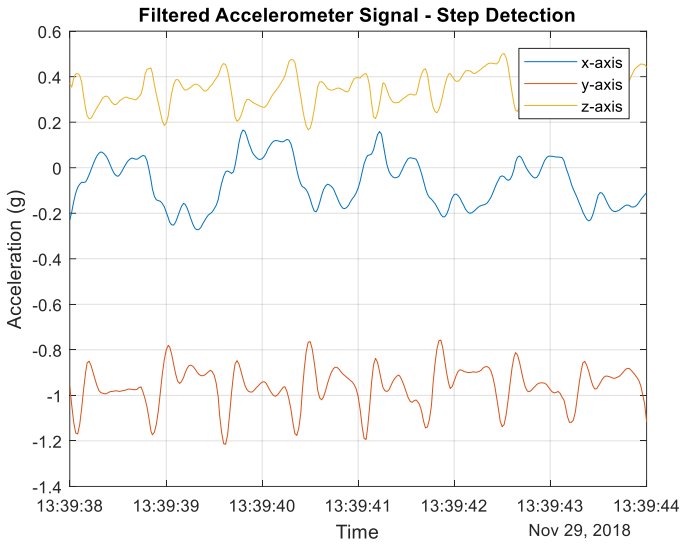

Figure 3.4-10 Subject 01BLO1L filtered accelerometer signal in the x, y, z-direction.

Lastly, centering the acceleration signals in the x, y, and z-direction to zero prior to applying the filter and processing the data improved the accuracy of the step counts, as seen below in Figure 3.4-11 and Figure 3.4-12. Subtracting the mean of the signal from the original signal will remove the effects of gravitational body forces [22]. This decreases the range of acceleration, which helps when finding peaks based on the minimum peak heights.

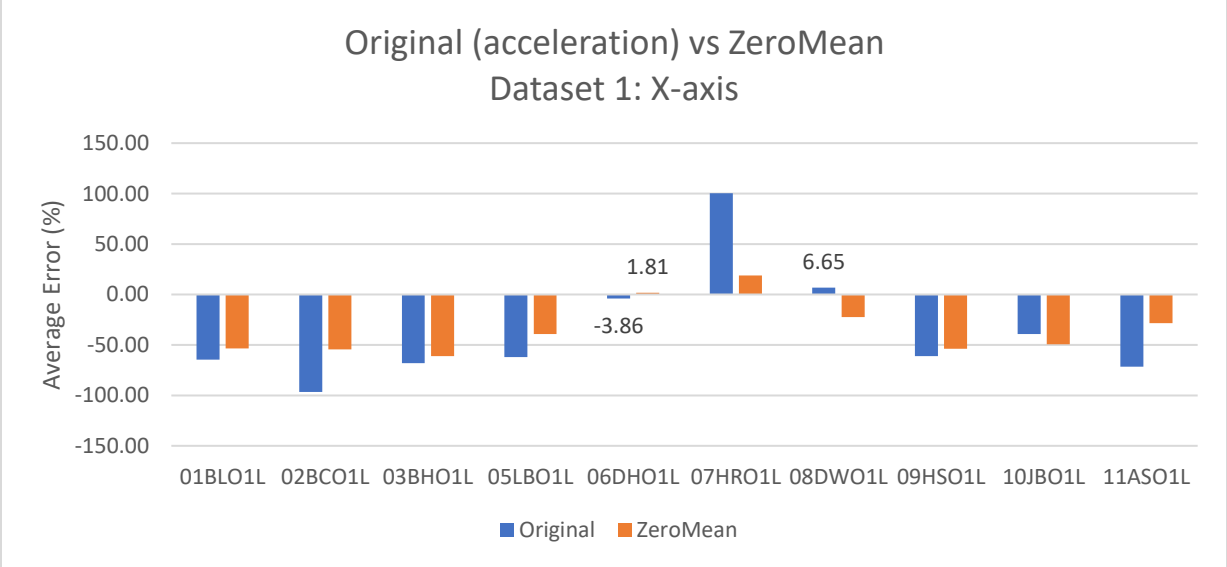

Figure 3.4-11 Dataset 1 average step count error based on the original algorithm without centering (zero mean) the accelerometer signal versus applying zero mean.

In Figure 3.4-12, the x-axis had the lowest errors without centering the accelerometer data, but when applying zero mean to the data, the y-axis resulted in the lowest errors. The errors for dataset 1 still were in the negative direction, meaning the step detection algorithm undercounted the steps. Dataset 2 results are shown in Appendix F.

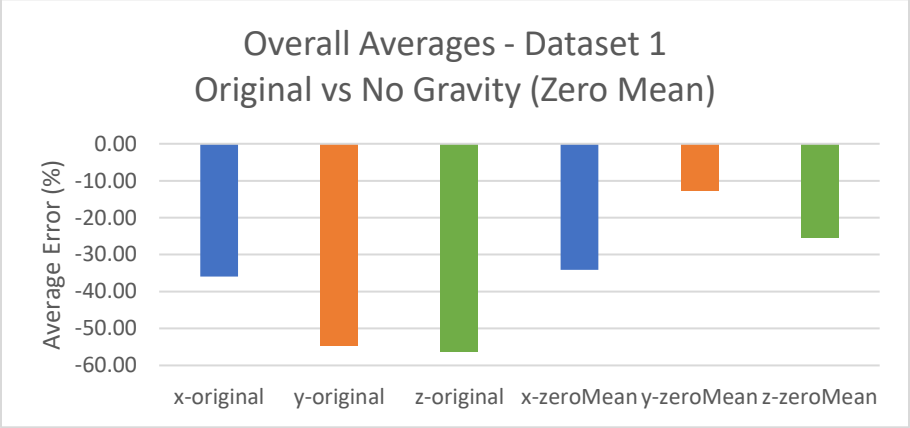

Figure 3.4-12 Overall average error for dataset 1. The y-zeroMean resulted in the lowest error.

3.5 Summary and Discussion

The step detection algorithm section further demonstrated the complexity of gait patterns, but the need for considering them for future devices older adults will use. Overall, the step count algorithm had high errors, but this thesis helped to understand the effects of different gaits. It was able to detect a similar cumulative step count per day and per hour as the ground truth. However, using a customized filter more appropriate to older adults would give better results. A few different lowpass filters were tested along with the filter discussed in this thesis, such as a 3rd-order median filter, 3rd-order elliptical filter, 3rd-order Butterworth filter, and 4th- order Butterworth filter with different cutoff frequencies ranging from 0.25 Hz to 20 Hz [23],[24], [25]. But the filter chosen performed best overall for both datasets.

Using the vector magnitude would be a good alternative to using only a single axis. However, for small wearable devices using a single axis is best for simplicity to minimize battery consumption. The x-axis showed the least amount of error for this age group in this study. However, the y-axis is used is typically used in practice with younger healthy adults. Future studies will be needed to validate if the x-axis should be used instead of the vertical y-direction with older adults in real-living environments.

4 Stand-to-sit / sit-to-stand (STS)

4.2 Background

Observing stand-to-sit and sit-to-stand is a common metric when assessing older adults' functional capabilities. Going from sit-to-stand requires a significant amount of muscle power and balance, which starts to decline in older adults [26]. Sometimes they will rock back and forth to gain momentum before attempting to stand. Also, it may take several attempts for them to fully stand. Just like we saw in the previous section with walks and steps, STS postural transitions vary a lot with older adults. But over time, detecting changes in the duration of STS may indicate health issues.

In this study, most of the participants fell into their seats after starting to descend from the standing position. It also took several attempts for them to fully stand. This is commonly seen with older adults. The stand-to-sit transition was shorter than the sit-to-stand transition. The sit-to-stand transition approximately took 3 seconds to 5 seconds for a person to stand. The STS average durations are compared in Figure 4.4-1 to the number of observed STS(s) in Figure 4.4-2. The number of STS data for this research was imbalanced with less than 1.5% of the data was either stand-to-sit or sit-to-stand, compared to 98.5% that was labeled as other. The other class label included walking,

standing, sitting, lying down, and step times. The spatial representation of the three classes is shown below in Figure 4.3-1.

4.3 Method

4.3.1 Training Data and Testing Data

For the STS classification section, all ten subjects from dataset 1 were used for training with a total of 101,018 samples. Eighteen subjects from dataset 2 were used to test the performance of the quadratic discriminate analysis (QDA) and RUSBoost classification models. Dataset 2 had 241,918 samples. Also, for a more realistic test, each subject was tested since the classification of STS would only be applied to a single person. On average there were about 10,000 samples per subject for testing.

There were two subject's data excluded from this section. Subject 17LPO1L only sat or laid in bed, therefore there is no STS ground truth data. Also, subject 20JJO1L did not have ground truth for STS because his main chair was not visible to the depth sensor.

4.3.2 Principle Component Analysis

The 3D principal component analysis (PCA) was performed to visually see the spatial representation of the three different classes reduced from the thirty-three features. The boundaries are difficult to identify because the hollow spherical shape has a few overlapping clusters. The black circle defines a separate cluster of data inside the sphere. It visually blended into the cluster behind it on the left. The yellow stand-to-sit (standSit) and cyan sit-to-stand (sitStand) were sparsely located within the black circle and scattered around the inside perimeter of the sphere. Overall, the 3D PCA shows there is a lot more

of the other class. The standSit and sitStand classes relatively clustered in a similar feature space.

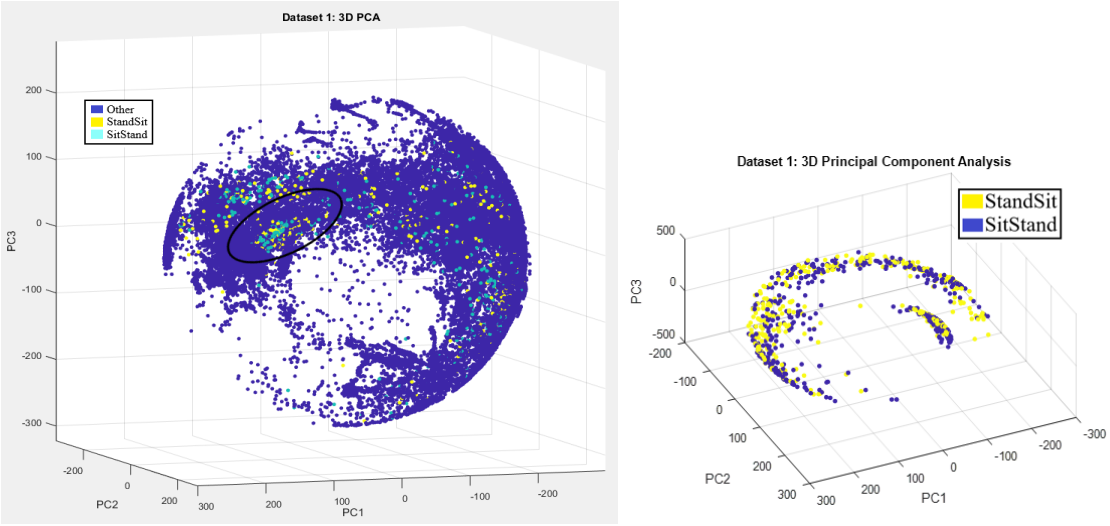

Figure 4.3-1 (left) A 3D PCA visualization of the thirty-three features of the three classes. (right) 3D PCA visualization of just the standSit and sitStand classes.

4.3.3 Ground Truth Labels

A window of 5-seconds was used to label the ground truth as either stand-to-sit (standSit), sit-to-stand (sitStand), or other. The other category as mentioned before included all the other activity times, such as walking, standing, steps, or lying down. The standSit was defined as the initial second the person started descending to sit in their chair until they sat down. And the sitStand was the initial second the person started to stand up. The depth sensor occasionally missed the sitStand due to not detecting the minimal movement or limited visibility. Also, for some subjects, the visibility of either sit-to-stand or stand-to-sit was limited due to low video resolution or the depth sensor missing the full postural transitions.

The windows were labeled either stand-sit or sit-stand if there were at least one of these states, else the window was labeled as the most frequent state. The time vectors were resized based on if the time was at the beginning STS, else the most frequent time was labeled. And for all the other states, the most frequent time was labeled.

4.3.4 Signal Processing and Feature Extraction

The raw (unfiltered) tri-axis accelerometer data collected at either 50 Hz or 100 Hz was filtered using a digital fourth-order Butterworth filter with a recommended cutoff frequency [27] for postural transition movements. The filter smooths the noise from the unfiltered signal shown in Figure 4.3-2. This figure also, shows the postural transition events between sitting and standing. It is easy to see the start and end of a standSit or sitStand, where there is a large decrease in amplitude. The signals shown below were from subject 23JWO1L. She sat down at a normal pace, which was a gradual descend before fully sitting. However, the large narrow peak indicates when she stood up fast.

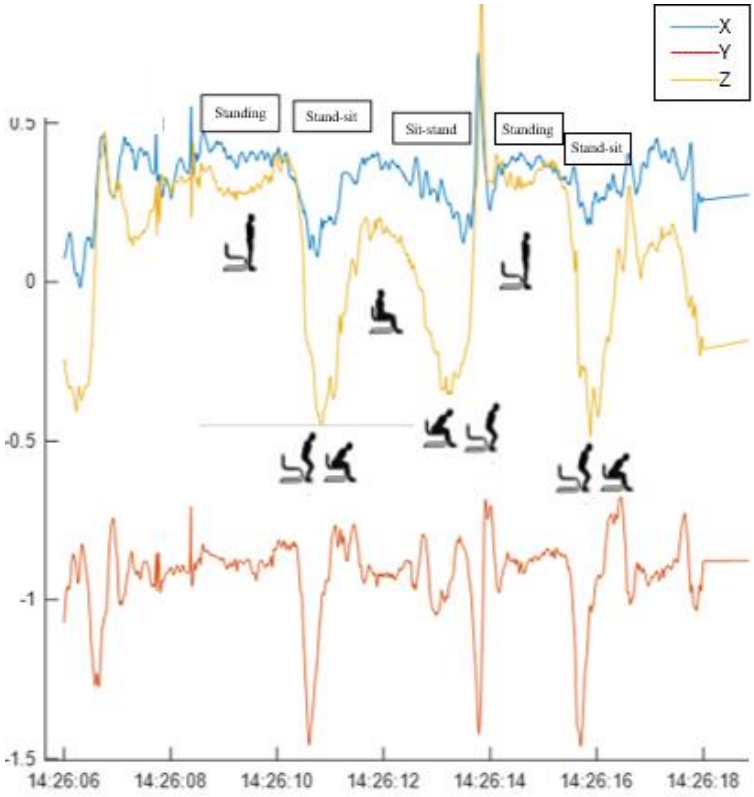

Figure 4.3-2 Subject 23 unfiltered ActiGraph accelerometer signal in the x, y, and z-direction showing transitional states between sitting and standing.

Next, the filtered signal was sampled over a 5-second window to extract thirty-three time-domain features. These sets of descriptive features for STS detection were also reported in [28][29]–[31]. The features used in this study are shown in the table below. Jerk is the first time derivative of acceleration and velocity is the first integral of acceleration with respect to the change in time.

Table 4.3-1 List of features calculated from several statical estimations.

Features	**Statistical Estimations**
Acceleration in x, y, z-direction	Mean, standard deviation, variance, maximum, jerk, velocity
Vector magnitude (VM) of acceleration	Mean, standard deviation, variance, maximum, jerk, velocity
yaw, pitch, roll angles	Mean, standard deviation, and maximum
Jerk in x, y, z-direction, and VM	mean
Velocity in x, y, z-direction, and VM	mean

4.3.5 Machine Learning Classifier

The supervised learning classification process used labeled ground truth data to fit a model to identify stand-to-sit and sit-to-stand transitional periods from the ActiGraph accelerometer data. A 5-fold cross-validation was used to ensure proper separation of training and validation data to limit overfitting. The training data was split into five equally sized random subsets, leaving one for validation and the remainder for training. From the five rounds of training, the average accuracy was computed.

The first classifier model was performed using quadratic discriminate analysis (QDA) that can handle multiple classes and creates nonlinear boundaries. It uses density estimation (δ_k) based on a multivariant Gaussian distribution that assumes variance of the means and covariances for each class. The centered covariances (Σ_k) can be estimated using singular value decomposition (SVD) shown in Equation 2, which is based on the general eigen decomposition transformation. Where (X_k) is the input and (U_k) and (V_k^T) are identity matrices, which leaves the diagonal of (Σ_k) as the estimated covariances.

Equation 2

$$X_k = U_k \Sigma_k V_k^T$$

For each kth class the prior probability (π_k), mean (μ_k), and covariances (Σ_k) are used to calculate the estimated discriminate score in Equation 3. Then then the classifier assigns the maximum score to the kth class. In general, the QDA uses a distance metric from the means of each class after applying a transformation [32].

Equation 3

$$\delta_k(x) = -\frac{1}{2}\log|\Sigma_k| - \frac{1}{2}(x-\mu_k)^T\Sigma_k^{-1}(x-\mu_k) + \log\pi_k$$

The second classifier model was performed using a random under-sampling boost (RUSBoost). This hybrid model uses two techniques, data sampling and boosting to reduce the effects of imbalanced data. It resamples the data by taking the class with the lowest number of observations and under samples the class with the highest number of observations [21], which would be the Other class in this study. The AdaBoost ensemble adds the weak weighted models sequentially attempting to correct errors to create a stronger classifier. This is where RUSBoost can be computationally expensive more than QDA. However, both models do not have hyperparameters, which keeps the computational costs lower than other popular models like support vector machine (SVM).

4.4 Overall Results

For each subject, the average standSit and sitStand ground truth durations were totaled and compared to the ground truth number of instances observed during their data collection. Subjects 09HSO1L and 33BEO1L took the longest to stand up and sit down. Based on Figure 4.4-1, most of the subjects took 1 to 2 seconds to either standSit or sitStand. Subject 33BEO1L, STS durations varied a lot between 1 second to 30 seconds. Overall, sitStands took about the same time as standSit, if not longer. A full table of STS average durations can be seen in Appendix G.

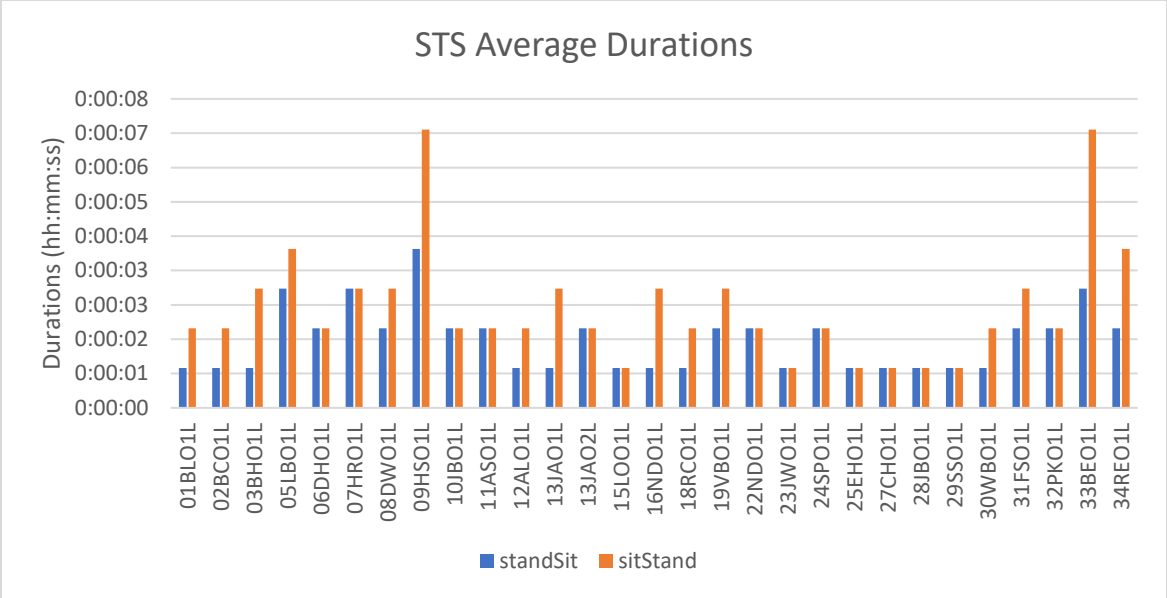

Figure 4.4-1 Ground truth STS average durations for each subject.

Figure 4.4-2 shows the ground truth number of STS instances observed. The other class is not shown below because it would outweigh the small number of STS that would barely be visible. However, the variation between the standSit and sitStand categories can be seen below. Subject 24SPO1L and 25EHO1L had the largest contrast, with hardly any sitStand. There were a few that had more standSits like 03BHO1L, 07HRO1L, 13JAO1L/13JAO2L, 16NDO1L, 30WBO1L,32PKO1L, and 33BEO1L.

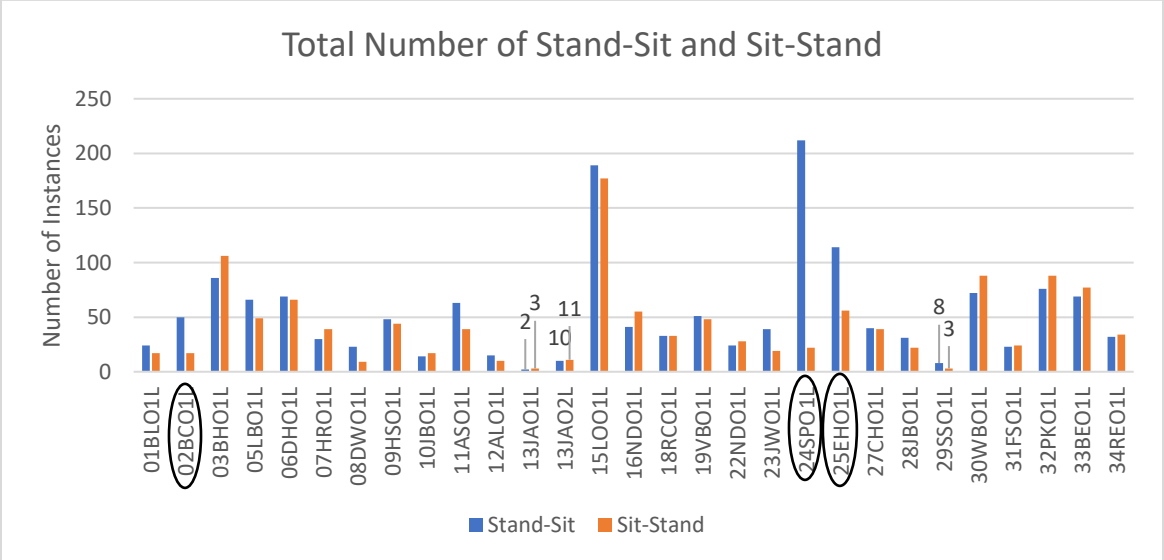

Figure 4.4-2 Ground truth total number of STS observed for each subject.

Next, the validation accuracies from the trained QDA and RUSBoost models are shown in Table 4.4-1. The confusion matrix shows the results as percentages instead of the number of observations. The percentages were calculated by taking the number of observed over the total number from the true class. Also, the true positive rates are shaded in green separate from the misclassifications. The darker green indicates a higher percentage of a class being classified correctly. For the misclassifications, a darker red indicates a higher percentage of a class being misclassified. Also, the class other, misclassifications are shaded relative to each other separate from the STS because of weighted differences. Out of the few misclassifications, the QDA training model misclassified both the other and sitStand class as standSit. Even though the percentages are relatively low, they are shaded dark red to indicate the maximum misclassified class.

Based on the results the training validation accuracy for both QDA and RUSBoost was about 93% . The QDA model mostly was confused with the standSit class and RUSBoost confused the sitStand class, shown in red.

Table 4.4-1 The validation accuracy from QDA and RUSBoost using dataset 1.

Dataset 1 - Validation Accuracy							
		QDA			RUSBoost		
TRUE	other	93.54%	4.82%	1.64%	93.53%	1.28%	5.19%
	stand-sit	8.68%	79.16%	12.16%	1.48%	67.44%	31.08%
	sit-stand	7.61%	24.95%	67.44%	1.74%	5.96%	92.31%
QDA	**93.40%**	other	stand-sit	sit-stand	other	stand-sit	sit-stand
RUS	**93.20%**	Predicted					

From dataset 2 the test accuracy for the QDA model was 92.33% and 91.3% accuracy for RUSBoost. This is only about a 1.5% decrease from the validation accuracy. Even with high accuracy, there was still a lot of confusion between standSit and sitStand.

The RUSBoost misclassified the standSit and other classes with the sitStand more than the QDA model. And the sitStand class was mostly misclassified as standSit.

Table 4.4-2 The test accuracy from QDA and RUSBoost using dataset 2.

Dataset 2 - Testing Accuracy							
		QDA			RUSBoost		
TRUE	other	92.69%	2.01%	5.31%	91.59%	1.43%	6.98%
	stand-sit	26.09%	43.11%	30.80%	21.92%	40.43%	37.65%
	sit-stand	18.28%	28.32%	53.41%	6.45%	18.52%	75.03%
QDA	92.33%	other	stand-sit	sit-stand	other	stand-sit	sit-stand
RUS	91.30%	Predicted					

Figure 4.4-3 below shows the individual test accuracies for each subject.

The QDA shown in blue and RUSBoost shown in orange showed similar performance. The overall average was about 90%, except for subjects 07HRO1L, 10JBO1L, 13JAO1L/13JAO2L, 29SSO1L, and 31FSO1L who underperformed. These individuals' results are explained more in-depth in the case study section. If these five individuals' results were excluded from this graph, there would not be large peaks if the y-axis limits were not scaled the same, else the graph would look smoother.

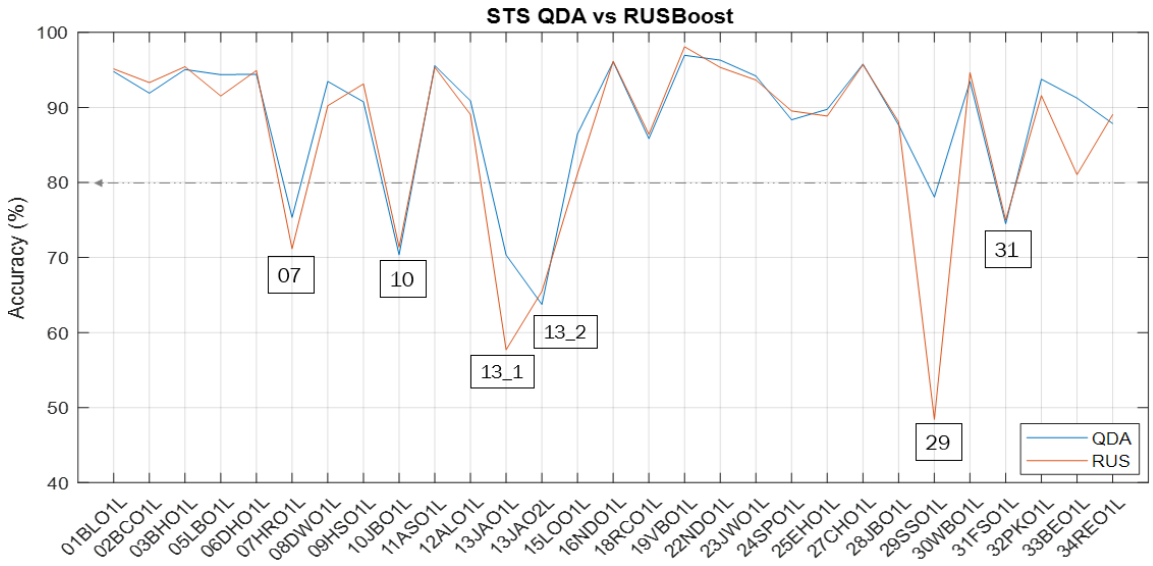

Figure 4.4-3 STS QDA and RUSBoost test accuracies for each subject.

In addition to looking at the overall test accuracies, evaluating the true positive rates shown in Table 4.4-3 and Table 4.4-4 were used to get a better understanding of the different classes' performance for each subject. The higher the true positive rate means the model was able to predict the correct class. A low true positive rate indicates a high number of misclassified classes. Based on both the QDA and RUSBoost results shown below, 07HRO1L, 09HRO1L, and 10JBO1L had low StandSit true positive rates. And 08DWO1L had low SitStand true positive rates. Overall, the QDA model misclassified the StandSits, which the RUSBoost model results said the same. Since the other class is weighted higher due to a larger number of observations, 07HSO1L and 10JBO1L lower true positive rates lowered the overall test accuracy as indicated above in Table 4.4-3.

Table 4.4-3 The true positive rates from dataset 1.

	True Positive Rates					
	D1 - QDA			D1 - RUS		
	Other	StandSit	SitStand	Other	StandSit	SitStand
01BLO1L	94.85%	75.00%	94.12%	95.21%	70.83%	100.00%
02BCO1L	91.93%	88.00%	94.12%	93.47%	72.00%	94.12%
03BHO1L	95.11%	80.23%	96.23%	95.51%	75.58%	96.23%
05LBO1L	94.99%	59.09%	81.63%	91.89%	74.24%	79.59%
06DHO1L	94.53%	75.36%	92.42%	95.11%	56.52%	93.94%
07HRO1L	75.38%	50.00%	92.31%	71.02%	53.33%	94.87%
08DWO1L	93.56%	95.65%	33.33%	90.29%	82.61%	77.78%
09HSO1L	91.08%	52.08%	70.45%	93.42%	39.58%	97.73%
10JBO1L	70.62%	21.43%	82.35%	71.55%	14.29%	100.00%
11ASO1L	95.68%	65.08%	71.79%	95.37%	90.48%	82.05%

In Table 4.4-4, the QDA results either had low StandSit or SitStand true positive rates under 60% except for 13JAO2, 29SSO1L, and 27CHO1L. For the RUSBoost model, only 13JAO1L, 23JWO1L, 25EHO1L, and 32PKO1L had a low true positive rate for sitStand. The standSit class results were like the QDA model. For the other class, 13JAO1L/13JAO2L, 29SSO1L, and 31FSO1L had the lowest true positive rates, which

caused a lower overall test accuracy. Again, this is consistent with Table 4.4-3, which showed large spikes for these three subjects.

Table 4.4-4 The true positive rates for dataset 2.

	True Positive Rates					
	D2 - QDA			D2 - RUS		
	Other	StandSit	SitStand	Other	StandSit	SitStand
12ALO1L	91.06%	60.00%	80.00%	89.22%	53.33%	90.00%
13JAO1L	70.36%	100.00%	33.33%	57.70%	100.00%	33.33%
13JAO2L	63.48%	80.00%	90.91%	65.25%	80.00%	90.91%
15LOO1L	87.03%	50.79%	52.54%	81.46%	47.09%	80.23%
16NDO1L	96.27%	31.71%	47.27%	96.30%	29.27%	78.18%
18RCO1L	86.06%	39.39%	81.82%	86.65%	42.42%	78.79%
19VBO1L	97.23%	56.86%	72.92%	98.41%	27.45%	93.75%
22NDO1L	96.44%	25.00%	42.86%	95.42%	29.17%	78.57%
23JWO1L	94.32%	74.36%	31.58%	93.79%	64.10%	47.37%
24SPO1L	90.63%	10.38%	77.27%	91.81%	10.85%	86.36%
25EHO1L	90.23%	50.88%	42.86%	89.34%	49.12%	39.29%
27CHO1L	95.90%	37.50%	64.10%	95.78%	45.00%	84.62%
28JBO1L	88.71%	19.35%	50.00%	88.96%	19.35%	72.73%
29SSO1L	78.21%	62.50%	66.67%	48.37%	50.00%	66.67%
30WBO1L	93.67%	59.72%	56.82%	94.78%	51.39%	87.50%
31FSO1L	74.82%	73.91%	54.17%	75.59%	30.43%	79.17%
32PKO1L	94.04%	48.68%	53.41%	91.80%	60.53%	56.82%
33BEO1L	93.33%	55.07%	32.47%	81.54%	62.32%	76.62%
34REO1L	88.12%	62.50%	44.12%	89.24%	56.25%	70.59%

4.5 Case Study – STS

4.5.1 07HRO1L

For subject 07HRO1L, both models QDA and RUSBoosts showed almost identical results. Her normal stand-to-sit and sit-to-stand she leaned forward more than other subjects with her chest down. She also used her arms to help her slowly sit down or assist herself up. She would stand up straight before sitting or after standing up before starting to walk. On average it took her 3 seconds to sit down or stand up.

For the other class and standSit class, they were mostly misclassified as sitStand, shaded dark red in Table 4.5-1. Before sitting she leaned forward holding on to her walker or reaching down to hold on to her chair. In extreme cases, the angle of her chest was parallel to the floor. Before sitting down, her chest would already be at an angle instead of starting from a vertical standing position. Another example, she held onto her walker right before she sat down by falling into her seat.

The one instant when the QDA model misclassified sitStand as standSit, occurred when she reached down on the floor right before she began to stand up. The other times when the model misclassified sitStand, she never fully stood up before starting to walk. She either reached forward to grab her walker or reach over to hold on to furniture and continue to walk with her chest down. Overall, both models were able to identify the STS transitional periods, but difficulties were classifying the standSit events.

Table 4.5-1 Subject 07HRO1L ground truth average duration and a number of observations.

Avg GT Duration		Number of Observations		
StandSit	**SitStand**	**Other**	**Stand-Sit**	**Sit-Stand**
0:00:03	0:00:03	2567	30	39

Table 4.5-2 Subject 07HRO1L prediction results from testing the QDA and RUSBoost model.

07HRO1L							
		QDA			RUS		
TRUE	other	75.38%	3.27%	21.35%	71.02%	3.35%	25.63%
	stand-sit	16.67%	50.00%	33.33%	10.00%	53.33%	36.67%
	sit-stand	5.13%	2.56%	92.31%	5.13%	0.00%	94.87%
QDA	**75.34%**	other	stand-sit	sit-stand	other	stand-sit	sit-stand
RUS	**71.17%**	Predicted					

4.5.2 10JBO1L

Subject 10JBO1L had the lowest standSit true positive rates for both models. Looking at subject 10JBO1L predicted results, both QDA and RUSBoost model found all

the same STS transitions, except for a few instances that are shown in Figure 4.5-1 and Figure 4.5-2. These two figures, only show the standSit and sitStand misclassifications. The GT are shown in blue and the QDA results in orange.

Table 4.5-3 Subject 10JBO1L ground truth average duration and number of observations

Avg GT Duration		Number of Observations		
StandSit	**SitStand**	**Other**	**Stand-Sit**	**Sit-Stand**
0:00:02	0:00:02	1940	14	17

Table 4.5-4 Subject 10JBO1L prediction results from testing the QDA and RUSBoost model.

10JBO1L							
		QDA			**RUS**		
TRUE	other	70.62%	3.45%	25.93%	71.55%	1.34%	27.11%
	stand-sit	7.14%	21.43%	71.43%	0.00%	14.29%	85.71%
	sit-stand	0.00%	17.65%	82.35%	0.00%	0.00%	100.00%
QDA	**70.37%**	other	stand-sit	sit-stand	other	stand-sit	sit-stand
RUS	**71.39%**	**Predicted**					

Looking at the first figure, the three GT large blue peaks (sitStand = 2) are where the QDA model misclassified the sitStand (2) as standSit (1), in which the blue peak is covering the short orange peak. The RUSBoost model classified these correctly, therefore not seen in Figure 4.5-2. At the first blue peak, she slightly rocked back and forth twice to gain momentum before standing. She normally does not rock back and forth but uses just her arms to help herself up. One of the last two peaks, she leaned forward more when she stood up from sitting on a couch. The couch was lower than the hard chair she normally sat in. Another time she stood up with her upper body slightly turned to look over her shoulder and start walking right after.

Next, the short blue GT peaks (standSit = 1) are where the QDA model misclassified the standSit (1) as sitStand (2), which was the lowest true positive rate out of dataset 1 subjects. She did sit in a hard chair compared to a couch or a recliner like the other subjects. She also sat down with a straighter posture, using more of her leg muscles

than the other subjects. All, but one standSit was misclassified. The states prior to her sitting down varied more than others. For example, she would reach forward over the table and continue to lean forward before sitting, when normally she had a straight posture. Another time she took steps sideways and sat down without pausing to stand.

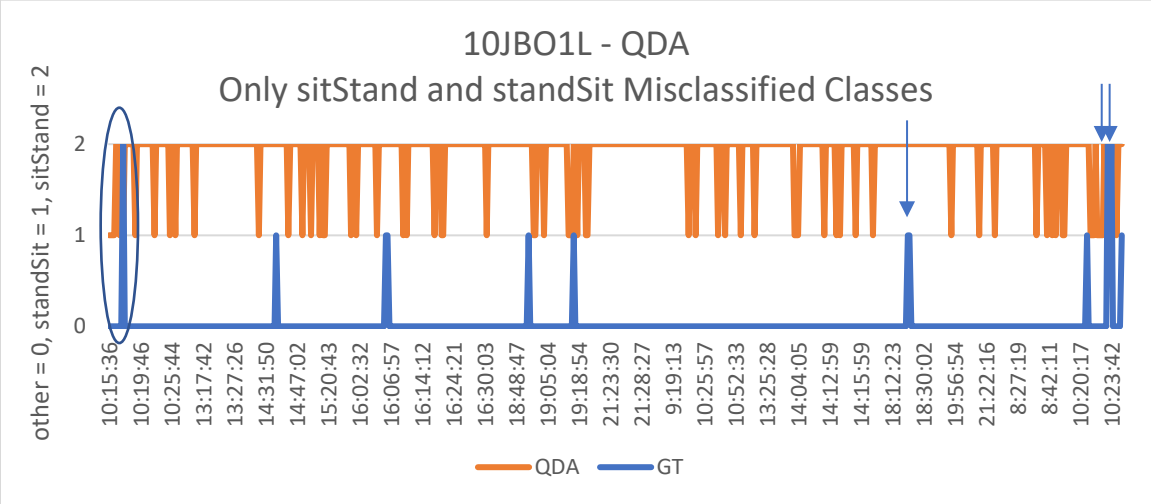

Figure 4.5-1 Subject 10JBO1L predicted QDA sitStand and standSit compared to the GT.

The RUSBoost model misclassified three standSits different from the QDA model. There is one on the left located by the arrow and the two on the right that has the same time. This is possible because the 5-second window was labeled as sitStand or standSit if either was present. In one of these instances, she leaned forward and quickly yank the chair closer to her. Another time she took a step while leaning forward and pulling the chair towards her. Once again, the prior events make a difference.

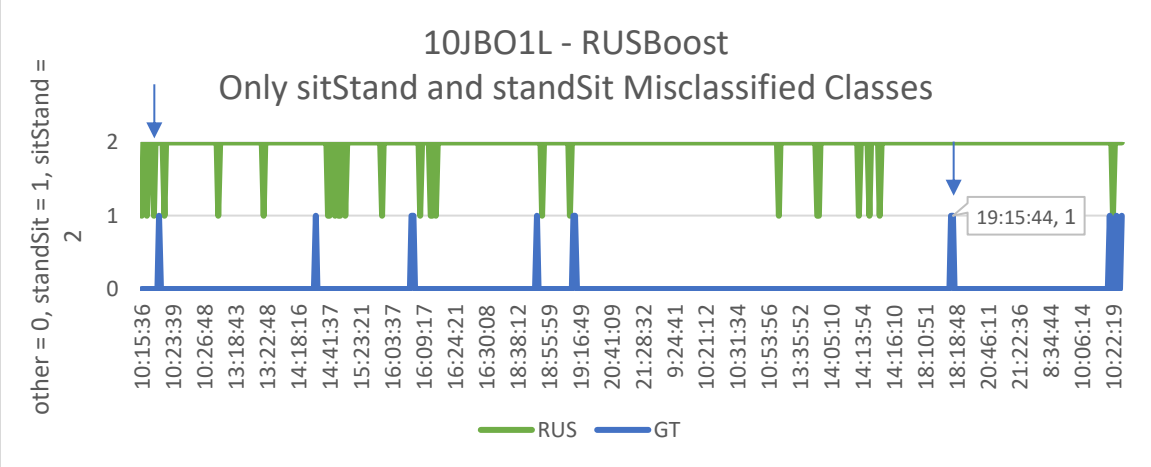

Figure 4.5-2 Subject 10JBO1L predicted RUSBoost sitStand and standSit results compared to the GT. The times are relative to the larger number of misclassifications found using the RUSBoost model than QDA.

4.5.3 13JAO1L / 13JAO2L

Subject 13JAO1L / 13JAO2L had the second to lowest overall test accuracy about 70% for QDA and about 65% for the RUSBoost model. Both data collection session results are shown below for comparison. For his first session, 13JAO1L was the only subject that had a 100% true positive rate for standSit class, but there were only two standSits ground truths observed. The two out of three sitStands were misclassified as standSits, which resulted in the lowest true positive rate of 33.33%. And the other class commonly had a few instances misclassified as sitStand. The confusion matrices are shown in Appendix G.2. Instead, the QDA and RUSBoost misclassification results are shown below for both 13JAO1L and 13JAO2L.

Table 4.5-5 Subject 13JAO1L and 13JAO2L ground truth average duration and number of observations.

Data collection sessions	Avg GT Duration		Number of Observations		
	StandSit	**SitStand**	**Other**	**Stand-Sit**	**Sit-Stand**
13JAO1L (34 hours)	0:00:01	0:00:03	2038	2	3
13JAO2L (24 hours)	0:00:02	0:00:02	1695	10	11

Subject 13JAO1L normally sat in his recliner chair that was out of the depth sensor's view. When he sat down and stood up, he typically had a moderate forward lean,

used both hands on his knees for assistance, or held onto something for stability like a table. The sitStand and standSits observed during the first data collection were from two different chairs. The first one was from when he sat at his dining table in a hard leather chair with wheels. As mentioned above for both the QDA and RUSBoost model, the sitStands were misclassified as standSits indicated by the large blue GT peaks. Before standing he rolled counter-clockwise 90 degrees, leaned forward, and held on to the kitchen counter close by. The second chair was a leather reclining chair, but different from his main chair. He did not recline back, but it took two attempts to stand up by leaning forward and using his arm to push off his knees.

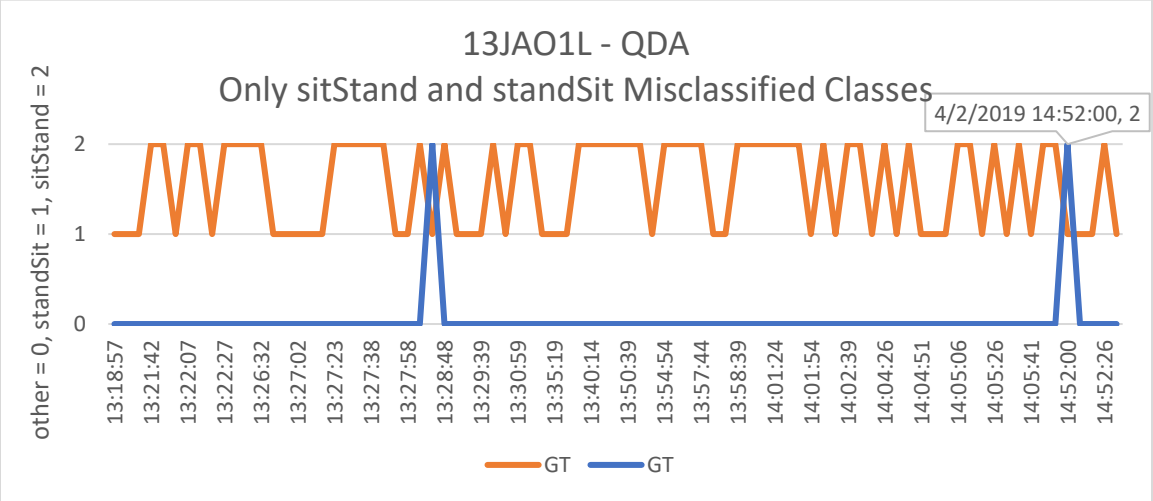

Figure 4.5-3 Subject 13JAO1L QDA misclassified sitStand and standSit. See Appendix G.2 for more detail

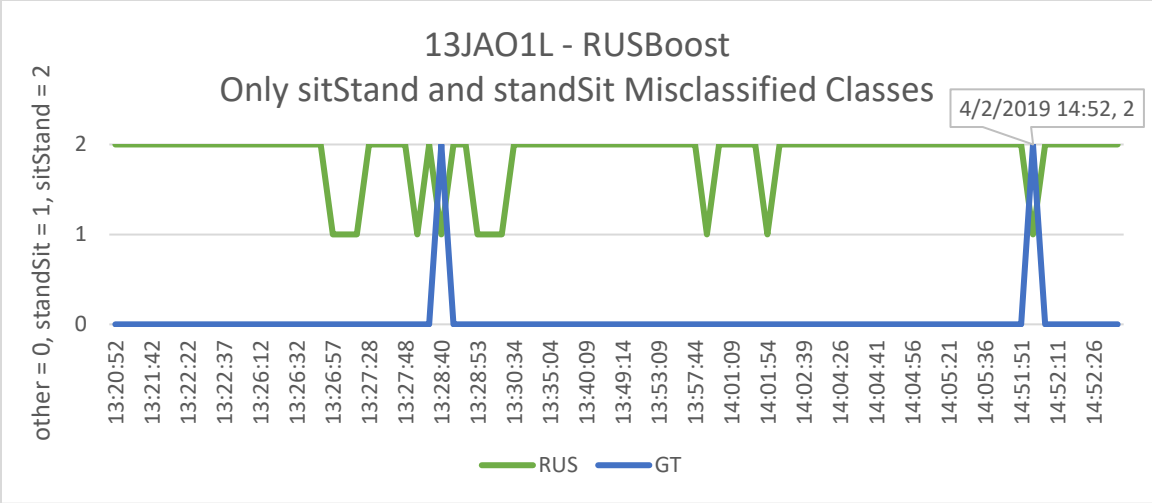

Figure 4.5-4 Subject 13JAO1L QDA misclassified sitStand and standSit. See Appendix G.2 for more detail.

For his second session, the STSs were only observed when he sat in the leather rolling chair at the kitchen table. The standSit class showed a slightly lower true positive rate of 80%, but a 90.91% rate for the sitStand class. That is almost a 60% increase from his first data collection session for the sitStand class. Both the QDA and RUSBoost misclassified two standSits located by the GT peaks below. In the first two instances, he took a side step, leaned extremely far forward with his chest about parallel to the floor, and the chair rolled slightly. The last instant is where the models misclassified one sitStand as standSit. Here his chest was forward, but he twisted his upper body and held onto the table for support. After standing he continued to lean forward. Overall, both models were able to identify the STS periods even with a limited number of observations.

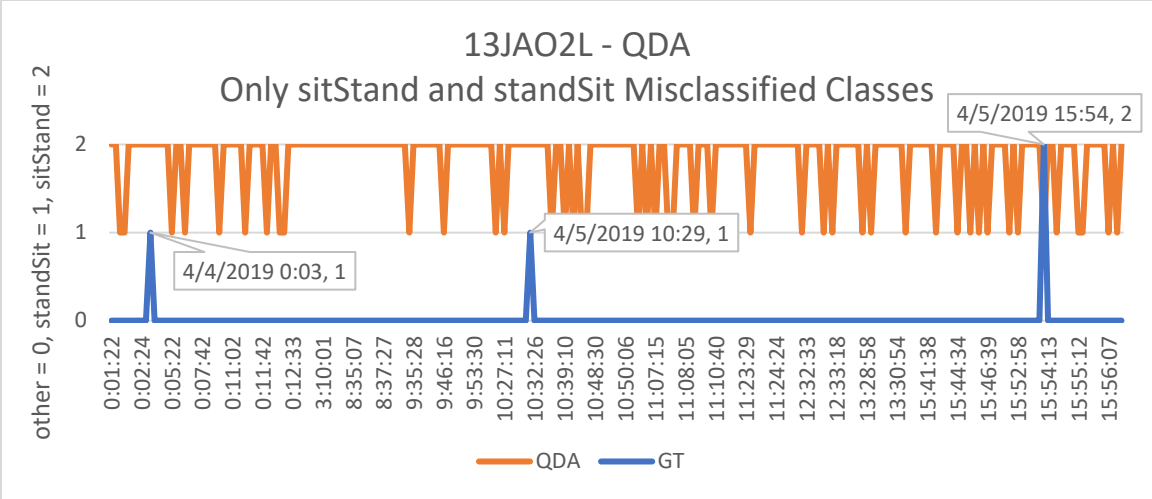

Figure 4.5-5 Subject 13JAO2L QDA misclassified sitStand and standSit. See Appendix G.2 for more detail.

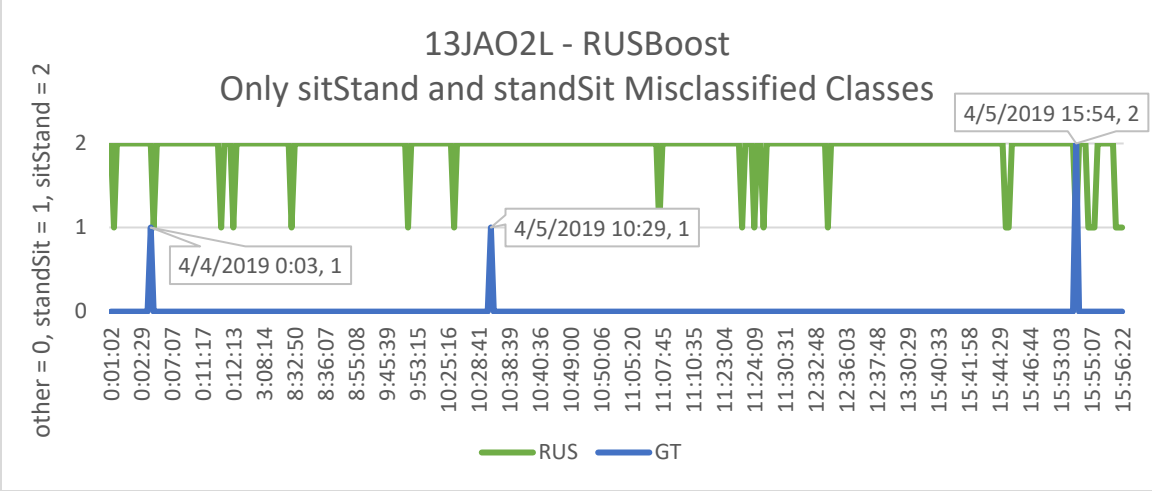

Figure 4.5-6 Subject 13JAO2L RUS misclassified sitStand and standSit. See Appendix E.4 for more detail.

4.5.4 29SSO1L

Subject 29SSO1L sitStand and standSits were difficult to view from the depth sensor due to low visibility. She sat in a gliding rocking chair that moved forward and backward. There were only two times she sat on the couch. One of them the RUSBoost model misclassified a sitStand as standSit. Oddly, this looks like a normal sitStand. She leaned forward and stood up with a moderate speed. But the other sitStand that was classified correctly, she sat on the rocking chair and stood up with a normal forward lean.

From the RUSBoost model, half the standSit class was classified as sitStand. The other half was correctly identified. During these times she moderately leaned forward and sat down quickly causing the rocker to move after sitting. This was also seen with the QDA model, where only two standSits were misclassified as sitStand or the other class. Overall subject 29SSO1L had some of the lowest true positive rates, especially seen with the RUSBoost model. The common cause was the rocking chair, which moved forward and back after sitting.

Table 4.5-6 Subject 29SSO1L ground truth average duration and the number of observations.

Avg GT Duration		Number of Observations		
StandSit	**SitStand**	**Other**	**Stand-Sit**	**Sit-Stand**
0:00:01	0:00:01	1042	8	3

Table 4.5-7 Subject 29SSO1L prediction results from testing the QDA and RUSBoost model.

29SSO1L							
		QDA			**RUS**		
TRUE	other	78.21%	2.69%	19.10%	48.37%	9.02%	42.61%
	stand-sit	12.50%	62.50%	25.00%	0.00%	50.00%	50.00%
	sit-stand	33.33%	0.00%	66.67%	0.00%	33.33%	66.67%
QDA	**78.06%**	other	stand-sit	sit-stand	other	stand-sit	sit-stand
RUS	**48.43%**	**Predicted**					

4.5.5 31FSO1L

Subject 31FSO1L sits in a recliner chair that also rocks. He normally leans forward before sitting and standing. To stand, he uses his cane and one armrest to help stand or sit down. The results between the QDA model and the RUSBoost model vary more than the previous four subjects. The RUSBoost had a higher sitStand true positive case than the QDA model that had a rate of 54.17%. Oppositely, the QDA model had a higher standSit true positive rate than the RUSBoost model that had a rate of 30.43%.

The sitStands for the QDA model were misclassified as either the other class or standSit class. At these instances, he either leaned forward more than usual or took multiple attempts to try to stand up which caused the same sitStand to show up twice. This was previously seen with subject 10JBO1L. The standSit class was mostly misclassified by the RUSBoost model as sitStands. He either turned his upper body to look behind him to check where he was going to sit or reach down to hold on to the armrest for support along with his cane. Occasionally, he would fall into his recliner chair, which caused it to rock back and forth, which is a similar motion to how some older adults stand up.

Table 4.5-8 Subject 31FSO1L ground truth average duration and the number of observations.

Avg GT Duration		Number of Observations		
StandSit	**SitStand**	**Other**	**Stand-Sit**	**Sit-Stand**
0:00:02	0:00:03	1561	23	24

Table 4.5-9 Subject 31FSO1L prediction results from testing the QDA and RUSBoost model.

31FSO1L							
		QDA			**RUS**		
TRUE	other	74.82%	3.07%	22.10%	75.59%	0.51%	23.89%
	stand-sit	8.70%	73.91%	17.39%	13.04%	30.43%	56.52%
	sit-stand	20.83%	25.00%	54.17%	20.83%	0.00%	79.17%
QDA	**74.50%**	other	stand-sit	sit-stand	other	stand-sit	sit-stand
RUS	**75.00%**	Predicted					

4.6 Summary and Discussion

Reviewing other studies, there is a wide range of accuracies being reported. The higher accuracies are typically conducted in a research or clinical environment with younger subjects [33],[34], [35]. The lower accuracies were conducted in real living environments [27], [28], [31]. One study that was performed in a real living environment, used a hip-worn accelerometer and trained their model using a random forest classifier.

They reported accuracies for sit-to-stand 52% and stand-to-sit 51% [27]. Another study used an accelerometer and gyroscope placed on the lower back. They used a combination of signal processing techniques to identify STS, which includes analyzing the signals using a discrete wavelet transformation (DWT), a six-degrees-of-freedom fusion algorithm, and vertical displacement estimation. They reported overall accuracies of 85% for older adults used the combination of title angle estimation.[26].

Overall, both the QDA and RUSBoost model in this study performed well with an average test accuracy computed from each subject of 89% for dataset 1 and 86% for dataset 2. The QDA had slightly higher accuracies and it was quicker to train, which was about 11 seconds. Even though RUSBoost only took about 40 seconds to train, a simpler and quicker model is best for low powered accelerometers to minimize battery consumption. The other category typically had high performance around 90%. There were significantly more observations for this class. Most of these other activities were either sitting or walking. Sitting is easier to classify since it is a stationary activity that produces a constant signal and normally has longer durations. Walks are non-stationary but also are longer in duration than STS. As seen in the step detection section, walks and steps have a unique cyclic pattern, but with older adults, their gaits vary a lot.

Both models were able to find almost all the sit-to-stands and stand-to-sit events. These postural transitions had a unique waveform in the accelerometer signal different from other class activities. However, comparing stand-to-sit to sit-to-stand the accelerometer signals were similar. Most of the misclassifications were between the two classes. For example, the stand-to-sit were misclassified as sit-to-stand and vice versa. Earlier shown, subject 07HRO1L extremely leaned forward and subject 10JBO1L had a

straighter posture during these STS transitions. Occasionally the way they sat down or stood up changed causing misclassification. The stand-to-sit class was the hardest to classify. The most variation occurred prior to sitting. This indicates the importance of identifying the preceding events.

For future work, implementing different features like angular velocity correlated with the duration of continuous states may increase the performance of finding the STS periods [36], [37],[9]. Another improvement to the STS algorithm may use a post validation process using a steady-state machine that defines states based on an event or a sequence of events before sit-to-stand or stand-to-sit. The order of when the person sits is an important feature because the sitting time is typically longer than these postural transitional movements. For evaluation, considering which subject rocks back and forth or takes several attempts to stand up could help understand the results from the model for each person. And lastly, computing several different output features such as the total STS durations, trunk angles, and angular velocity would be valuable information to detect changes over time.

5 Motion Density – Accelerometer Based

5.2 Background

Monitoring physical activity is a common way to get insight into a person's overall level of health. As stated in an article in a sports medicine section of the Springer Journal, physical activity is movement, and energy expenditure is defined as "a reflection of gender, age, and body mass, in addition to movement and efficiency of movement [7]. Sensors can provide continuous monitoring of various health information that can give insight into daily functional patterns. The current in-home systems at facilities like TigerPlace captures motion density using four motion sensors to track activity level over time [7]. And motion density is a set of motion over a unit of time. To accurately measure activity density in a home, the time the home was vacant was detected. Further details of how time away from home (TAFH) was determined is explained in the next section.

An in-home motion sensor network is not able to identify individual activity levels when there are multiple people living in the same space or visitors. And activity outside of the home can only be tracked using personal activity trackers or mobile devices that can track activity. However, there are several limitations to using a mobile device, such as the person must always have it with them. For this study, we used the ActiGraph to capture motion density. The overall goal is to determine a person's daily level of activity and detect any changes from the norm. The data collected for this research is not long enough to determine significant changes. This thesis uses the current motion sensor system and ground truths obtained from the depth sensor videos to compare the motion density computed using the ActiGraph accelerometer signals.

5.3 Method

The depth sensor was used to classify stationary versus non-station events. From the short amount of daily physical activity among elderly adults, the non-stationary events captured from the ActiGraph accelerometer in the z-direction were mostly walking events. Also, the non-stationary events had to be at least 10 seconds or more to be detected by the ActiGraph. The ground truths were labeled as walking times when the subject was in view of the depth sensor. Walking events were counted when a person took three or more steps. Again, these are non-stationary events that were used to calculate motion density.

Motion density calculated from the ActiGraph was based on the number of active instances over a unit of time. For example, each hour the person was in view of the depth sensor the number of active minutes was totaled. The ground truth was calculated similarly but with the total number of labeled walking instances every hour. At mentioned before, the motion sensor density was computed as the number of all motion sensor hits during an hour divided by the time at home during that hour [38].

The ground truth of only walking periods was compared to the ActiGraph motion density. Also, the ground truth is compared to the density motion computed from the Zigbee motion sensors. Below is the table, which shows an outline of the data used in this section.

Table 5.3-1 A list of motion density data used for comparison.

Data	**Motion Density Metric**
Ground Truth (labeled data)	Labeled walking instances (events)
ActiGraph Accelerometer	Detected activity instances
Motion Sensor (Zigbee)	Detected motion hits every 7 seconds

5.4 Overall Results

The results in this section compare daily motion density from the ground truth and ActiGraph data to the motion sensor density. First looking at dataset 1 in Figure 5.4-1, the top three subjects 02BCO1L, 03BHO1L, and 06DHO1L had the highest amount of activity detected from the ActiGraph and GT. But looking at Figure 5.4-2, the motion sensors detected the least amount of motion for these three individuals. Subject 03BHO1L sat in the living room or would walk to the kitchen, but his living room motion sensor was not working at the time. Therefore, the motion sensor density did not accurately show his level of activity. Now looking at the motion sensor results first, 05LBO1L, 07HRO1L, and 11ASO1L had the highest densities, while looking at the GT and ActiGraph they had some of the lowest densities.

Overall the ActiGraph accelerometer resulted in lower densities than the GT in dataset 1, but relatively the moving average was similar. There were a few exceptions, such as 07HRO1L and 09HSO1L had significantly lower ActiGraph densities than the GT. And comparing the GT and ActiGraph, there were a few major differences in the moving averages caused by the six subjects previously mentioned.

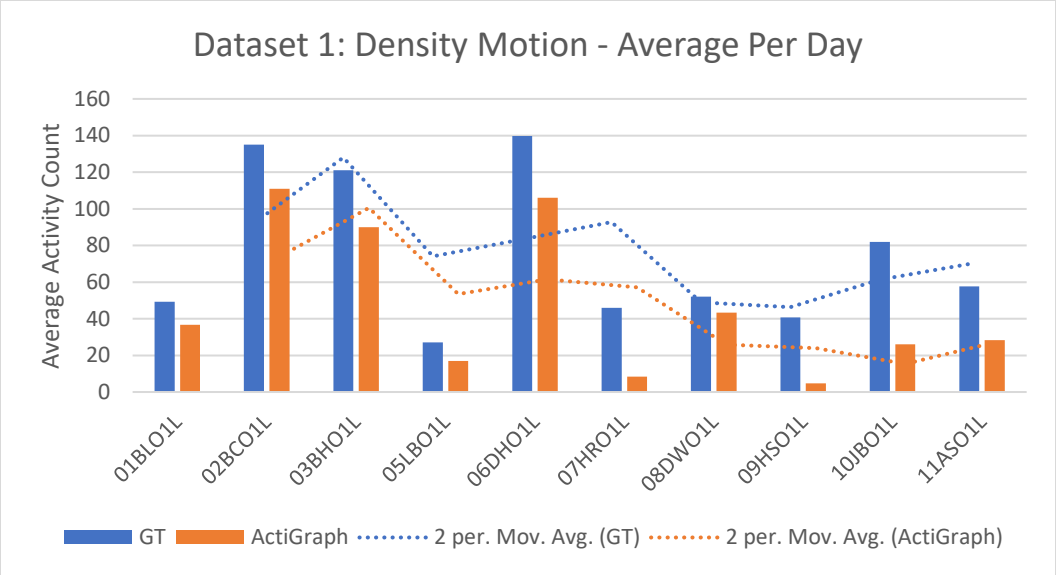

Figure 5.4-1 Dataset 1 overall motion density per day from the GT and ActiGraph accelerometer. GT and ActiGraph has a similar trend.

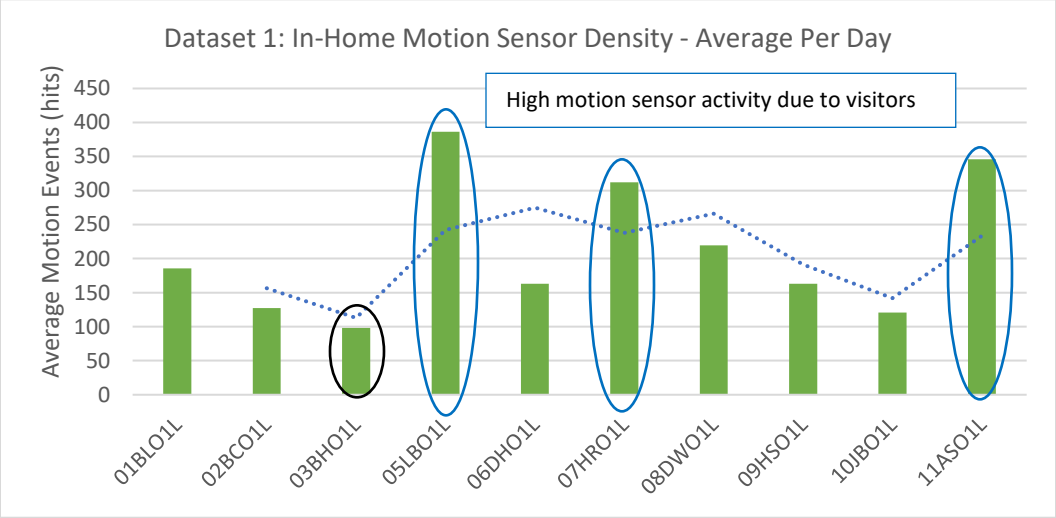

Figure 5.4-2 Dataset 1 overall motion density per day from in-home motion sensors that fire every 7 seconds (sensor hits) when it detects movement. The blue circles show the motion sensors have high density motion vs GT & ActiGraph. Subject 03BHO1L had inactive bedroom and living room motion sensor.

From dataset 2 in Figure 5.4-3, looking at both the GT and ActiGraph, subjects 13JAO1L and 27CHO1L had a higher density than detected from the motion sensors. There were a few cases where the ActiGraph showed higher densities than the GT, such as 13JAO1L, 18RCO1L, 25EHO1L, and 27CHO1L. Oppositely, there were cases where the Actigraph showed significantly lower densities than the GT, such as with 15LOO1L,

31FSO1L, and 33BEO1L. Overall the moving averages were similar between the GT and motion sensors but slightly less similar compared to the ActiGraph.

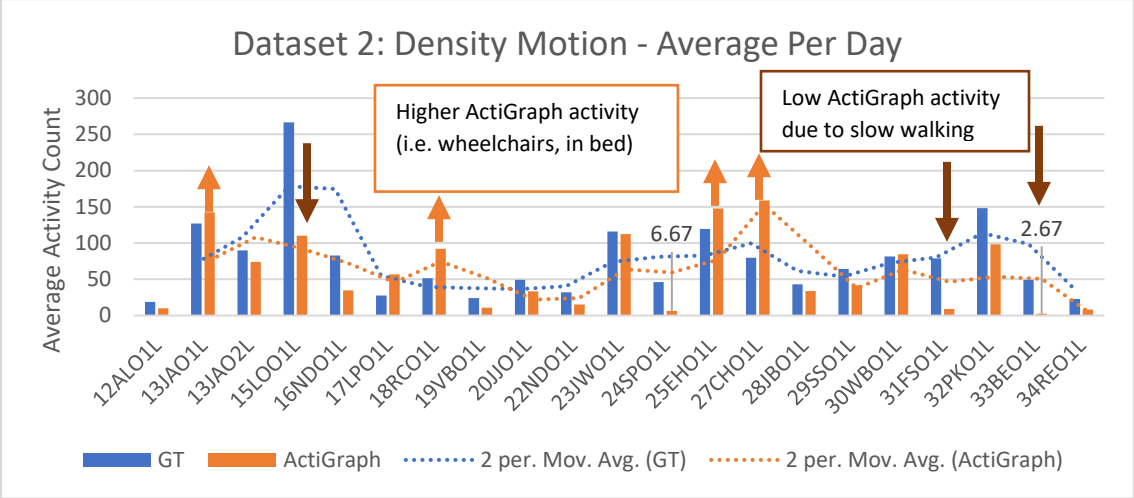

Figure 5.4-3 Dataset 2 overall motion density per day from the GT and ActiGraph accelerometer. The orange arrows show higher ActiGraph motion than GT. And the brown arrow show the ActiGraph lower than the GT

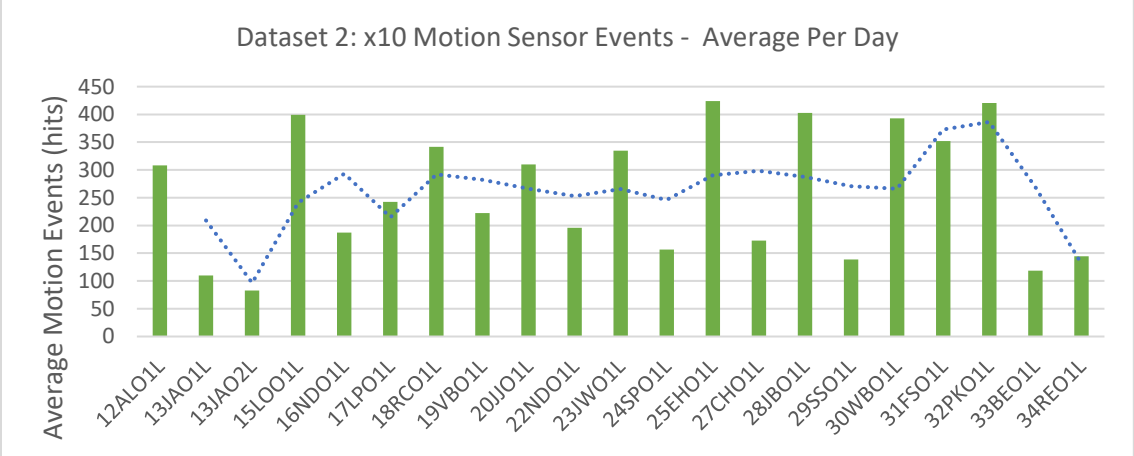

Figure 5.4-4 Dataset 2 overall motion density per day from in-home motion sensors that fire every 7 seconds (sensor hits) when it detects movement.

5.5 Case Study – Motion Density

The case studies shown below looks at the motion density on an hourly precision. The subjects chosen were based on the special cases mentioned above to represent similar situations.

5.5.1 Case 1: Subject 05BLO1L

Subject 05BLO1L showed high motion sensor density compared to the GT and ActiGraph results. The GT and ActiGraph accelerometer motion densities were similar, but the ActiGraph was still slightly less dense. Looking closer at the individual hours, the ActiGraph there was one significantly higher density on the second day at 9:00 located by the red arrow. The ground truth reported no motion and the motion sensor detected some motion, but not the highest. The reason for the large differences was caused by her doing sit-to-stand and stand-to-sit exercises consecutively. Even though individually these movements are only a few seconds, as a set of events the ActiGraph and living room motion was able to detect the movements. Now, the reason for the motion sensors having a higher density was caused by the visitors. She had a person with her during the day to help and there were multiple staff entering and exiting for short periods.

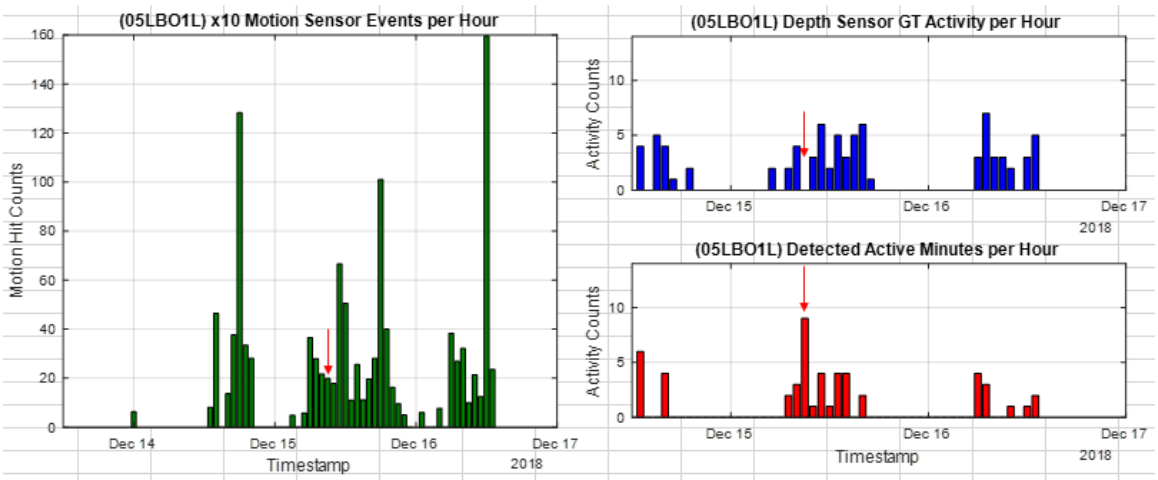

Figure 5.5-1 Subject 05LBO1L motion density results per hour from the motion sensors (left – green), GT (top right - blue), and ActiGraph accelerometer (bottom right – red).

5.5.2 Case 2: Subject 33BEO1L

Subject 33BEO1L had very low ActiGraph motion density and a relatively large difference between the Actigraph and GT. The ActiGraph density was very sparse, also observed from 15LOO1L and 31FSO1L who were mentioned earlier. Most likely the ActiGraph did not detect activity because her slow walks were not considered at least 10 seconds. She took only a few steps at a time before taking more. Throughout the day she sat in her chair or got up to either go to the bathroom or to leave for a meal.

The motion sensors detected more activity than both the GT and ActiGraph. This was partly due to the bedroom and bathroom motion not being filtered out. There were a few times when there was only a visitor in the apartment when she left. For example, on the first day at 14:00 located by the red arrow.

Looking at the third day at 7:00 located by the dashed green arrow, the ActiGraph had a higher motion density than the GT. Only one walking event was labeled as GT and was about 10 seconds. However, the ActiGraph was most likely detected when she sat in her wheelchair and she was being pushed by the nurse. The nurse repeatedly started to

push the wheelchair for a few seconds then stopped about four times before they both left the apartment. Overall, the few hours the ActiGraph detected active events there was GT and the motion density.

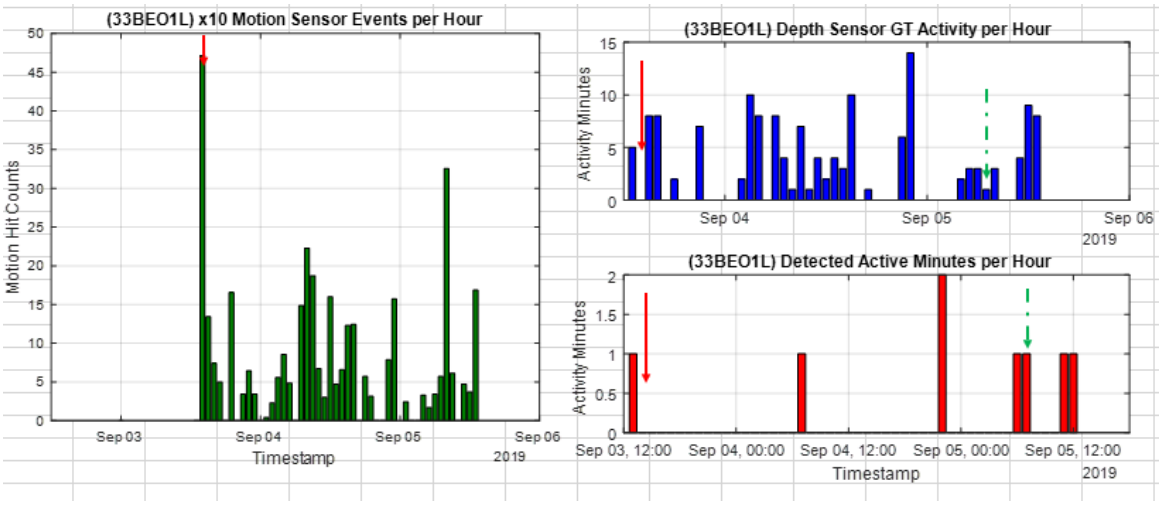

Figure 5.5-2 Subject 33BEO1L motion density results per hour from the motion sensors (left – green), GT (top right - blue), and ActiGraph accelerometer (bottom right – red).

5.5.3 Case 2: Subject 27CHO1L

Subject 27 was mostly in bed for all three days. She had most of her meals brought to her apartment, except in the morning. The times she was out of bed, included walking to the bathroom or in the living room to get the food that was delivered. The first night at 20:00 located by the red arrow, she was in bed the entire hour. Based on watching the depth sensor videos, she moved the most during the beginning of this hour. She leaned over to reach something a few times and switched sides she was laying on several times. The bedroom motion sensor across the room was able to detect motion. During this hour there was no GT recorded and the ActiGraph motion density was low. All the blue dotted circles identify the times when she was in bed and there was motion density for the bedroom motion sensor and ActiGraph. But again, there was a lack of GT recorded.

The last two hours located by the red circle showed similar motion densities for the ActiGraph and motion sensors. Looking at the last hour, the motion sensor density was higher because she had a visitor. The ActiGraph was mostly higher because she performed a few sit-to-stands consecutively and exercises in the bed by rolling side to side. Overall, 27CHO1L motion densities produced by the ActiGraph and motion sensors were similar.

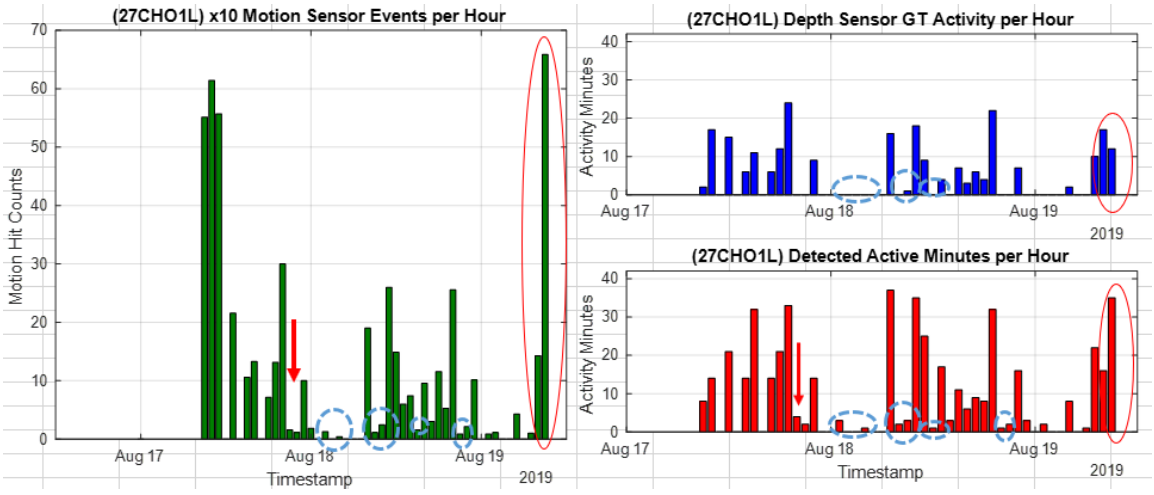

Figure 5.5-3 Subject 27CHO1L motion density results per hour from the motion sensors (left – green), GT (top right - blue), and ActiGraph accelerometer (bottom right – red).

5.6 Summary and Discussion

Overall, the ActiGraph showed similar levels of motion density as the GT, but most importantly the in-home motion sensors. However, the results showed that if there is more motion caused by the visitor, the motion sensor density would not be a good representation of their overall activity levels as seen with 05BLO1L and 33BEO1L. Therefore, a wearable sensor would provide a better option for environments with multiple people or frequent visitors.

For all subjects in dataset 1, the ActiGraph resulted in lower densities than the ground truth. This was not a surprise because the ActiGraphs are sensitive to activity

produced at least 10 seconds, which were mostly walking events. For dataset 2, 13JAO1L, 17LPO1L, 18RCO1L, 25EHO1L, and 27CHO1L had slightly higher motion densities from the ActiGraph than the ground truth. As explained by the three cases, it is possible to produce activities that are non-walking events. Specifically, the ActiGraph had a higher motion density when subject 05LBO1L and 27CHO1L performed short consecutive movements like sit-to-stand and stand-to-sits.

For future work, the motion sensor density should be computed in a related way to the ActiGraph for a better comparison. The motion sensor hits should be added each hour, but only during the time, the subject was in view of the depth sensor divided by the time they were in view during that hour.

6 Vacancy Detection

6.2 Background

Detecting vacancy along with capturing motion density helps estimate a person's daily level of activity. It has been estimated that older adults spend 60% of their day sitting [7]. If the subjects in this study were not sitting in their favorite chair, they left their apartment to eat a meal or attend an activity. Most of the apartments were studios or one-bedroom that did not allow for a lot of room to walk around. There were four motion sensors. One placed in the bathroom, bedroom, living room, and on the ceiling above the front door.

The current vacancy algorithm developed by S.Wang uses the motion sensor data was based on the old x10 motion sensor system that fired every 7 seconds [7]. This algorithm tracks whether each sensor event is a front door sensor or another sensor like a bedroom or bathroom. The time away from home (TAFH) is the entire duration of continuous chronological front door sensor events. The final decision uses a fuzzy logic system to calculate confidence when the apartment was vacant. Ideally, the duration of the door sensor events before leaving and after returning should be a lot shorter than the duration of no sensor events to be call TAFH.

In the future, the goal is to use the true firing of the Zigbee motion sensor system that only captures the start time when motion is first detected and end time when there is no motion without the extended firings in between. No motion is when there is no differential change between the two IRs embedded in the Zigbee sensors, such as heat given off from a person's body. There have been concerns with the accuracy of the current system since switching to a new one. Along with the motion density, the vacancy

algorithm can give insight into ambiguous sensor-based parameters. For example, when motion density decreases within the apartment during the day, it may look like a person is less active. In facilities like TigerPlace, the caveat could be fewer caregivers entering because the person started feeling better.

6.3 Method

The vacancy algorithm proposed in this thesis uses crisp decision results with a steady-state machine approach to determine the start and ending TAFH periods. Figure 6.3-1 illustrates the three main states for motion sensor events; front door, no motion, and other motion that includes bedroom and living room motion events. There can be continuous motion sensor events, such as if a person continuously stands in the doorway or walks around in their apartment a lot.

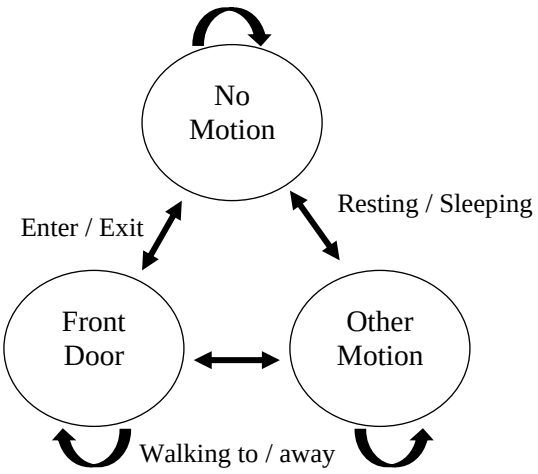

Figure 6.3-1 Steady-state diagram shows the three main motion sensor events in an apartment.

The proposed vacancy algorithm is described in Figure 6.3-3. For the purpose of testing, the algorithm was tested offline using motion sensor data between each subject's data collection. The Figure 6.3-2 shows an example of a vacancy detection sequence from subject 01BLO1L.The TAFH for this proposed algorithm is the duration between the end time of the first front door motion event and the start time of the next front door

motion event, shown by the short orange bracket. There must be prior other motion before exiting and other motion after returning, shown by the green brackets. Also, the apartment must be vacant for at least a threshold of 1.5 minutes. This threshold is longer than if someone steps out of the apartment for a few seconds. Also, the time between the last front door motion event right before exiting and entering, must be greater than the threshold. This reduces short front door motion events that cause false positives.

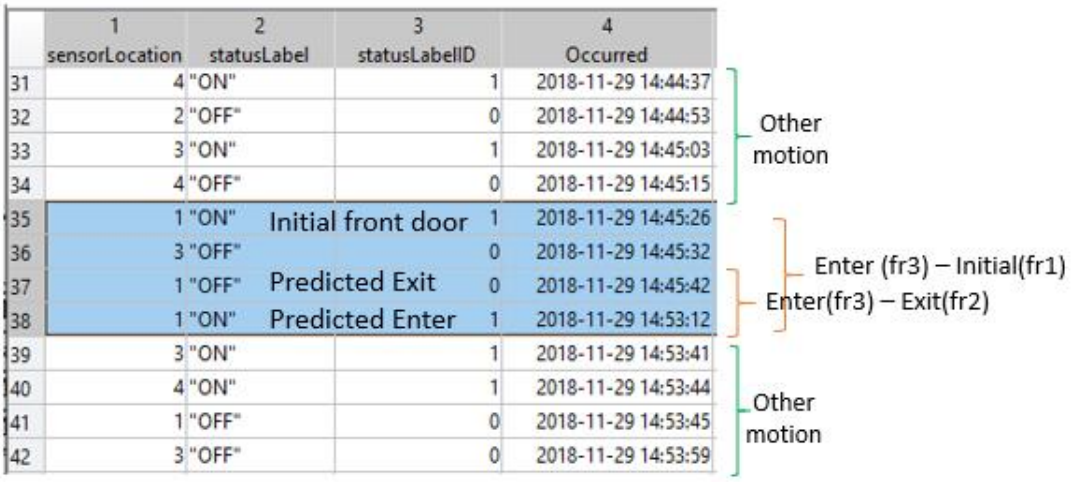

Figure 6.3-2 Example of proposed vacancy detection sequence from subject 01BLO1L. The green brackets show there was other motion prior to exiting and after entering her apartment. The long orange bracket is the duration between the predicted enter and initial front door motion event. The short orange bracket is the duration between the enter and exit times.

Proposed Vacancy Algorithm:

For k = BeginDetection : EndDetection

1) Find other motion prior to exitTime. OtherMotion = k
2) Find the initial front door event with the ON status. fr1 = k.
3) Find the front door event (k) with the OFF status. fr2 = k. This is the possible exitTime.
    a. **If** the next (k+2) motion even is the front door and the status is ON
        i. **If** there are continuous front door motion hits find the last front door event in sequence. **Then** fr3 = k. This is the possible enterTime.
        ii. **If** there is NOT continuous front door motion hits. fr3 = k. This is the possible enterTime.
    b. **If** the duration proposed enterTime (fr3) – initial front door (fr1) and proposed enterTime(fr3) – exitTime(fr2) are greater than the threshold (TR). **Then** record enterTime (fr3) and exitTime (fr2).
        i. proposed enterTime (fr3) – initial front door (fr1), this avoids short front door hits. And calculate the duration.
4) Check **for** other motion event hits prior to exitTime
    a. **If** there is no motion prior to exitTime, **Then** remove the predicted exitTime and associated enterTime
5) Check for other motion event hits after exitTime
    a. **If** there is motion after exitTime, **Then** remove the predicted exitTime and associated enterTime

End

Figure 6.3-3 Proposed vacancy algorithm using Zigbee start and end motion sensor events only.

The current S.Wang algorithm and the proposed algorithm results were compared to the ground truth labels that were manually recorded from the depth sensor videos. These labels consisted of times when the resident entered and exited their apartment. Any ground truth times or times detected from the current algorithm under the minimum threshold were eliminated.

Table 6.3-1 Vacancy detection algorithm dataset and ground truth metrics.

Data	**Metric**
Ground Truth	Labeled Exit/Enter Times
S.Wang Vacancy (current)	Motion sensor hits every 7 seconds
Proposed Vacancy (Zigbee)	Motion sensor start time & end time

A few subjects, unfortunately, had technical difficulties with their motion sensors during the collection periods. For the vacancy section, the individuals without motion sensor data were not included. From dataset 1, only subject 02BCO1L had missing data. For dataset 2, subject 13JAO1L/13JAO2L, 15LOO1L, and 33BEO1L.

6.4 Results

Figure 6.4-1 and Figure 6.4-2 demonstrates an overall performance of both the current algorithm and proposed algorithm against the ground truth. The average TAFH durations below were calculated from each subject's total TAFH per hour. If the algorithms had a perfect performance the durations would match, like 05LBO1L, 07HRO1L, and 32PKO1L. For dataset 1, 03BHO1L, 06DHO1L, 08DWO1L, and 11ASO1L had the largest differences from the ground truth. The details of these specific cases are discussed in the case study section 6.5.

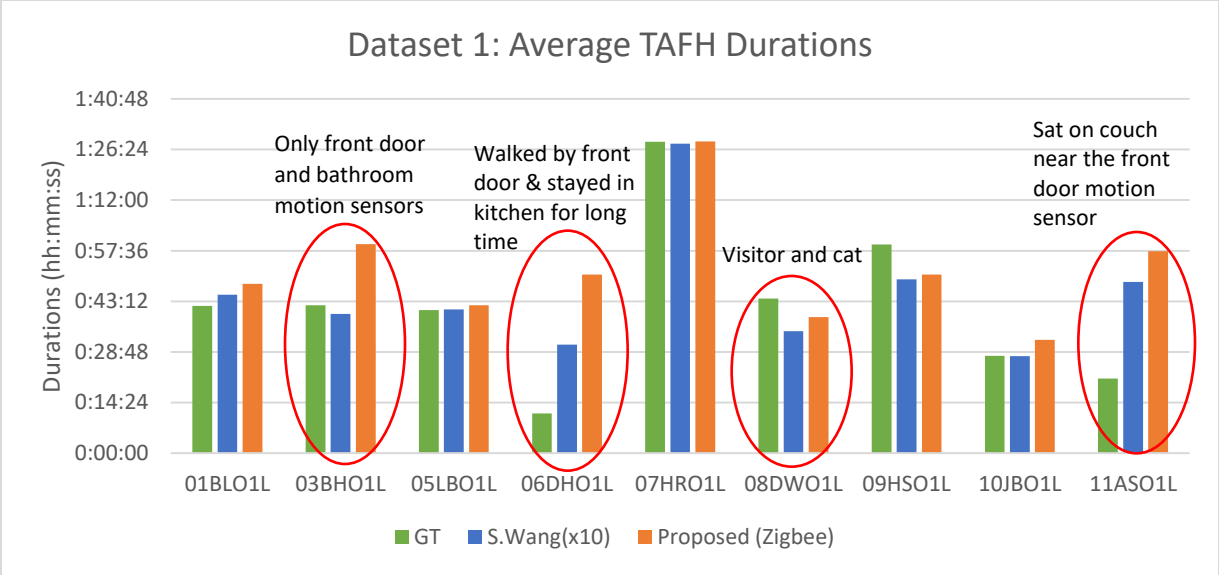

Figure 6.4-1 Dataset 1: Average TAFH durations with respect to hourly precision.

For dataset 2, 18RCO1L, 19VBO1L, 20JJO1L, 22NDO1L, 25EHO1L, 28JBO1L, and 34REO1L had the largest differences compared to the ground truth. Some of the common pitfalls were visitors interrupting the common TAFH sequences or inefficient motion sensor placements. Also, another weakness of the proposed algorithm is that it would record the enter time as the last front door motion sensor in series right before it detected other motion in the apartment. Most of the time this occurred when there was continuous front door motion due to someone standing in the doorway or frequently walked past the door without triggering other motion sensors.

The residents from dataset 2 that had several visitors include, 18RCO1L and 19VBO1L. Subject 20JJO1L main rolling desk chair is right by the front door, where he spends a lot of time. Sometimes it was difficult to tell if he left his apartment because the front door was not in view of the depth sensor frame. For subject 34, two out of four TAFH were interrupted by a visitor entering the apartment from the patio door without a motion sensor.

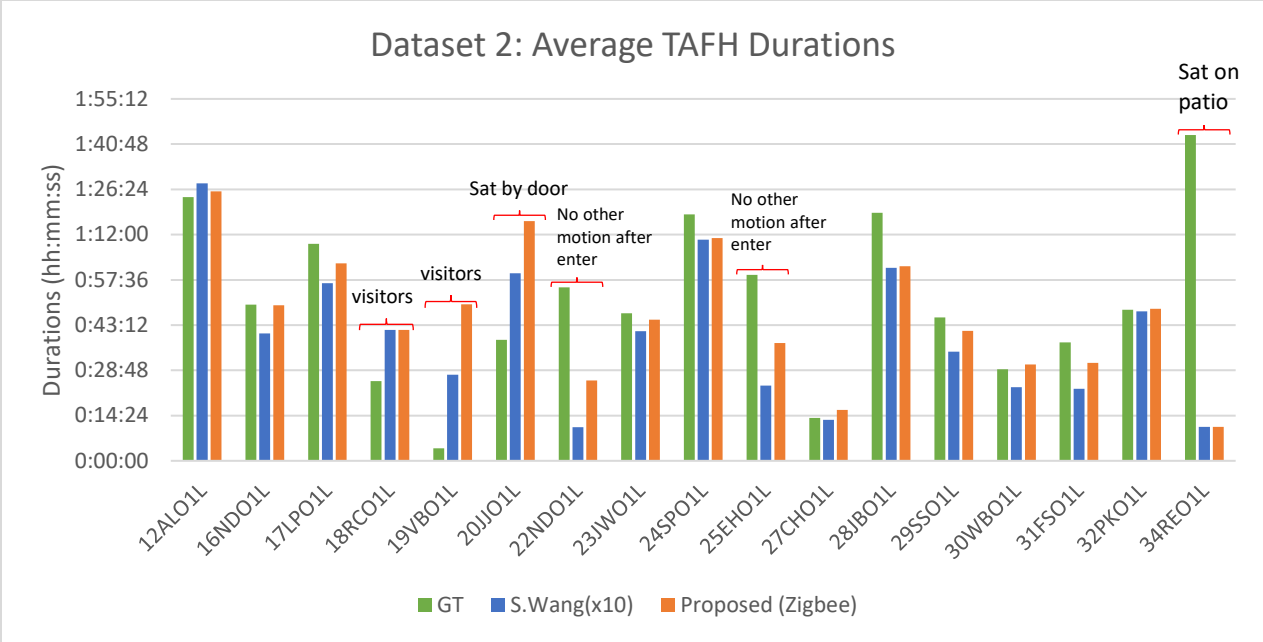

Figure 6.4-2 Dataset 2: Average TAFH durations with respect to hourly precision.

6.5 Case Study – Vacancy Detection

6.5.1 Case 1: 03BHO1L

Subject 03BHO1L unfortunately only had the front door and bathroom motion sensors active during the data collection period. Therefore, an exitTime or enterTime was only counted if there was prior bathroom motion or post bathroom motion after he entered. If he did not go to the bathroom after entering the apartment, the vacancy algorithms both would miss the times he entered his apartment. This is seen in Figure 6.5-1, where both the current algorithm is shown in blue and the proposed algorithm is shown in orange are missing TAFH durations at hours 15:00 and 17:00 on December 10th, 14:00 and 15:00 on December 11th, and 13:00 on December 12th. For the proposed algorithm where the durations were significantly longer at 10-Dec 17:00, 11-Dec 18:00, and 12-Dec 8:00 the algorithm searched for the next motion other than the front door, which was only the bathroom. Sometimes 03BHO1L would not enter the bathroom hours after entering his apartment. Also, the proposed algorithm's recorded the last front door

event in series right before the other motion sensors were detected rather than recording the first front door event.

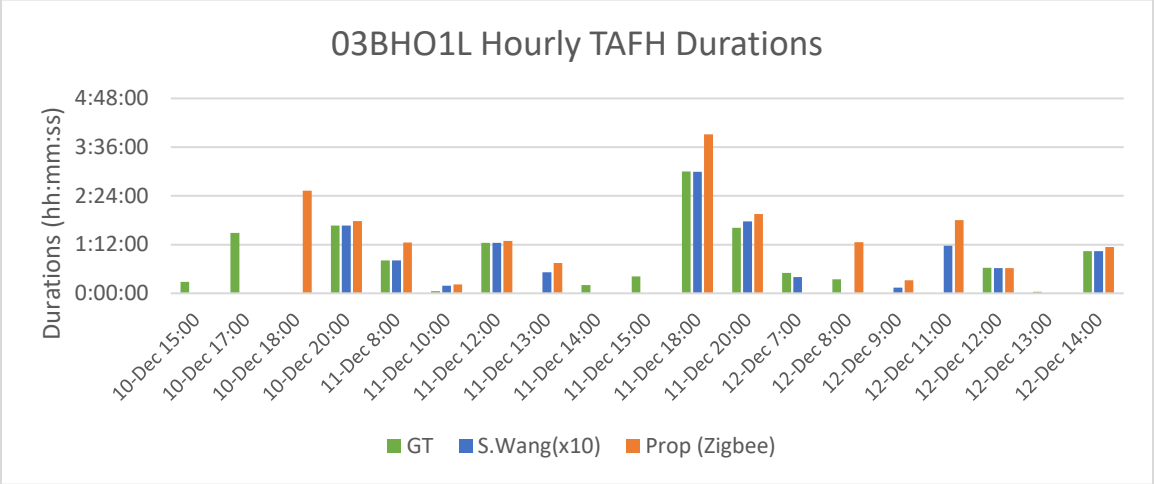

Figure 6.5-1 Subject 03BHO1L hourly TAFH durations.

6.5.2 Case 2: 06DHO1L

Subject 06DHO1L has a larger apartment, shown in Figure 6.5-3. He mainly left his apartment for dinner and rarely there were visitors. The proposed algorithm found almost all the same enter times that the current algorithm detected, but the exit times are sometimes detected earlier. Opposite from before, the proposed algorithm would record the first exit time in series instead of the last exit time. Both the current and proposed algorithms detected more TAFH than the ground truth, as seen in Figure 6.5-2. The proposed algorithm did detect a similar exit time as the ground truth on 12-Feb 18:00. The entered time was not detected because there were no other motion sensors detected except for the front door. This also explains the large time difference on 12-Feb 21:00 because the TAFH continued. Another reason for the false positives was because he frequently walked past the front door into the kitchen and would stay there for long periods of time, which looked like he left.

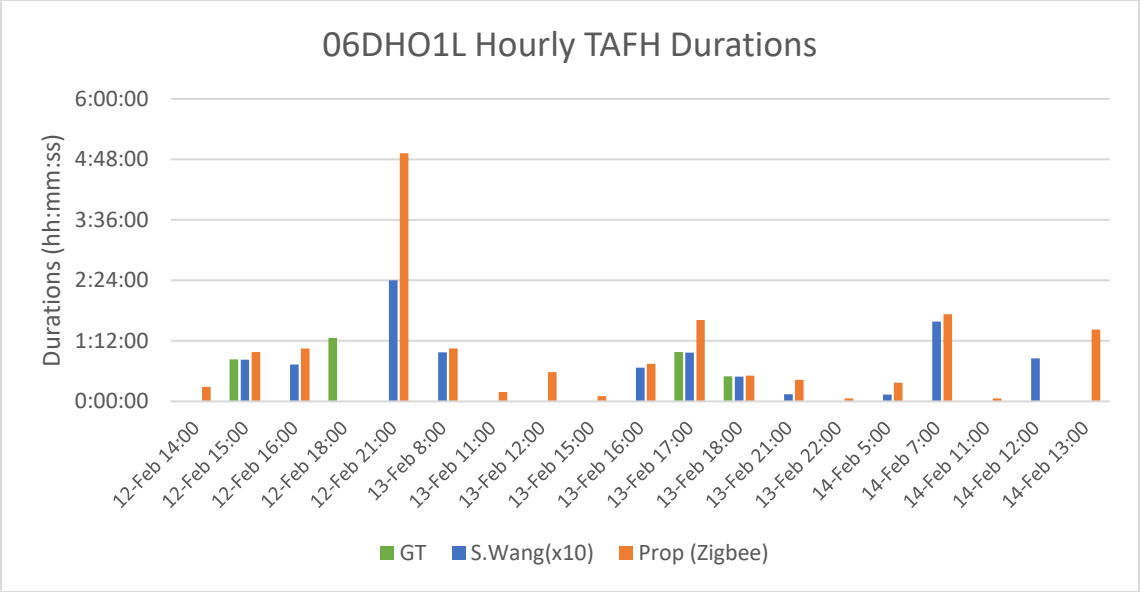

Figure 6.5-2 Subject 06DHO1L hourly TAFH durations. Only four ground truth TAFH.

Occasionally, after he entered his apartment, the living room motion sensor did not detect movement. Instead, the first bedroom motion sensor was the second motion sensor triggered after entering his apartment. Oddly, a few times after he entered his apartment the first motion sensor triggered was the bedroom door other than the front door was the bedroom. The battery level was even reported as 2.6 V, which is considered good.

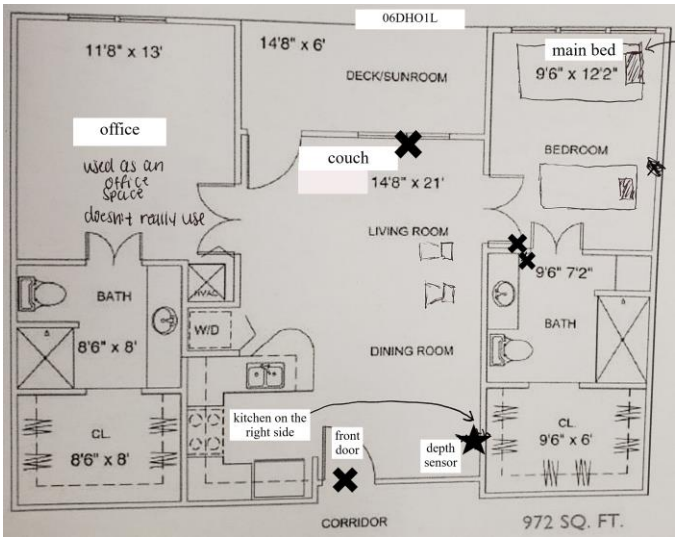

Figure 6.5-3 06DH1OL apartment layout. The 'X' represents the motion sensors placements and the star represents the placement of the depth sensor.

6.5.3 Case 3: 08DWO1L

Subject 08DWO1L was the only resident with a cat that would occasionally produce motion sensor events when jumping on to the bathroom counter. This caused both the current and proposed algorithm to not detect a vacant period as seen in Figure 6.5-5 at 16-Feb 18:00. Another significant difference occurred between 15-Feb 10:00 and 15-Feb 11:00. The proposed algorithm detected the same exit time as the ground truth but missed the time she entered her apartment. There was no other motion detected until after 11:00 am, which caused the proposed algorithm TAFH duration to be extended.

Next, the current and proposed algorithm detected vacancy at 16-Feb 16:00, when it should have not. In this case, 08DWO1L left the apartment, but there was a visitor still in the apartment cleaning in a room without motion sensors. The apartment was large enough that when the visitor walked into the common area, they walked to the front door without producing a living room motion event. Soon after, they walked into the bedroom, which triggered the correct series of events to look like someone entered the apartment. The path the visitor took after 08DWO1L left is shown in Figure 6.5-4 with red arrows.

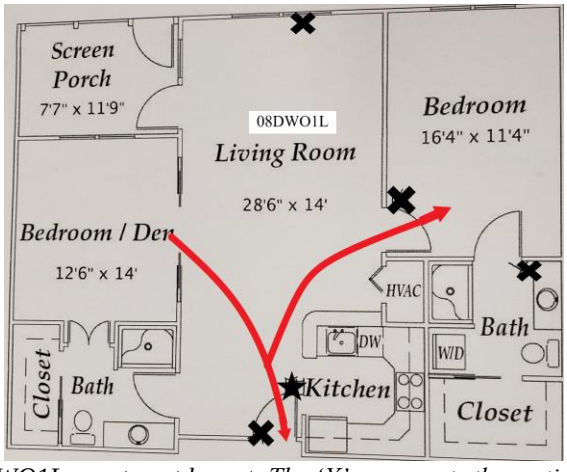

Figure 6.5-4 Subject 08DWO1L apartment layout. The 'X' represents the motion sensors placements and the star represents the placement of the depth sensor. The red arrows were the path the visitor took that avoided triggering the living room motion sensor.

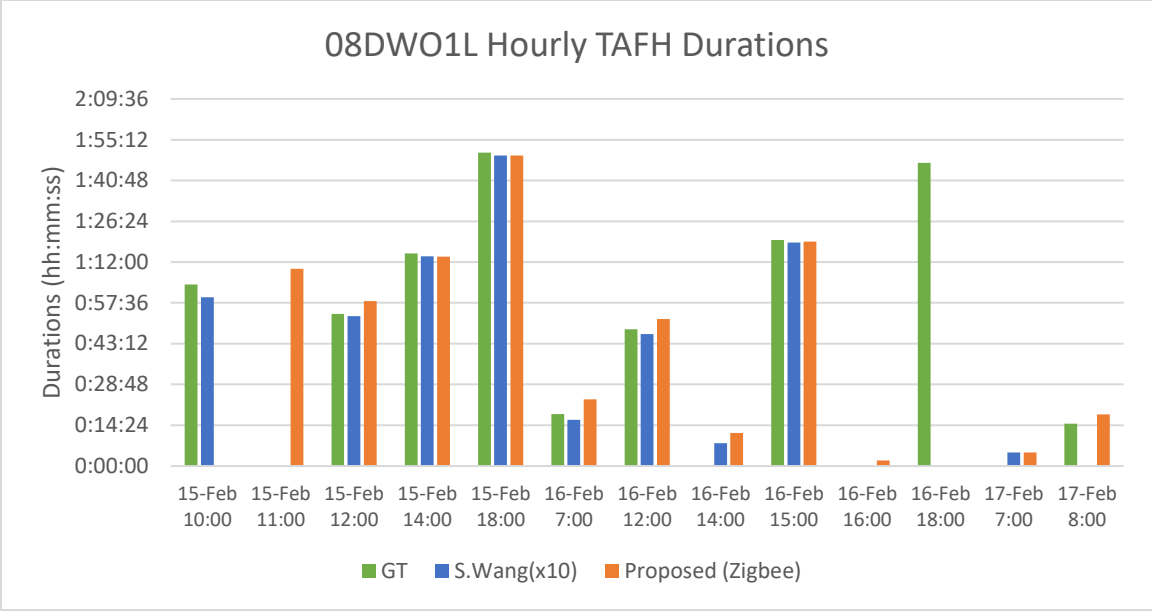

Figure 6.5-5 Subject 08DWO1L hourly TAFH durations.

6.5.4 Case 4: 11ASO1L

Subject 11ASO1L had a very small apartment that was only 340 square feet, shown in Figure 6.5-6. She typically would rest on the couch, which was right next to the front door. When she sat down or stood up from the couch, it triggered the front door motion rather than the living room. To trigger the living room motion sensor, she had to get up and take a few steps towards it. This confusion and the handful of visitors entering and exiting created several false positives, which can be seen below in Figure 6.5-6. Also, the differences in the current algorithm and the proposed algorithm were due to the proposed algorithm recording the enter times at a later time or the exit time early like mentioned before. Overall, both the algorithms detected similar vacancy periods as the ground truth.

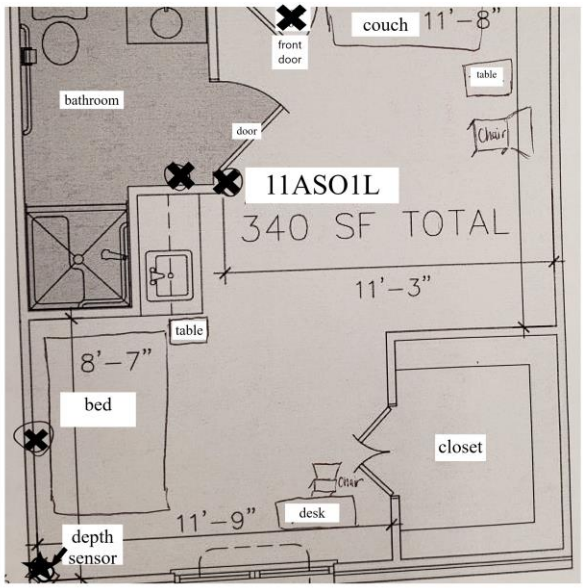

Figure 6.5-6 Subject 11ASO1L apartment layout. The 'X' represents the motion sensors placements and the star represents the placement of the depth sensor.

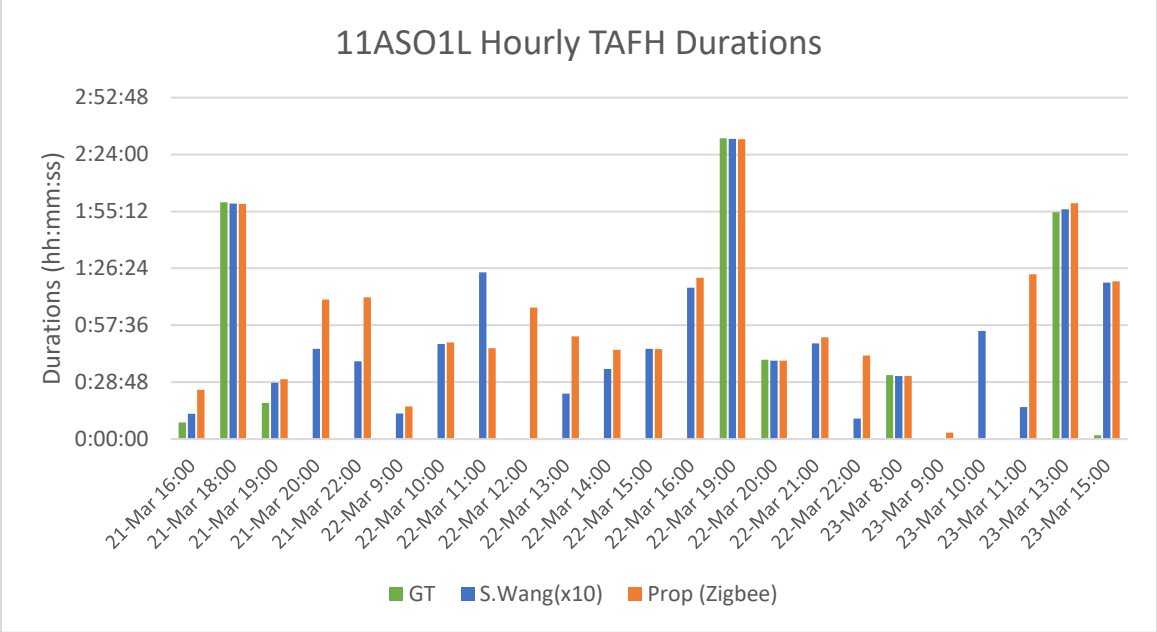

Figure 6.5-7 Subject 11ASO1L hourly TAFH durations.

6.6 Summary and Discussion

Overall, the proposed algorithm performed well even with several weaknesses recording exit times early or enter times late, visitors, pets, and times when the resident leaves the apartment using the patio door. The methodology of this new proposed

algorithm has a high potential over the old algorithm because it minimizes the need to use the simulated firing of 7-second motion. Instead, the proposed algorithm in this thesis focused on the true Zigbee motion sensor events that only fire at the beginning of a motion event and the end of a motion event.

The case studies further stress that the arrangement of the motion sensors should be strategically placed. For many of these small apartments, having a centralized living room motion sensor far enough away from the front door is critical, along with the front door motion sensor for the vacancy algorithm to work properly. For example, 03BHO1L only had the bathroom motion sensor other than the front door motion sensor. This specific case was an example of what happens when there is a sparse number of motion sensors. And where 11ASO1L sat during the day was close to the front door motion sensor caused a lot of false positives.

For future work, the algorithm could look at other thresholds to find one that works better to eliminate short continuous front door motion events. Also, the algorithm could check for the other in-home sensors to verify a person is not in the bed or the living space during the predicted TAFH duration. A person sitting still or sleeping for a long time, motion sensors might falsely detect the apartment as vacant. The depth sensor could be used to validate the living room for walking periods. The last suggestion would be to test the S.Wang algorithm using the true Zigbee motion sensor events for an equal comparison to the proposed algorithm.

7 Conclusion

In this study, several algorithms were developed and assessed to understand how different functional abilities and health may affect the results. These algorithms can be used as a continuum of monitoring health to identify early health problems. All the results were compared to the ground truth labels that were created from watching depth sensor videos.

In chapter 3, the step detection algorithm used a signal processing approach to counting steps from walking periods using the ActiGraph x-axis accelerometer signals. The different gait patterns that were looked at included a person's posture, walking speed, base-of-support, and gait cycles. This thesis explained the complexity of older adults' gait patterns and how they vary depending on how a person feels, time of day, or physical ability. It showed that a person with a forward posture and uses an assistive device greatly reduced the accuracy of counting steps. An assistive walking device produces additional noise in the accelerometer signal that resulted in a lot of false positives. And using the x-axis accelerometer signal was difficult to accurately count steps, but had the best results for the older adults in this study. The step detection algorithm was able to count individual steps but undercounted steps for a person with an average gait pattern, a straight posture, and no assistive device. Future studies will need to improve the accuracy along with combining a walking detection algorithm.

In chapter 4, the stand-to-sit and sit-to-stand classifier (STS) using the quadratic discriminate analysis (QDA) and random under-sampling boost (RUSBoost) based algorithms to identify postural transitions. Almost all the sit-to-stands and stand-to-sits were found separate from other activities. The case studies demonstrated different

instances where the models misclassified the three classes. It also determined that prior events to a stand-to-sit are important to identify to accurately classify it separate from sit-to-stands. Overall, the validation and test accuracy were over 90%.

In chapter 5, this thesis provided another method to identify motion density using accelerometers. The results were compared to the ground truth and the current motion density results that used in-home motion sensor data. The accelerometer eliminates the concern with visitors creating additional activity. But there were times when it showed higher motion density than the GT that indicated stationary activities like sitting or lying down. The ActiGraph accelerometer data produced less motion density than the ground truth. But overall, it provided similar results relative to the in-home motion sensors data.

In chapter 6, a proposed vacancy detection algorithm was developed to use Zigbee motion sensor data instead of the simulated x10 that fired every 7 seconds. The algorithm found almost all the time periods when the subject was away from home, but produced a lot of false-positive results as well. When someone used the patio door to exit or enter, the algorithm did not detect the apartment was vacant. Also, visitors sometimes confused the vacancy detection sequence. The placement of the motion sensors is important as we saw with subject 11ASO1L, who sat close to the front door motion sensor. For future work, the number of false-positive events needs to be reduced.

Appendix

Appendix A. Step Detection Program List

Directory: **ILA_LiaHowe/StepDection_LH**

Input: raw accelerometer data, timestamps, GT walk times

1. **Vector Magnitude Step Detection**
    a. stepDetection_vecMag_LH.mat
        i. output: vector magnitude step counts
2. **Dynamic Axis Selection Step Detection**
    a. stepDetection_selection_LH.mat
        i. output: step counts based on optimal axis per window
3. **Single Axis Step Detection (x, y, or z)**
    a. stepDectection_All3axes_LH.mat
        i. output: step counts based on chosen axis (x, y, or z)

Appendix B. STS Program List

Directory: **STS_LH**

Input: raw accelerometer data, timestamps, GT walk times

1. standSit_formatGT.m – formats the STS timestamps & finds matching raw data index
    a. input: original Timestamps, STS GT labeled times
    b. output: GT begin times & GT end times
    c. Additional functions:
        i. importStandSit.m
        ii. datetime2datestr.m
        iii. datetime2duration.m
2. preproces_standSit.m
    a. input: raw accelerometer data, timestamps, STS GT labeled times
    b. output: xdata (features), ydata (labels), userIDs, whole D1 xdata & ydata, whole D2 xdata & ydata
    c. Additional Functions:
        i. windowingFeatures.m
3. standSitclassifier.m
    a. input: xdata (features), ydata (labels), userIDs, whole D1 xdata & ydata, whole D2 xdata & ydata
    b. output: predicted QDA and predicted RUS labels
    c. Additional functions:
        i. confusionMatrix.m
        ii. charLabels2Num.m

Appendix C. Vacancy Program List

Directory: **Zigbee_LH**

testScript_HourlyDaily.m – main script used to run the vacancy algorithm

1. **sampleFiles.m –** loads info
    a. file input: motion sensor filenames, vacancy data collection range
2. **vacancyStartEndTimes.m**
    a. **OOAformat.m**
        i. formats the Zigbee motion sensor data & removes the simulated x10 motion sensor hits every 7 secs
        ii. input: filename 1, filename 2, filename 3, startTime, endTime, rootdir, relativefolder
        iii. output: data
    b. **getOldVacancyData.m**
        i. connects to the db.adl and fetches the predicted enterTime & exitTime for TAFH (S.Wang vacancy algorithm)
        ii. map of the original residentIDs associated to the userIDs used for this study
        iii. **CHANGE** : user path to dbConnection
    c. **importZigbee.m –** imports Zigbee motion sensor data
    d. **importGT.m –** imports ground truth labels
        i. input: filename
        ii. output: GTExit, GTEnter
3. **cmstats.m**
    a. input: groundtruthTAFH, predictedTAFH
    b. output: accuracy,sensitivity, specificity, precision, recall, FScore

Appendix D. Participant Information

Appx. Table D-1 Average biometric data for dataset 1 (10 volunteers) and dataset 2 (20 volunteers).

	GENDER (F:M)	AGE (years)	HEIGHT (in)	WEIGHT (lbs.)	BUILD (E:M:EN)
Dataset 1 - Average	8:1	87.5 ± 7.5	64.3 ± 7	148 ± 57	2:3:5
Dataset 1 - Female	8	87.86 ± 7.5	62.63 ± 5	137.63 ± 35	1:3:4
Dataset 1 - Male	2	85 ± 5	71 ± 3	189.5 ± 30.5	1:0:1
Dataset 2 - Average	14:6	83.7 ± 15	64.05 ± 9.5	158.1 ± 78.5	3:7:10
Dataset 2 - Female	14	83.14 ± 15	61.36 ± 7	144.21 ± 55	3:3:8
Dataset 2 - Male	6	85 ± 12.5	70.33 ± 1.5	190.5 ± 37.5	0:4:2

Appx. Table D-2 Dataset 1 subject information and data collection information

Dataset 1 - Subject Information

ID Name	Facility	Time Range	Sampling Rate (Hz)	Motion Sensor Status	Gender	Age	Physiological Build	Height (inches)	Weight (lbs)	Assistive Devices	Assistive Device during Calibration	Orientation attach Actigraph	Orientation remove Actigraph
01BLO1L	TigerPlace	48	50		F	84	Endomorph	63	172	none	none	sat in chair	sat in chair
02BCO1L	TigerPlace	24	50	no front, vaccant	F	89	Ectomorph	61	106	none	none	lying in bed*	standing
03BHO1L	TigerPlace	48	50	no bedroom, living	M	90	Endomorph	74	220	walker exit	none	standing	standing
05LBO1L	TigerPlace	48	100		F	94	Endomorph	70	176	walker	walker	lying in bed	lying in bed
06DHO1L	TigerPlace	48	100		M	80	Ectomorph	68	159	none	none	standing	standing
07HRO1L	Bluff Creek	48	100		F	92	Endomorph	62	130	walker	walker	sat in chair	sat in chair
08DWO1L	TigerPlace	48	100		F	88	Mesomorph	61	124	none	none	sat in chair	sat in chair
09HSO1L	Colony Pointe	48	100		F	89	Mesomorph	62	113	walker	walker	sat in chair	sat in chair
10JBO1L	TigerPlace	48	100		F	79	Endomorph	62	147	walker infrequent	none	sat in hard chair	sat in chair
11ASO1L	Hartmann	48	100		F	90	Mesomorph	60	133	walker	walker	lying in bed	lying in bed

Appx. Table D-3 Dataset 2 subject information and data collection information

Dataset 2 - Subject Information

ID Name	Facility	Time Range	Sampling Rate (Hz)	Motion Sensor Status	Gender	Age	Physiological Build	Height (inches)	Weight (lbs)	Assistive Devices	Assistive Device during Calibration	Orientation attach Actigraph	Orientation remove Actigraph
12ALO1L	Hartmann	48	100		F	83	Endomorph	60	178	walker	walker	lying down*	lying down
13JAO1L	TigerPlace	34	100	No front, vaccant	M	85	Mesomorph	72	165	walker	walker	sitting / reclining in chair	n/a
13JAO2L	TigerPlace	24	100	No front, vaccant	M	85	Mesomorph	72	165	walker	walker	lying	sit/recline*
15LOO1L	Hartmann	48	100	No front , vaccant (front 15 min precision)	F	92	Ectomorph	67	165	walker, cane	start: walker, end: cane	lying in bed	sat in chair
16NDO1L	Ashland Villa	48	100		F	79	Endomorph	62	185	cane rarely	none	lying in bed	lying in bed
17LPO1L	Ashland Villa	48	100		M	71	Endomorph	69	237	walker	none	lying in bed	sitting*
18RCO1L	Ashland Villa	48	100		M	87	Endomorph	70	193	wheelchair infrequent	none, end: wheelchair infrequent	sat in wheelchair	sat in bed
19VBO1L	TigerPlace	48	100	no living room	F	90	Ectomorph	57	80	walker	walker	lying back in recliner	sat in chair
20JJO1L	TigerPlace	48	100		M	91	Mesomorph	70	162	walker	walker	lying down	sat in chair
22NDO1L	Colony Pointe	48	100	front 15 min precision	F	90	Endomorph	60	130	walker	walker	sat in chair	lying down
23JWO1L	Colony Pointe	48	100	front hourly precision	F	74	Ectomorph	63	114	none	none	sat in chair	sat in chair
24SPO1L	TigerPlace	48	100		F	92	Mesomorph	64	130	walker	walker	lying in bed	sat in chair
25EHO1L	Bluff Creek	48	100		F	71	Endomorph	53	130	cane	start: cane, end: none	lying in bed	sat in bed
27CHO1L	TigerPlace	48	100		F	66	Endomorph	64	181	none	none	lying in bed	sat in chair
28JBO1L	Colony Pointe	48	100		F	79	Endomorph	55	110	none	none	lying in bed	lying in bed
29SSO1L	TigerPlace	48	100		F	81	Endomorph	65	175	cane	none	lying down	sat in chair
30WBO1L	Churchill	48	100		M	96	Mesomorph	70	181	walker	none, end: walker	sat in chair	sat in chair
31FSO1L	Churchill	48	100		M	80	Mesomorph	71	205	cane, wheelchair, walker	cane, end: walker	sat in chair	sat in chair
32PKO1L	Churchill	48	100		F	78	Endomorph	65	190	walker	start: none, except a walker during depth calibration, end: none	lying down	sat in chair
33BEO1L	TigerPlace	48	100	no front, vaccant	F	93	Mesomorph	62	135	walker	walker	lying down	sat in chair
34REO1L	TigerPlace	48	100		F	96	Mesomorph	62	116	walker, sometimes wheelchair	walker	lying down	lying down

* Orientations are reported to the best of our knowledge; however, there is some uncertainty.

Index	Resident ID	ILA ID	Collection start DATE	ACTIGRAPH INITIAL TIME	ACTIGRAPH Attachment Time	Collction end DATE	ACTIGRAPH Removal Time	ACTIGRAPH END Date	ACTIGRAPH Stop Time
1	3089	01BLO1L	11/29/2018	12:22:00 PM	12:22:00 PM	12/1/2018	1:13:18 PM	12/2/2018	2:00:00 PM
2	3125	02BCO1L	12/2/2018	11:19:00 AM	11:20:00 AM	12/3/2018	11:31:14 AM	12/3/2018	1:00:00 PM
3	3054	03BHO1L	12/10/2018	3:15:00 PM	3:17:05 PM	12/12/2018	3:12:25 PM	12/12/2018	4:00:00 PM
4	3026	05LBO1L	12/14/2018	1:10:00 PM	1:13:20 PM	12/16/2018	1:07:38 PM	12/16/2018	2:00:00 PM
5	3102	06DHO1L	2/12/2019	2:00:00 PM	2:01:00 PM	2/14/2019	2:08:35 PM	2/14/2019	3:00:00 PM
6	6103	07HRO1L	2/15/2019	10:00:00 AM	10:03:00 AM	2/17/2019	10:09:17 AM	2/17/2019	10:00:00 AM
7	3038	08DWO1L	2/15/2019	9:00:00 AM	9:36:00 AM	2/17/2019	11:06:00 AM	2/17/2019	12:00:00 PM
8	6304	09HSO1L	2/18/2019	1:00:00 PM	1:23:00 PM	2/20/2018	1:18:25 PM	2/20/2019	2:00:00 PM
9	3085	10JBO1L	2/23/2019	10:00:00 AM	10:00:00 AM	2/25/2019	10:28:47 AM	2/25/2019	11:00:00 AM
10	6417	11ASO1L	3/21/2019	3:33:00 PM	3:40:45 PM	3/23/2019	3:40:48 PM-3:41:00	3/23/2019	5:00:00 PM
11	6408	12ALO1L	3/21/2019	4:09:00 PM	4:15:10 PM	3/23/2019	4:23:00 PM	3/23/2019	6:00:00 PM
12	3107	13JAO1L	4/1/2019	1:09:00 PM	1:19:00 PM	4/3/2019	N/A	4/3/2019	1:20:00 PM
13	3107	13JAO2L	4/3/2019	1:25:00 PM	1:27:18 PM-1:31:05	4/4/2019	3:56:30 PM	4/4/2019	4:00:00 PM
14	6405	15LOO1L	4/5/2019	3:49:00 PM	3:51:34 PM	4/7/2019	3:41:40 PM	4/7/2019	5:00:00 PM
15	6003	16NDO1L	4/12/2019	11:27:00 AM	11:33:47 AM	4/14/2019	11:59:24 AM	4/14/2019	1:00:00 PM
16	6013	17LPO1L	4/12/2019	12:53:00 PM	12:55:44 PM	4/14/2019	12:50:55 PM	4/14/2019	2:00:00 PM
17	6018	18RCO1L	4/12/2019	1:16:00 PM	1:16:38 PM	4/14/2019	1:09:50 AM	4/14/2019	3:00:00 PM
18	3082	19VBO1L	7/18/2019	11:52:00 AM	11:56:29 AM	7/20/2019	11:46:44 AM	7/20/2019	12:30:00 PM
19	3129	20JJO1L	7/19/2019	1:01:00 PM	1:08:27 PM	7/21/2019	1:16:10 PM	7/21/2019	2:00:00 PM
20	44107	22NDO1L	7/22/2019	1:33:00 PM	1:42:15 PM	7/24/2019	2:07:06 PM	7/24/2019	2:30:00 PM
21	6325	23JWO1L	7/22/2019	2:15:00 PM	2:17:34 PM	7/24/2019	1:29:23 PM	7/24/2019	3:00:00 PM
22	3130	24SPO1L	8/13/2019	10:45:00 AM	10:53:00 AM	8/15/2019	10:19:50 AM	8/15/2019	4:00:00 PM
23	6123	25EHO1L	8/13/2019	7:18:00 PM	7:24:00 PM	8/15/2019	7:13:40 PM	8/15/2019	11:00:00 PM
24	3132	27CHO1L	8/17/2019	9:46:00 AM	9:53:50 AM	8/19/2019	9:28:38 AM	8/19/2019	11:00:00 PM
25	6311	28JBO1L	8/19/2019	1:28:00 PM	1:36:50 PM	8/21/2019	1:07:00 PM	8/21/2019	11:00:00 PM
26	3134	29SSO1L	8/20/2019	12:23:00 PM	12:30:00 PM	8/22/2019	12:26:17 PM	8/22/2019	11:00:00 PM
27	6207	30WBO1L	8/28/2019	2:07:00 PM	2:27:23 PM	8/30/2019	2:18:00 PM	8/30/2019	11:00:00 PM
28	6219	31FSO1L	8/28/2019	3:22:00 PM	3:29:16 PM	8/30/2019	3:16:07 PM	8/30/2019	11:00:00 PM
29	6215	32PKO1L	8/28/2019	4:15:00 PM	4:40:00 PM	8/30/2019	3:41:20 PM	8/30/2019	11:00:00 PM
30	3027	33BEO1L	9/3/2019	1:00:00 PM	1:45:00 PM	9/5/2019	1:45:00 PM	9/6/2019	11:00:00 PM
31	3140	34REO1L	9/3/2019	1:00:00 PM	3:40:00 PM	9/5/2019	3:14:00 PM	9/6/2019	11:00:00 PM
Index	Resident ID	ILA ID	Collection start DATE	ACTIGRAPH INITIAL TIME	ACTIGRAPH Attachment Time	Collction end DATE	ACTIGRAPH Removal Time	ACTIGRAPH END Date	ACTIGRAPH Stop Time
n/a	3115	04RKO1L	12/10/2018	4:08:00 PM	4:10:00 PM	12/12/2018	N/A	12/12/2018	5:00:00 PM
n/a	6409	14ERO1L	4/5/2019	3:15:00 PM	3:18:00 PM	4/7/2019	N/A	4/7/2019	5:00:00 PM
n/a	3127	21JSO1L	7/20/2019	2:33:00 PM	2:42:00 PM	7/22/2019	4:01:55 PM	7/22/2019	3:30:00 PM
n/a	3128	26BTO1L	8/16/2019	4:30:00 PM	4:35:49 PM	~8/17/2019	~21:10	8/19/2019	10:00:00 PM

Appendix E. Subject Living Space Information

Appendix E contains information about the subject's living space, such as the layout, pets, and additional notes about the subject.

Appx. Table E-1 Dataset 1 living space information.

Dataset 1 - Living Space Information

ID Name	Room Layout	Bed Tilt (degrees)	# Pillows	Pets	Bed in view	Bedroom Depth Sensor	Chair Sensor	Notes
01BLO1L	1 bed, 784 sqft	0	1 head	0	no	no	0	no Actigraph + Depth sensor calibration reference activity
02BCO1L	1 bed, 784 sqft	0	1 head	dog	no	no	0	
03BHO1L	1 bed, rectangle 648 sqft	0	1 head / 1 feet	0	yes	yes	0	
05LBO1L	2 bed, 1064 sqft	0	1 head	0	no	no	0	legally blind, daily morning helper
06DHO1L	2 bed, 972 sqft	30	2 head	0	no	no	0	
07HRO1L	studio 232 sqft	0	1 head	0	partial	no	0	
08DWO1L	2 bed, 1064 sqft	0	1 head / 1 knee	cat	no	no	0	
09HSO1L	1 bed, with kitchenette 499 sqft	0	1 head / 1 knees	0	partial	no	0	
10JBO1L	2 bed, 1064 sqft	0	1 head	0	no	no	0	
11ASO1L	studio, 340 sqft	0	1 head	0	partial	no	0	

Appx. Table E-2 Dataset 2 living space information. Resident 29SSO1L low visiblity due to a large apartment. Resident 30WBO1L depth sensor resolution was very grainy.

Dataset 2 - Living Space Information

ID Name	Room Layout	Bed Tilt (degrees)	# Pillows	Pets	Bed in view	Bedroom Depth Sensor	Chair Sensor	Notes
12ALO1L	1 bed, with kitchenette 499 sqft	0	1-2 head	0	no	no	0	felt sick 3/22/2019
13JAO1L	1 bed,784 sqft	0	1 head	0	no	no	0	part 1, no final calibration activities
13JAO2L	1 bed,784 sqft	0	1 head	0	no	no	0	part 2
15LOO1L	studio, 340 sqft	0	1 head	0	partial	no	0	
16NDO1L	studio, 260 sqft	0	1 head	0	partial	no	0	
17LPO1L	studio, 260 sqft	0	1 head	0	barely	no	0	only used bed, no chair
18RCO1L	studio, 260 sqft	0	1 head	0	barely	no	0	frequent friend visits & sometimes stays the night
19VBO1L	2 bed, 1064 sqft	20	1 head/ 1 knees	0	no	no	0	chair sensor stoped early, one of the 2 daughters, stayed full time during the data collection period
20JJO1L	1 bed, rectangle 648 sqft	0	1 head	0	no	no	0	rolling desk chair (main)
22NDO1L	studio, 273 sqft	0	1 head, sometimes no pillow	0	partial	no	1	
23JWO1L	studio, 414 sqft	0	2 head	small dog	yes	no	1	frequently goes outside
24SPO1L	2 bed, 1064 sqft	0	1 head	0	no	no	1	depth sensor videos very grainy, living room mostly black
25EHO1L	studio, 232 sqft	0	2 head / sometimes 1 back	0	yes	no	0	
27CHO1L	1 bed, rectangle 648 sqft	0	2-3 head	0	yes	yes	1	felt sick during data collection period
28JBO1L	1 bed, kitchenette 499 sqft	0	1 head	0	no	no	1	during initial calibration, depth sensor had technical difficulties and stopped recording for a few minutes. Leaves front door open, goes in/out of room a lot, twice the front door didn't catch exit time
29SSO1L	1 bed, 1080 sqft	0	1 head & 1 small knees	dog	no	no	1	
30WBO1L	studio, 245 sqft	0	1 head	0	yes	no	1	chair with sensor is out of view
31FSO1L	1 bed, 463 sqft	0	1 head	0	no	no	1	
32PKO1L	studio, 245 sqft	0	1 head	0	yes	no	1	shoulder immobility, therefore wasn't able to lay on right or left side
33BEO1L	2 bed, 972 sqft	0	1 head	0	no	no	1	legally blind
34REO1L	1bed, 540 sqft	0	1 head	0	no	no	1	

Appendix F. Step Detection Additional Information

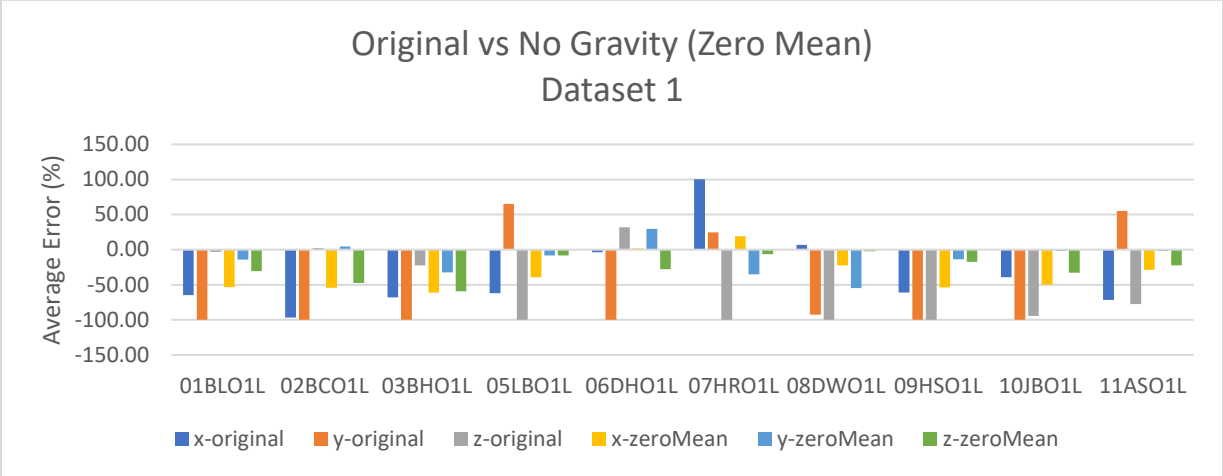

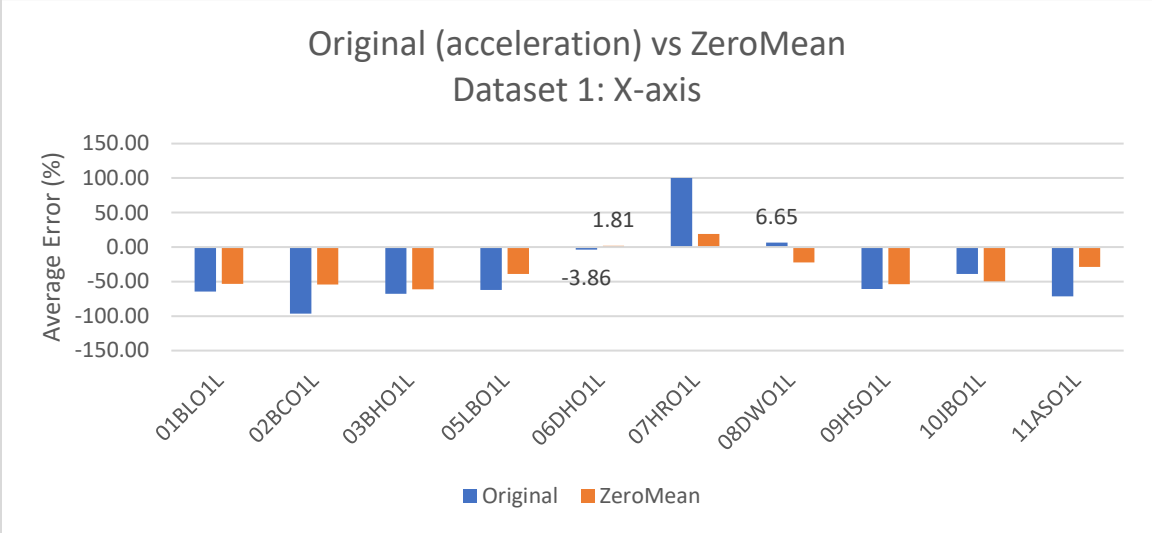

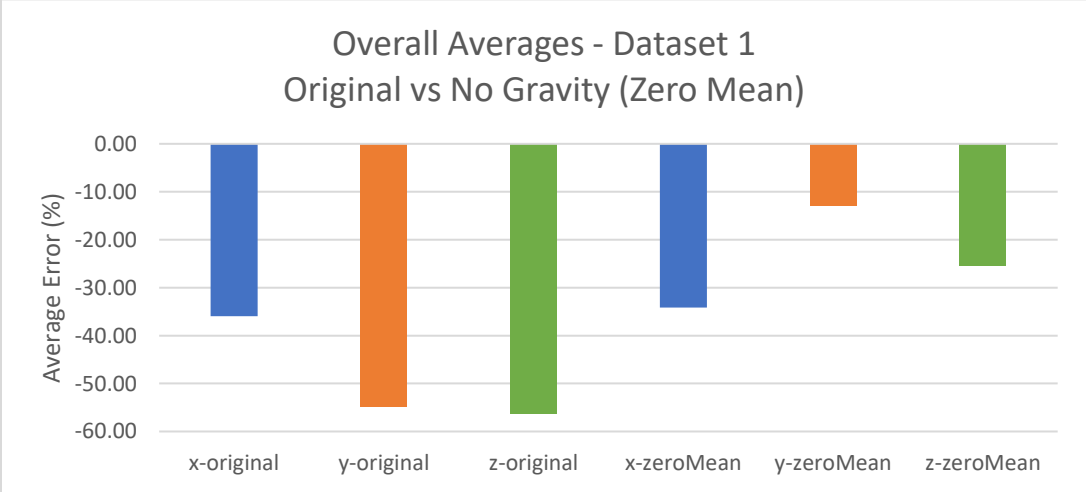

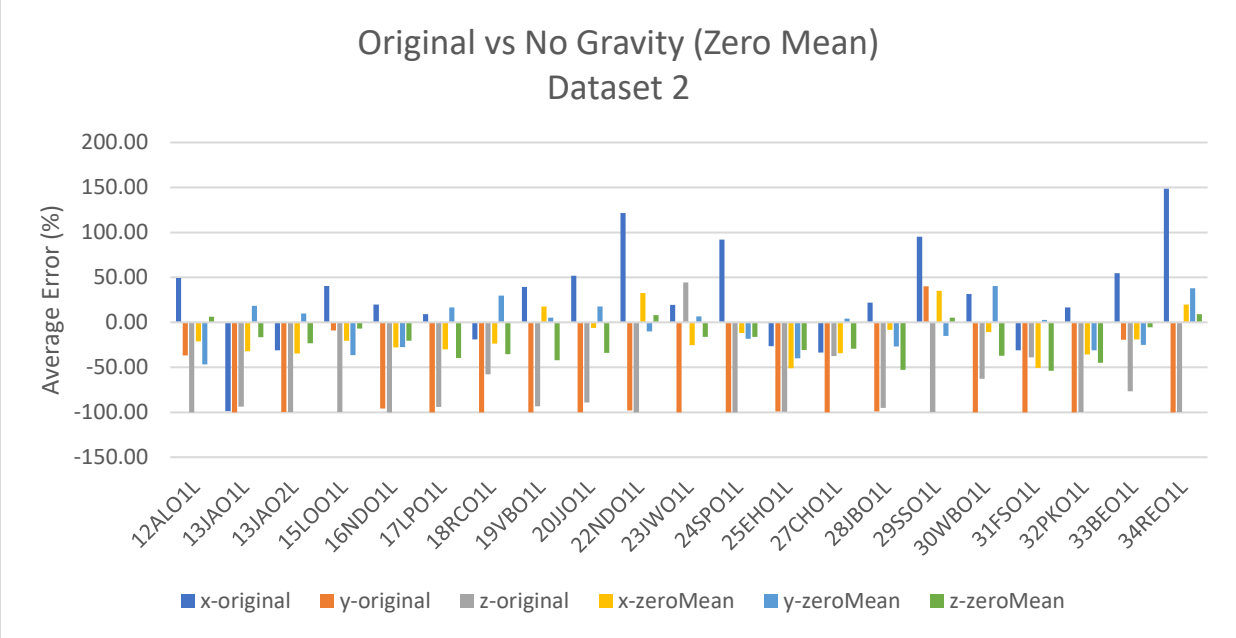
Original vs No Gravity (Zero Mean)
Dataset 2
Average Error (%)
200.00
150.00
100.00
50.00
0.00
-50.00
-100.00
-150.00
12ALO1L
13JAO1L
13JAO2L
15LOO1L
16NDO1L
17LPO1L
18RCO1L
19VBO1L
20JJO1L
22NDO1L
23JWO1L
24SPO1L
25EHO1L
27CHO1L
28JBO1L
29SSO1L
30WBO1L
31FSO1L
32PKO1L
33BEO1L
34REO1L
x-original
y-original
z-original
x-zeroMean
y-zeroMean
z-zeroMean

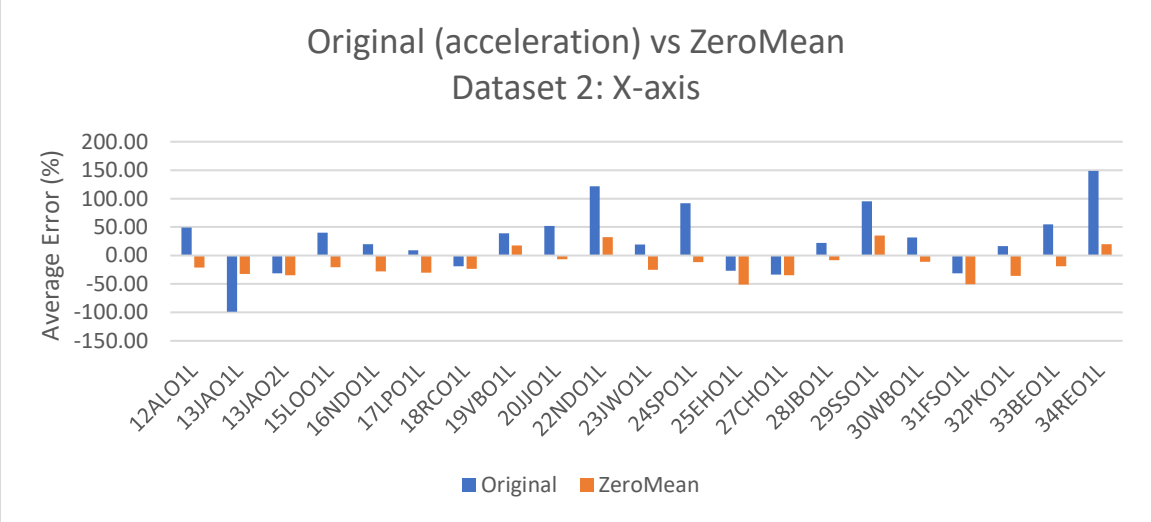
Original (acceleration) vs ZeroMean
Dataset 2: X-axis
Average Error (%)
200.00
150.00
100.00
50.00
0.00
-50.00
-100.00
-150.00
12ALO1L
13JAO1L
13JAO2L
15LOO1L
16NDO1L
17LPO1L
18RCO1L
19VBO1L
20JJO1L
22NDO1L
23JWO1L
24SPO1L
25EHO1L
27CHO1L
28JBO1L
29SSO1L
30WBO1L
31FSO1L
32PKO1L
33BEO1L
34REO1L
Original
ZeroMean

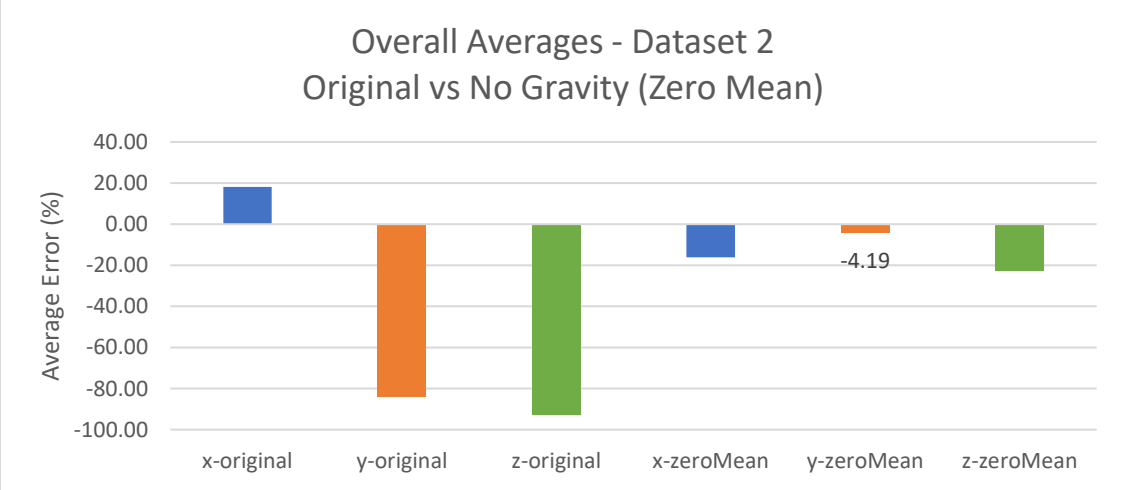
Overall Averages - Dataset 2
Original vs No Gravity (Zero Mean)
Average Error (%)
40.00
20.00
0.00
-20.00
-40.00
-60.00
-80.00
-100.00
-4.19
x-original
y-original
z-original
x-zeroMean
y-zeroMean
z-zeroMean

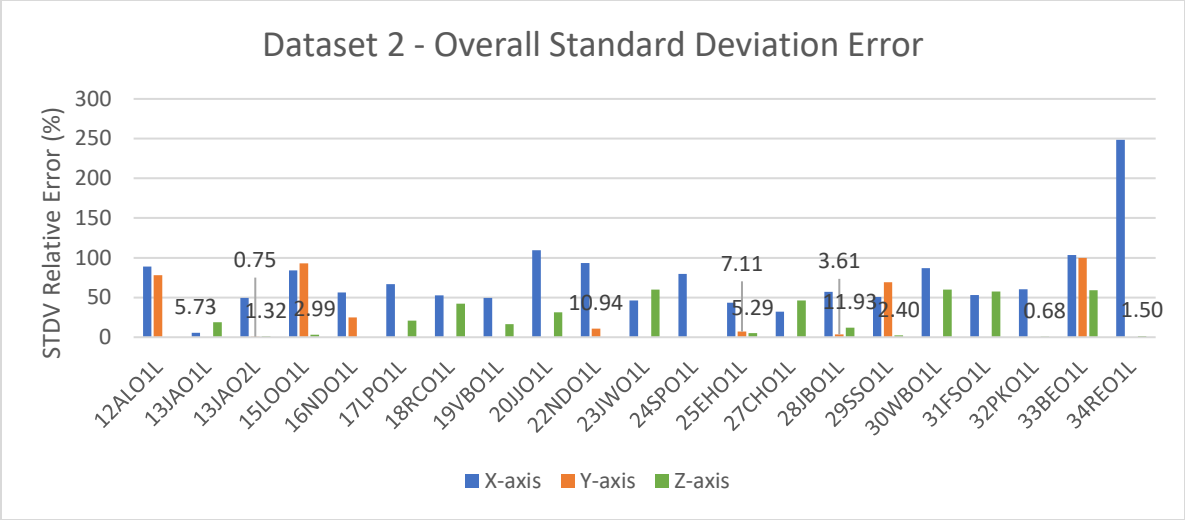
Dataset 2 - Overall Standard Deviation Error
STDV Relative Error (%)
300
250
200
150
100
50
0
0.75
7.11
3.61
5.73
1.32
2.99
10.94
5.29
11.93
2.40
0.68
1.50
12ALO1L
13JAO1L
13JAO2L
15LOO1L
16NDO1L
17LPO1L
18RCO1L
19VBO1L
20JJO1L
22NDO1L
23JWO1L
24SPO1L
25EHO1L
27CHO1L
28JBO1L
29SSO1L
30WBO1L
31FSO1L
32PKO1L
33BEO1L
34REO1L
X-axis
Y-axis
Z-axis

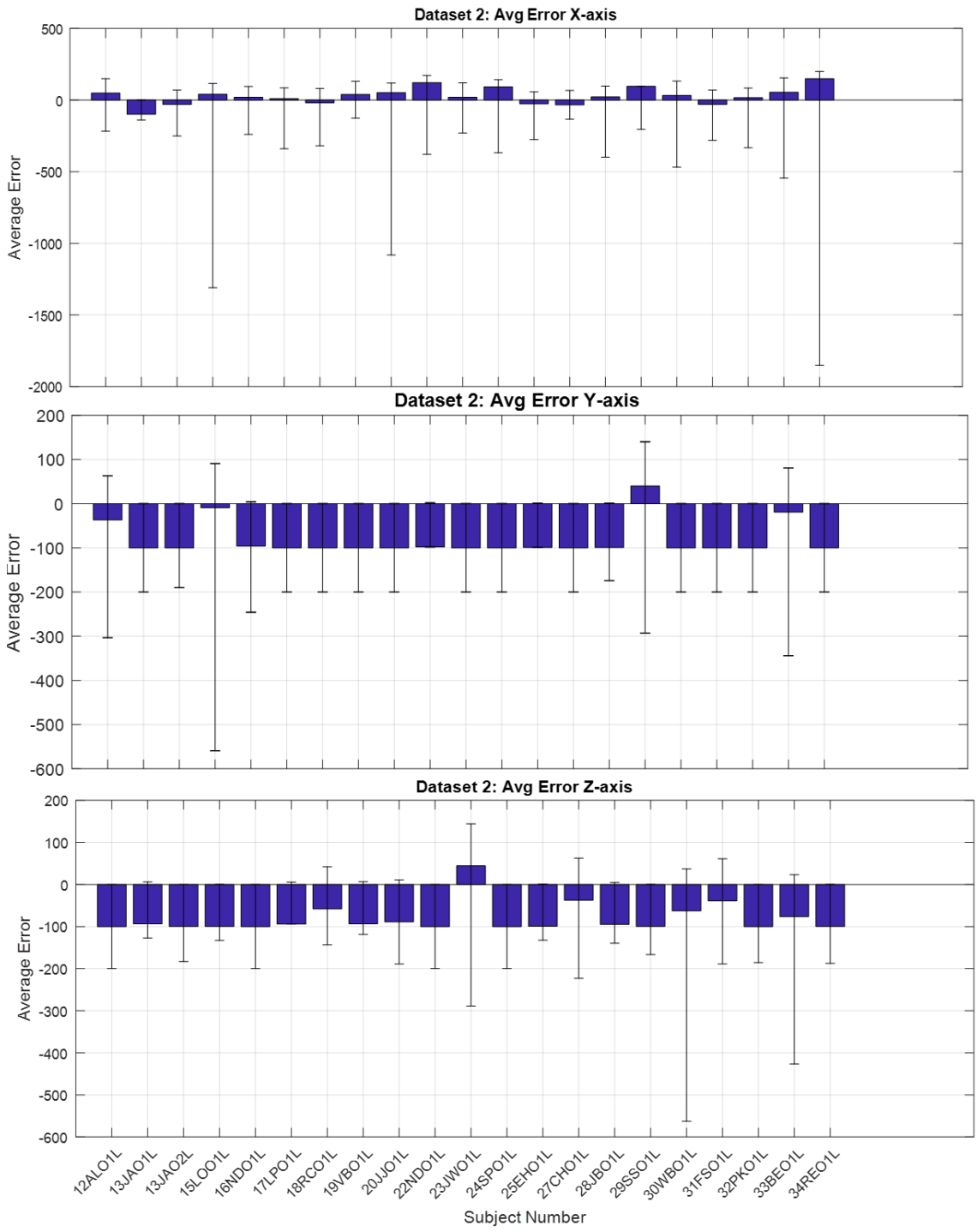
Dataset 2: Avg Error X-axis
Average Error
500
0
-500
-1000
-1500
-2000
Dataset 2: Avg Error Y-axis
Average Error
200
100
0
-100
-200
-300
-400
-500
-600
Dataset 2: Avg Error Z-axis
Average Error
200
100
0
-100
-200
-300
-400
-500
-600
12ALO1L
13JAO1L
13JAO2L
15LOO1L
16NDO1L
17LPO1L
18RCO1L
19VBO1L
20JJO1L
22NDO1L
23JWO1L
24SPO1L
25EHO1L
27CHO1L
28JBO1L
29SSO1L
30WBO1L
31FSO1L
32PKO1L
33BEO1L
34REO1L
Subject Number

Appendix F.1. Gait Patterns

Appx. Table F-1 Weighted percentage of subjects for each gait pattern category.

assistive device		walking speed		shuffle		heel strike & toe-off		posture		BOS	
DATASET 1											
noWalker	40.0%	fast	10.0%	full	0%	full	50%	normal	60%	narrow	40%
infreqDevice	20.0%	moderate	30.0%	medium	0%	medium	20%	forward	40%	normal	60%
walker	40.0%	slow	50.0%	minimal	0%	minimal	30%			wide	0%
multiDevice	0.0%	Very slow	10.0%	min_none	0%	min_none	0%				
				none	100%	none	0%				
DATASET 2											
noWalker	19.0%	fast	0.0%	full	19%	full	66.7%	normal	42.9%	narrow	23.8%
infreqDevice	9.5%	moderate	33.3%	medium	0%	medium	4.8%	forward	57.1%	normal	57.1%
walker	57.1%	slow	42.9%	minimal	0%	minimal	14.3%			wide	19.0%
multiDevice	14.3%	Very slow	23.8%	min_none	0%	min_none	9.5%				
				none	81%	none	4.8%				

Appx. Table F-2 Additional weighted percentage of subjects for gait pattern categories leg swing, arm swing, and gait symmetry.

leg swing		arm swing		symmetry	
DATASET 1					
full	60%	full_none	20%	symmetric	70%
medium	20%	full	40%	partSym	0%
minimal	10%	medium	10%	asymmetric	30%
min_none	10%	min_none	0%		
none	0%	none	30%		
DATASET 2					
full	61.9%	full_none	9.5%	symmetric	42.9%
medium	14.3%	full	28.6%	partSym	23.8%
minimal	14.3%	medium	0.0%	asymmetric	33.3%
min_none	4.8%	min_none	4.8%		
none	4.8%	none	57.1%		

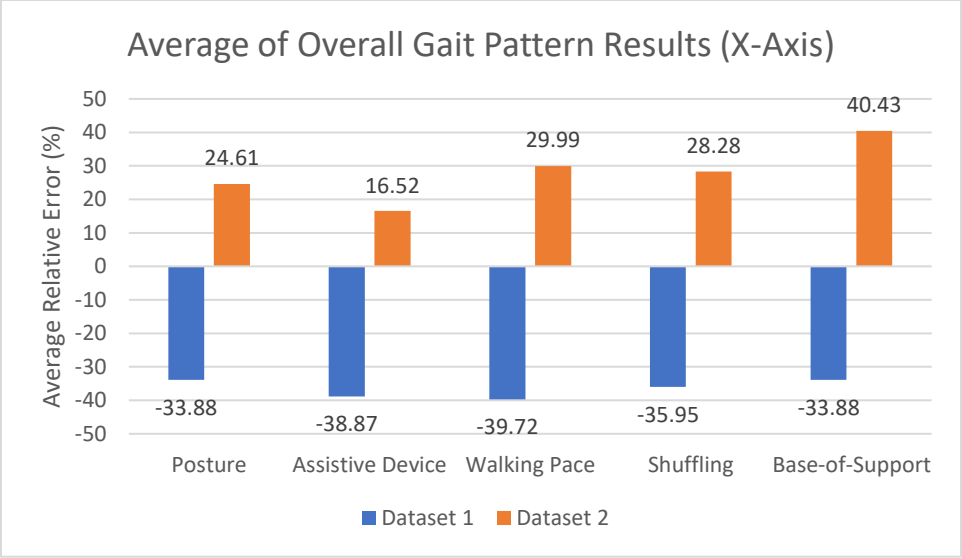

Appx. Figure F-1, shows the results separated into the different assistive devices people used in dataset 1. The first four subjects shaded in blue did not use a walker. The next two, 03BHO1L and 10JBO1L shaded in orange both infrequently used a cane. Next, four subjects shaded in green used walkers. And lastly, there were no subjects in dataset 1 that used multiple assistive devices. This supports the earlier results shown in Figure 3.4-3, that the walker caused a significant error. Interestingly, subjects 06DHO1L and 08DWO1L had the lowest error because

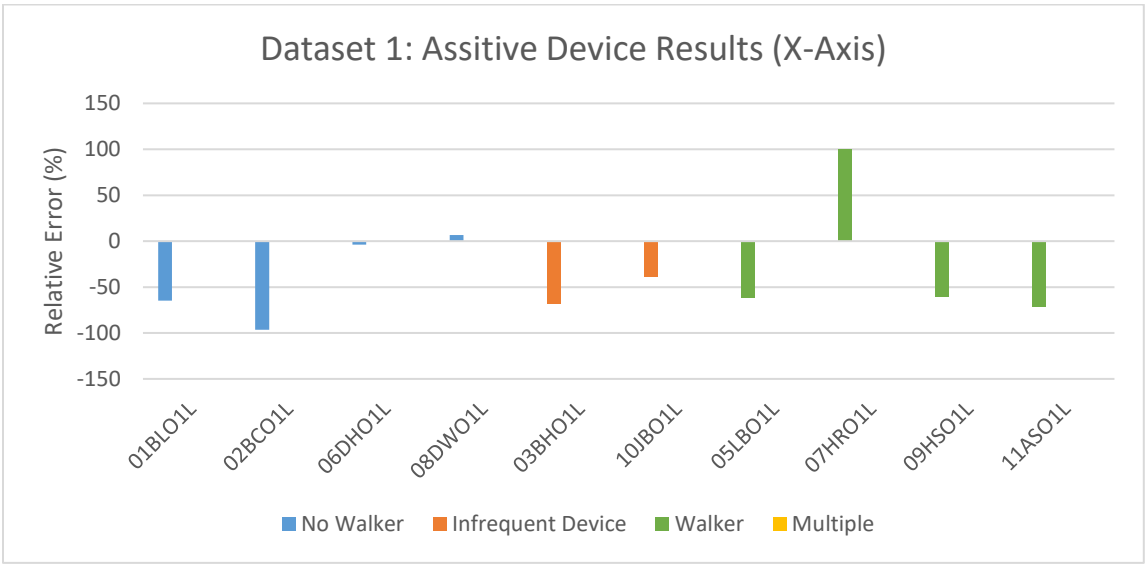

Appx. Figure F-1 Individual results from dataset 1 looking at the effects of different assistive devices.

01BLO1L	X
02BCO1L	X
03BHO1L	X
05LBO1L	X
06DHO1L	X
07HRO1L	y
08DWO1L	y
09HSO1L	X
10JBO1L	X
11ASO1L	x

12ALO1L	y
13JAO1L	x
13JAO2L	x
15LOO1L	x
16NDO1L	x
17LPO1L	x
18RCO1L	z
19VBO1L	z
20JJO1L	z
22NDO1L	y
23JWO1L	x
24SPO1L	z
25EHO1L	x
27CHO1L	z
28JBO1L	z
29SSO1L	z
30WBO1L	z
31FSO1L	x
32PKO1L	z
33BEO1L	y
34REO1L	z

Appx. Figure F-2 Using a dynamic axis selection method, this table shows which axis is best for each subject based on the results

Appendix G. Overall STS Additional Results

Appx. Table G-1 Ground truth number of STS observations

Participant	Number of Observations: Other	Stand-Sit	Sit-Stand
01BLO1L	6101	24	17
02BCO1L	7059	50	17
03BHO1L	23027	86	106
05LBO1L	4750	66	49
06DHO1L	14395	69	66
07HRO1L	2567	30	39
08DWO1L	5499	23	9
09HSO1L	8493	48	44
10JBO1L	1940	14	17
11ASO1L	26311	63	39
12ALO1L	3366	15	10
13JAO1L	2038	2	3
13JAO2L	1695	10	11
15LOO1L	23176	189	177
16NDO1L	27869	41	55
18RCO1L	7640	33	33
19VBO1L	11713	51	48
22NDO1L	23862	24	28
23JWO1L	15516	39	19
24SPO1L	7365	212	22
25EHO1L	15055	114	56
27CHO1L	30501	40	39
28JBO1L	2791	31	22
29SSO1L	1042	8	3
30WBO1L	27615	72	88
31FSO1L	1561	23	24
32PKO1L	25009	76	88
33BEO1L	3374	69	77
34REO1L	8812	32	34

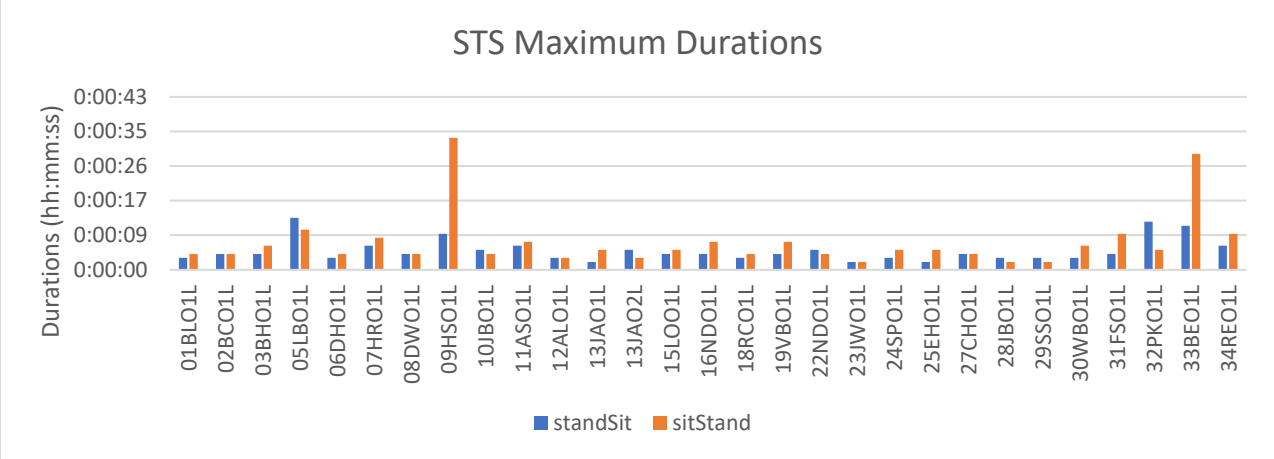

Appx. Figure G-1 Ground truth maximum STS durations

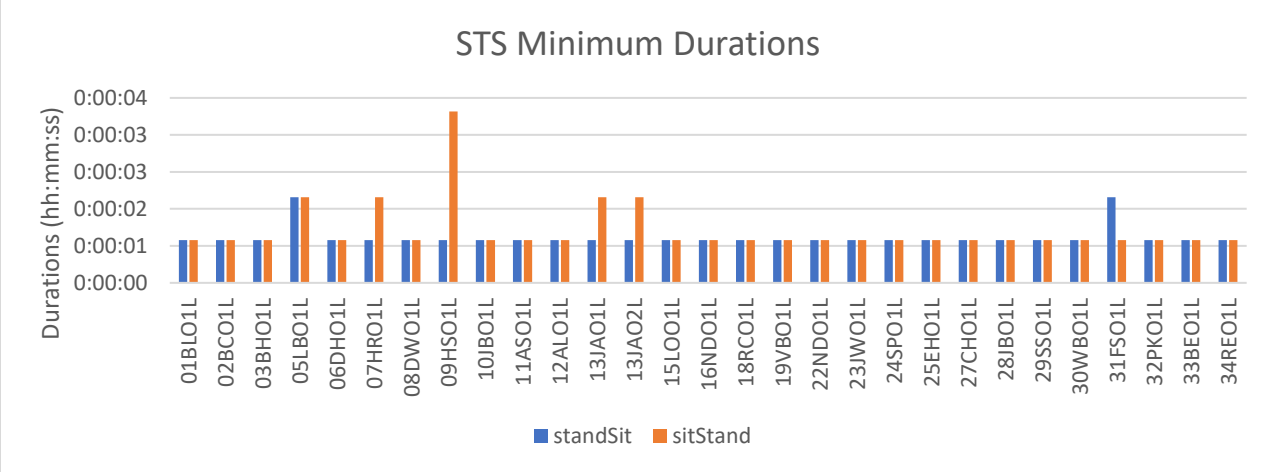

Appx. Figure G-2 Ground truth minimum STS durations.

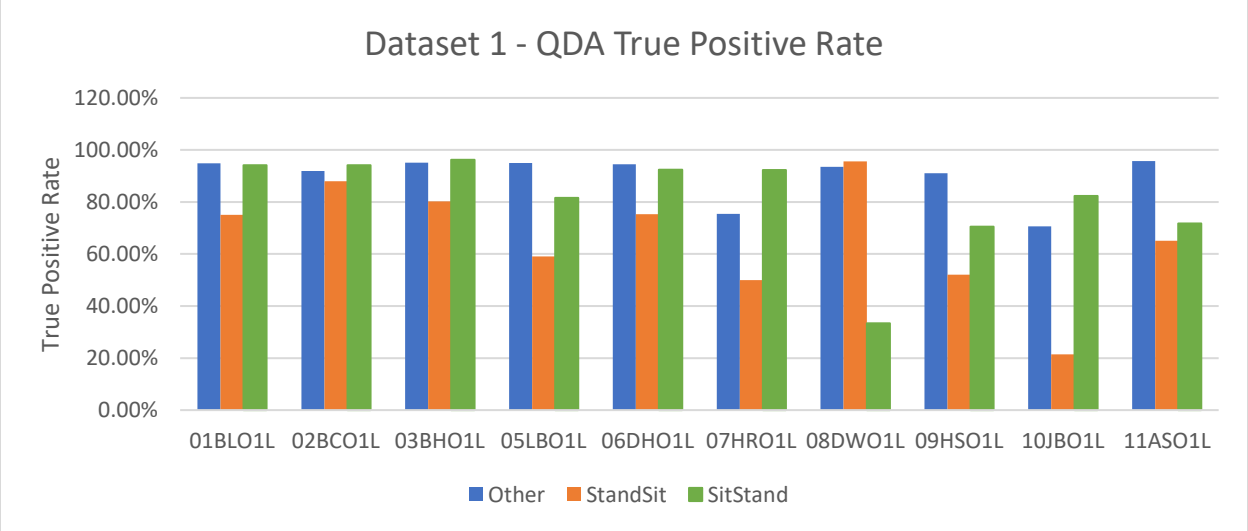

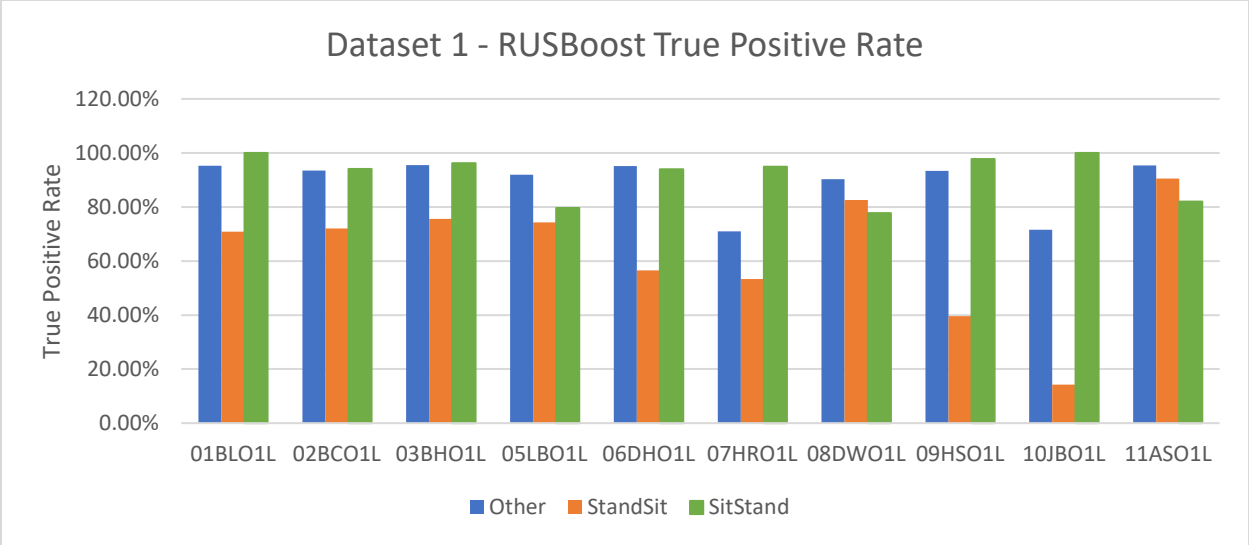
Dataset 1 - RUSBoost True Positive Rate
True Positive Rate
120.00%
100.00%
80.00%
60.00%
40.00%
20.00%
0.00%
01BLO1L
02BCO1L
03BHO1L
05LBO1L
06DHO1L
07HRO1L
08DWO1L
09HSO1L
10JBO1L
11ASO1L
Other
StandSit
SitStand

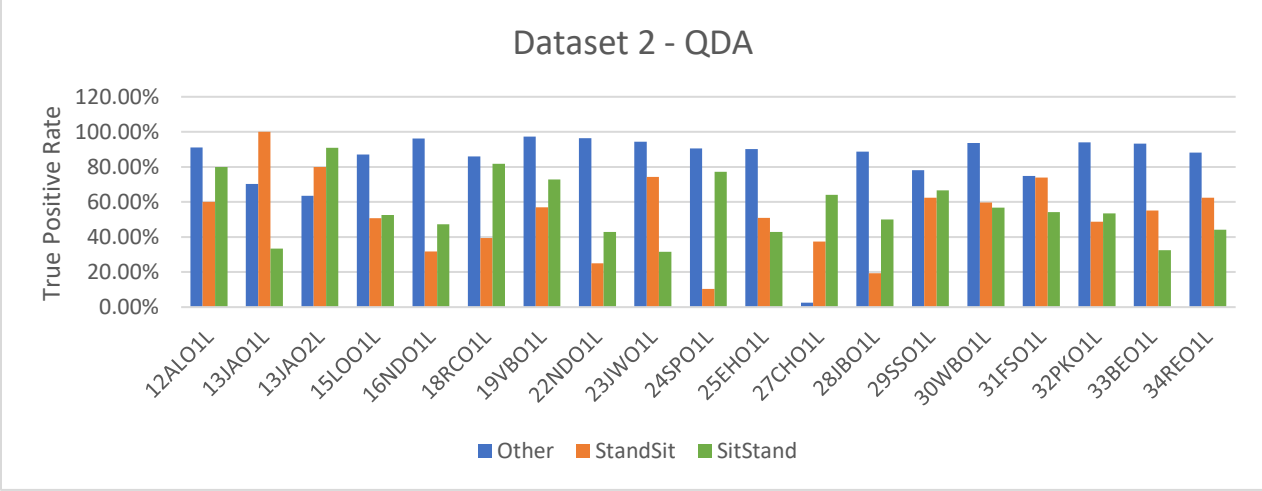
Dataset 2 - QDA
True Positive Rate
120.00%
100.00%
80.00%
60.00%
40.00%
20.00%
0.00%
12ALO1L
13JAO1L
13JAO2L
15LOO1L
16NDO1L
18RCO1L
19VBO1L
22NDO1L
23JWO1L
24SPO1L
25EHO1L
27CHO1L
28JBO1L
29SSO1L
30WBO1L
31FSO1L
32PKO1L
33BEO1L
34REO1L
Other
StandSit
SitStand

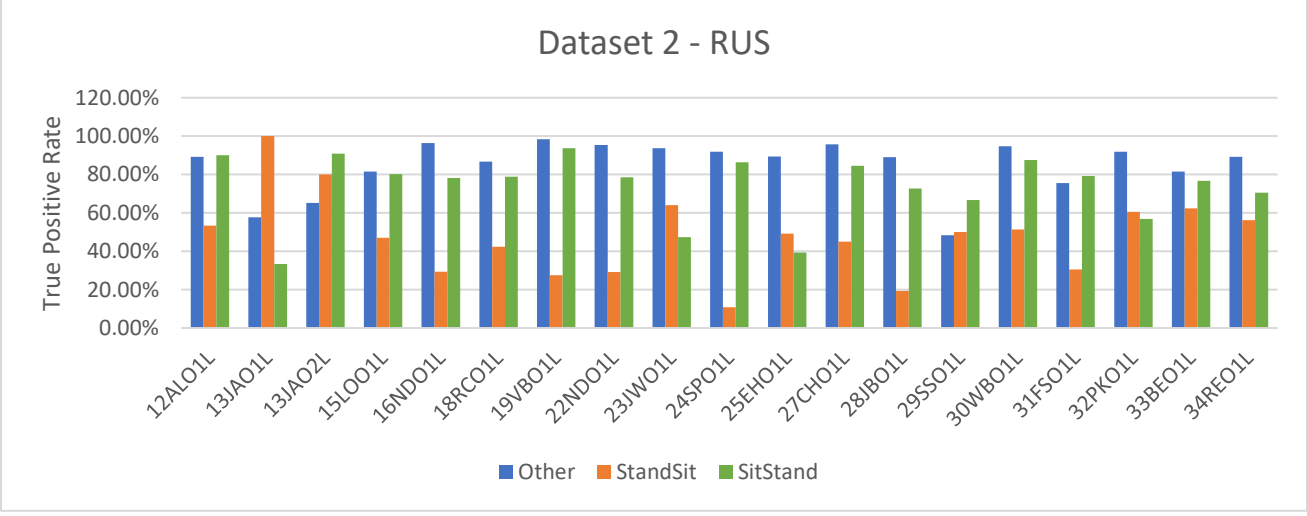
Dataset 2 - RUS
True Positive Rate
120.00%
100.00%
80.00%
60.00%
40.00%
20.00%
0.00%
12ALO1L
13JAO1L
13JAO2L
15LOO1L
16NDO1L
18RCO1L
19VBO1L
22NDO1L
23JWO1L
24SPO1L
25EHO1L
27CHO1L
28JBO1L
29SSO1L
30WBO1L
31FSO1L
32PKO1L
33BEO1L
34REO1L
Other
StandSit
SitStand

Individual subjects' classifier performance				
	Dataset 1		Dataset 2	
Averages	QDA	RUSBoost	QDA	RUSBoost
Total	89.60%	89.16%	87.44%	84.48%
Sensitivity	78.95%	81.29%	65.68%	68.61%
F1	44.54%	46.96%	38.99%	39.75%
Stand-Sit	66.19%	62.95%	52.56%	47.79%
Sit-Stand	80.88%	91.63%	56.58%	73.24%

Appendix G.1. Individual STS Additional Results – Dataset 1

01BLO1L							
		QDA			RUS		
TRUE	other	94.85%	1.34%	3.80%	95.21%	0.74%	4.05%
	stand-sit	0.00%	75.00%	25.00%	0.00%	70.83%	29.17%
	sit-stand	0.00%	5.88%	94.12%	0.00%	0.00%	100.00%
QDA	94.77%	other	stand-sit	sit-stand	other	stand-sit	sit-stand
RUS	95.13%	Predicted					

02BCO1L							
		QDA			RUS		
TRUE	other	91.93%	2.07%	6.01%	93.47%	0.75%	5.78%
	stand-sit	2.00%	88.00%	10.00%	0.00%	72.00%	28.00%
	sit-stand	5.88%	0.00%	94.12%	5.88%	0.00%	94.12%
QDA	91.90%	other	stand-sit	sit-stand	other	stand-sit	sit-stand
RUS	93.32%	Predicted					

03BHO1L							
		QDA			RUS		
TRUE	other	95.11%	1.03%	3.87%	95.51%	0.28%	4.21%
	stand-sit	2.33%	80.23%	17.44%	3.49%	75.58%	20.93%
	sit-stand	2.83%	0.94%	96.23%	0.94%	2.83%	96.23%
QDA	95.06%	other	stand-sit	sit-stand	other	stand-sit	sit-stand
RUS	95.43%	Predicted					

05LBO1L							
		QDA			RUS		
TRUE	other	94.99%	0.95%	4.06%	91.89%	2.04%	6.06%
	stand-sit	10.61%	59.09%	30.30%	0.00%	74.24%	25.76%
	sit-stand	12.24%	6.12%	81.63%	2.04%	18.37%	79.59%
QDA	94.37%	other	stand-sit	sit-stand	other	stand-sit	sit-stand
RUS	91.53%	Predicted					

06DHO1L							
		QDA			RUS		
TRUE	other	94.53%	0.94%	4.54%	95.11%	0.38%	4.51%
	stand-sit	0.00%	75.36%	24.64%	0.00%	56.52%	43.48%
	sit-stand	3.03%	4.55%	92.42%	1.52%	4.55%	93.94%
QDA	94.43%	other	stand-sit	sit-stand	other	stand-sit	sit-stand
RUS	94.92%	Predicted					

07HRO1L							
		QDA			RUS		
TRUE	other	75.38%	3.27%	21.35%	71.02%	3.35%	25.63%
	stand-sit	16.67%	50.00%	33.33%	10.00%	53.33%	36.67%
	sit-stand	5.13%	2.56%	92.31%	5.13%	0.00%	94.87%
QDA	75.34%	other	stand-sit	sit-stand	other	stand-sit	sit-stand
RUS	71.17%	Predicted					

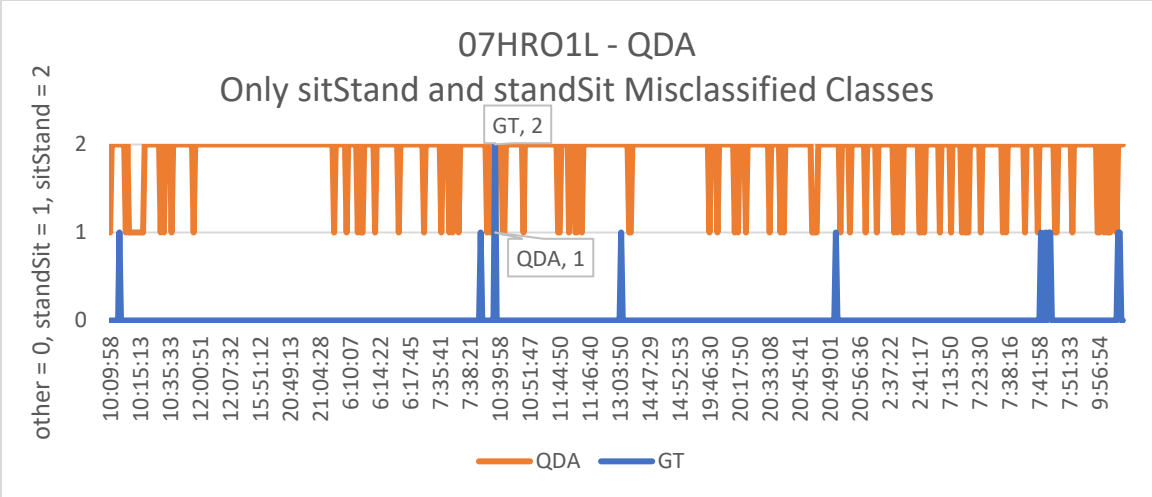

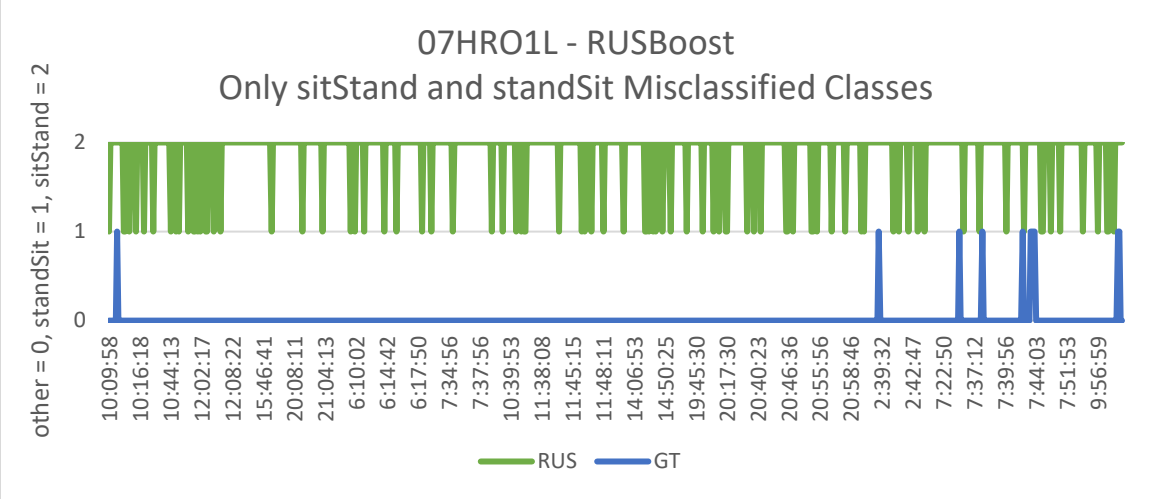

08DWO1L							
		QDA			RUS		
TRUE	other	93.56%	2.95%	3.49%	90.29%	2.05%	7.66%
	stand-sit	0.00%	95.65%	4.35%	0.00%	82.61%	17.39%
	sit-stand	22.22%	44.44%	33.33%	0.00%	22.22%	77.78%
QDA	**93.47%**	other	stand-sit	sit-stand	other	stand-sit	sit-stand
RUS	**90.24%**	Predicted					

09HSO1L							
		QDA			RUS		
TRUE	other	91.08%	1.93%	6.99%	93.42%	0.33%	6.25%
	stand-sit	18.75%	52.08%	29.17%	2.08%	39.58%	58.33%
	sit-stand	29.55%	0.00%	70.45%	2.27%	0.00%	97.73%
QDA	**90.75%**	other	stand-sit	sit-stand	other	stand-sit	sit-stand
RUS	**93.14%**	Predicted					

10JBO1L							
		QDA			RUS		
TRUE	other	70.62%	3.45%	25.93%	71.55%	1.34%	27.11%
	stand-sit	7.14%	21.43%	71.43%	0.00%	14.29%	85.71%
	sit-stand	0.00%	17.65%	82.35%	0.00%	0.00%	100.00%
QDA	**70.37%**	other	stand-sit	sit-stand	other	stand-sit	sit-stand
RUS	**71.39%**	Predicted					

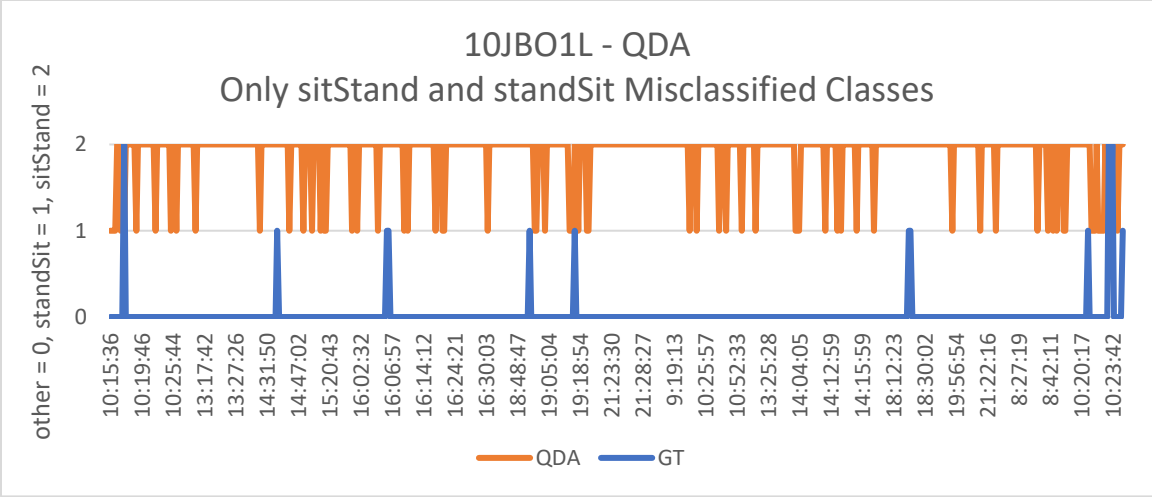

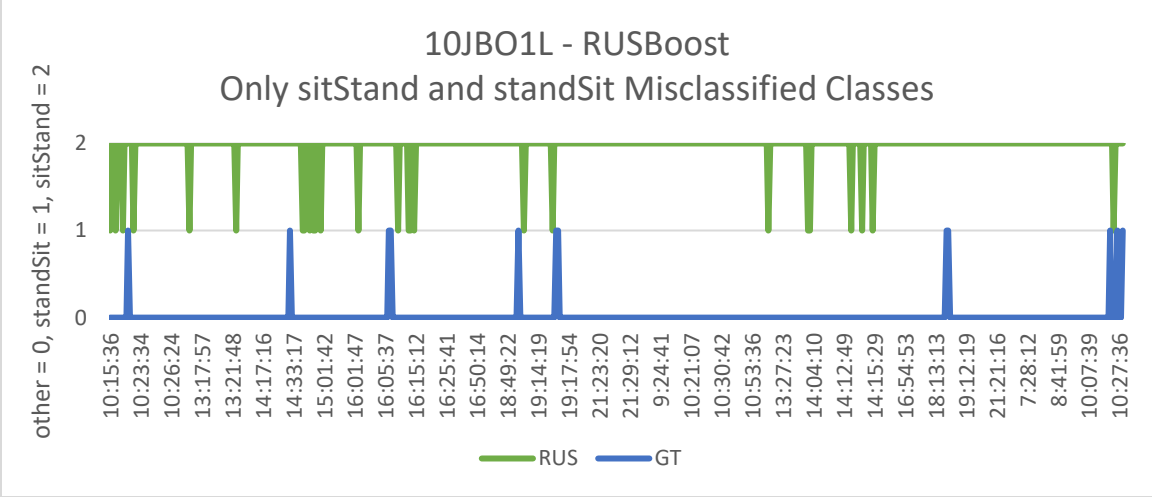

11ASO1L							
		QDA			RUS		
TRUE	other	95.68%	1.71%	2.60%	95.37%	2.72%	1.91%
	stand-sit	15.87%	65.08%	19.05%	0.00%	90.48%	9.52%
	sit-stand	12.82%	15.38%	71.79%	0.00%	17.95%	82.05%
QDA	**95.57%**	other	stand-sit	sit-stand	other	stand-sit	sit-stand
RUS	**95.34%**	Predicted					

Appendix G.2. Individual STS Additional Results – Dataset 2

12ALO1L							
		QDA			RUS		
TRUE	other	91.06%	1.31%	7.64%	89.22%	1.66%	9.12%
	stand-sit	6.67%	60.00%	33.33%	6.67%	53.33%	40.00%
	sit-stand	0.00%	20.00%	80.00%	0.00%	10.00%	90.00%
QDA	**90.89%**	other	stand-sit	sit-stand	other	stand-sit	sit-stand
RUS	**89.06%**	Predicted					

13JAO1L							
		QDA			RUS		
TRUE	other	70.36%	14.77%	14.87%	57.70%	2.11%	40.19%
	stand-sit	0.00%	100.00%	0.00%	0.00%	100.00%	0.00%
	sit-stand	0.00%	66.67%	33.33%	0.00%	66.67%	33.33%
QDA	**70.34%**	other	stand-sit	sit-stand	other	stand-sit	sit-stand
RUS	**57.71%**	Predicted					

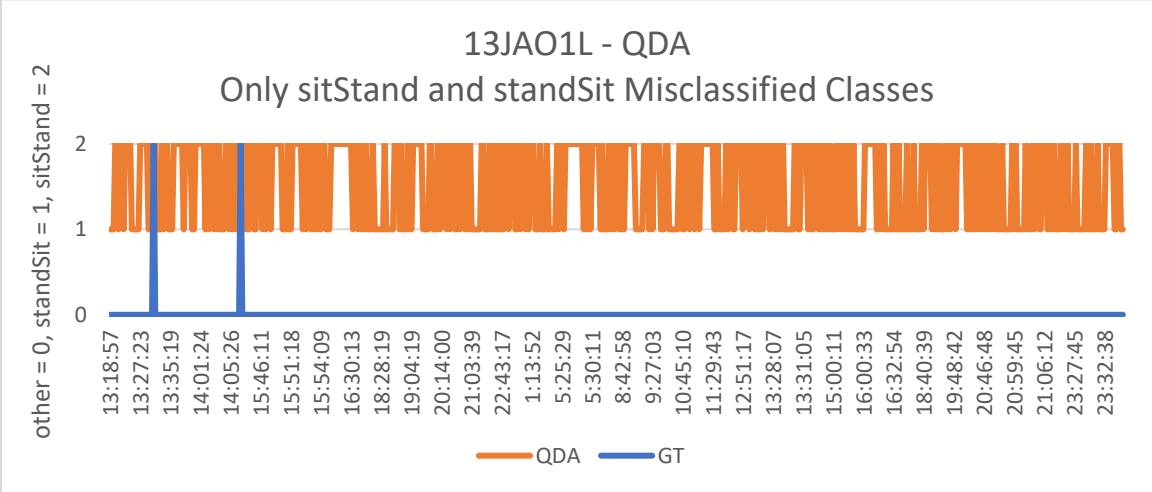

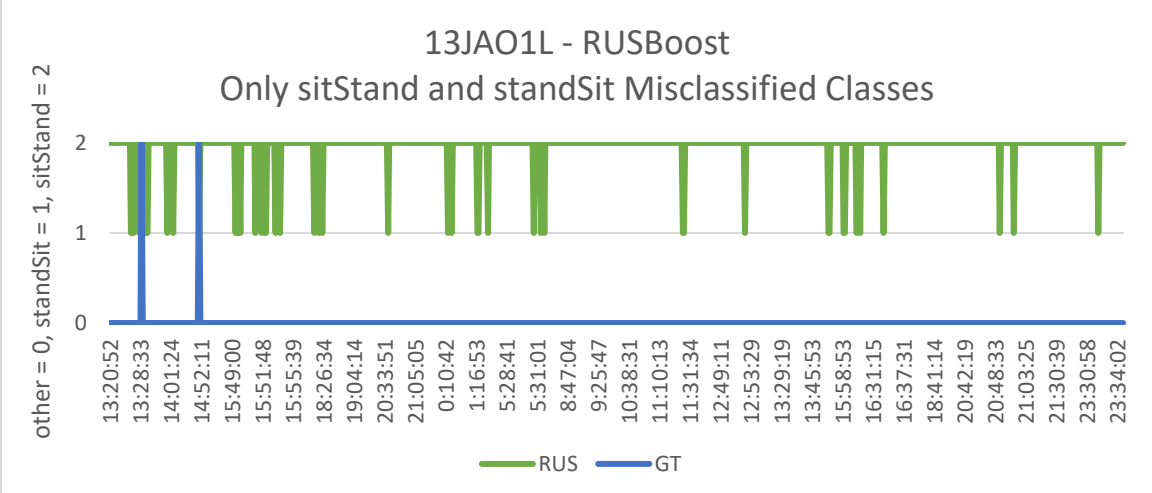

13JAO2L							
		QDA			RUS		
TRUE	other	63.48%	4.66%	31.86%	65.25%	1.77%	32.98%
	stand-sit	0.00%	80.00%	20.00%	0.00%	80.00%	20.00%
	sit-stand	0.00%	9.09%	90.91%	0.00%	9.09%	90.91%
QDA	63.75%	other	stand-sit	sit-stand	other	stand-sit	sit-stand
RUS	65.50%	Predicted					

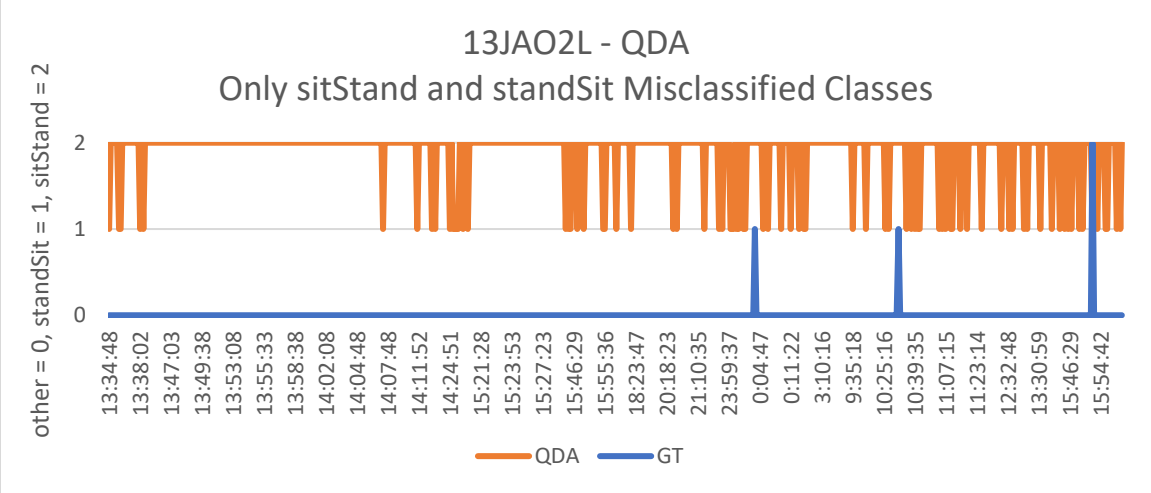

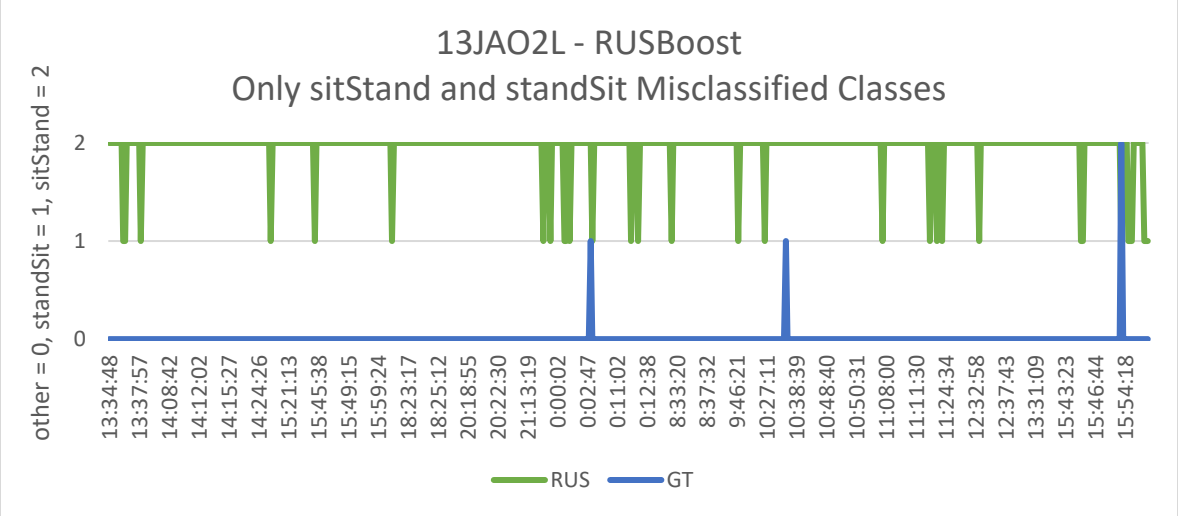

15LOO1L							
		QDA			RUS		
TRUE	other	87.03%	4.10%	8.87%	81.46%	3.51%	15.03%
	stand-sit	13.23%	50.79%	35.98%	6.35%	47.09%	46.56%
	sit-stand	16.95%	30.51%	52.54%	3.95%	15.82%	80.23%
QDA	86.48%	other	stand-sit	sit-stand	other	stand-sit	sit-stand
RUS	81.17%	Predicted					

16NDO1L							
		QDA			RUS		
TRUE	other	96.27%	1.15%	2.58%	96.30%	0.96%	2.74%
	stand-sit	9.76%	31.71%	58.54%	0.00%	29.27%	70.73%
	sit-stand	10.91%	41.82%	47.27%	1.82%	20.00%	78.18%
QDA	96.08%	other	stand-sit	sit-stand	other	stand-sit	sit-stand
RUS	96.16%	Predicted					

18RCO1L							
		QDA			RUS		
TRUE	other	86.06%	2.28%	11.66%	86.65%	0.71%	12.64%
	stand-sit	3.03%	39.39%	57.58%	3.03%	42.42%	54.55%
	sit-stand	3.03%	15.15%	81.82%	3.03%	18.18%	78.79%
QDA	85.84%	other	stand-sit	sit-stand	other	stand-sit	sit-stand
RUS	86.43%	Predicted					

19VBO1L							
		QDA			RUS		
TRUE	other	97.23%	0.31%	2.47%	98.41%	0.03%	1.55%
	stand-sit	9.80%	56.86%	33.33%	3.92%	27.45%	68.63%
	sit-stand	10.42%	16.67%	72.92%	2.08%	4.17%	93.75%
QDA	96.95%	other	stand-sit	sit-stand	other	stand-sit	sit-stand
RUS	98.09%	Predicted					

22NDO1L							
		QDA			RUS		
TRUE	other	96.44%	1.27%	2.29%	95.42%	1.23%	3.34%
	stand-sit	16.67%	25.00%	58.33%	0.00%	29.17%	70.83%
	sit-stand	25.00%	32.14%	42.86%	7.14%	14.29%	78.57%
QDA	96.30%	other	stand-sit	sit-stand	other	stand-sit	sit-stand
RUS	95.34%	Predicted					

23JWO1L							
		QDA			RUS		
TRUE	other	94.32%	2.01%	3.67%	93.79%	0.48%	5.74%
	stand-sit	12.82%	74.36%	12.82%	12.82%	64.10%	23.08%
	sit-stand	0.00%	68.42%	31.58%	0.00%	52.63%	47.37%
QDA	**94.19%**	other	stand-sit	sit-stand	other	stand-sit	sit-stand
RUS	**93.66%**	Predicted					

24SPO1L							
		QDA			RUS		
TRUE	other	90.63%	2.44%	6.92%	91.81%	2.51%	5.68%
	stand-sit	82.08%	10.38%	7.55%	80.19%	10.85%	8.96%
	sit-stand	9.09%	13.64%	77.27%	4.55%	9.09%	86.36%
QDA	**88.35%**	other	stand-sit	sit-stand	other	stand-sit	sit-stand
RUS	**89.54%**	Predicted					

25EHO1L							
		QDA			RUS		
TRUE	other	90.23%	2.74%	7.03%	89.34%	2.54%	8.12%
	stand-sit	25.44%	50.88%	23.68%	25.44%	49.12%	25.44%
	sit-stand	3.57%	53.57%	42.86%	1.79%	58.93%	39.29%
QDA	**89.76%**	other	stand-sit	sit-stand	other	stand-sit	sit-stand
RUS	**88.85%**	Predicted					

27CHO1L							
		QDA			RUS		
TRUE	other	95.90%	1.15%	2.95%	95.78%	0.28%	3.94%
	stand-sit	2.50%	37.50%	60.00%	0.00%	45.00%	55.00%
	sit-stand	5.13%	30.77%	64.10%	2.56%	12.82%	84.62%
QDA	**95.78%**	other	stand-sit	sit-stand	other	stand-sit	sit-stand
RUS	**95.70%**	Predicted					

28JBO1L							
		QDA			RUS		
TRUE	other	88.71%	2.47%	8.81%	88.96%	2.26%	8.78%
	stand-sit	0.00%	19.35%	80.65%	0.00%	19.35%	80.65%
	sit-stand	13.64%	36.36%	50.00%	18.18%	9.09%	72.73%
QDA	**87.66%**	other	stand-sit	sit-stand	other	stand-sit	sit-stand
RUS	**88.08%**	Predicted					

29SSO1L							
		QDA			RUS		
TRUE	other	78.21%	2.69%	19.10%	48.37%	9.02%	42.61%
	stand-sit	12.50%	62.50%	25.00%	0.00%	50.00%	50.00%
	sit-stand	33.33%	0.00%	66.67%	0.00%	33.33%	66.67%
QDA	**78.06%**	other	stand-sit	sit-stand	other	stand-sit	sit-stand
RUS	**48.43%**	Predicted					

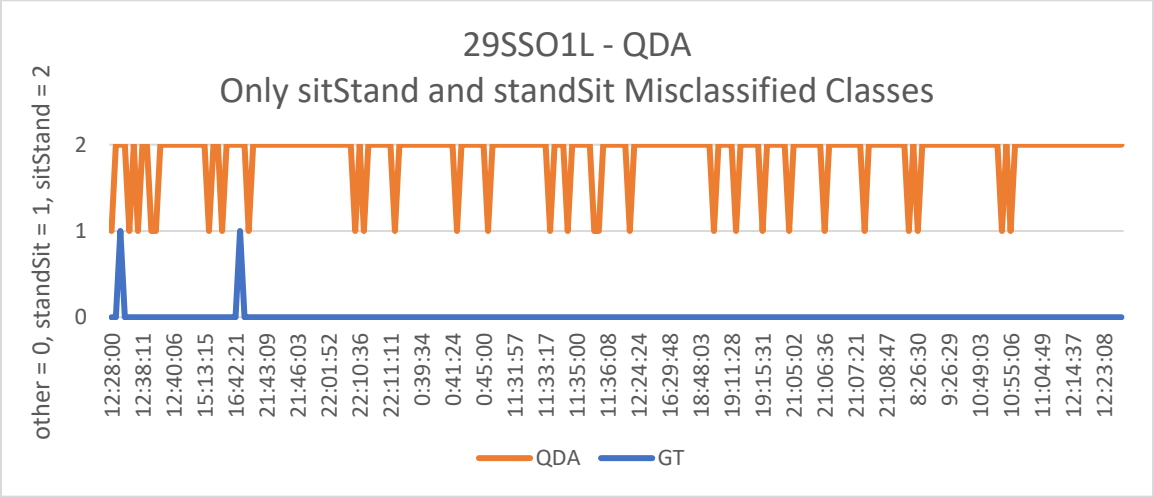

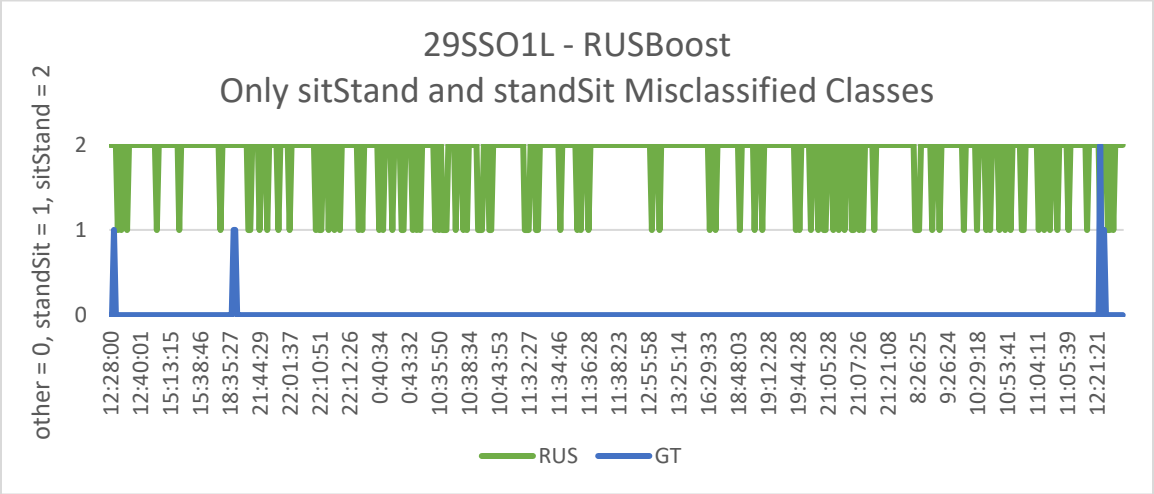

30WBO1L							
		QDA			RUS		
TRUE	other	93.67%	1.73%	4.60%	94.78%	0.37%	4.85%
	stand-sit	4.17%	59.72%	36.11%	2.78%	51.39%	45.83%
	sit-stand	6.82%	36.36%	56.82%	5.68%	6.82%	87.50%
QDA	**93.47%**	other	stand-sit	sit-stand	other	stand-sit	sit-stand
RUS	**94.64%**	Predicted					

31FSO1L							
		QDA			RUS		
TRUE	other	74.82%	3.07%	22.10%	75.59%	0.51%	23.89%
	stand-sit	8.70%	73.91%	17.39%	13.04%	30.43%	56.52%
	sit-stand	20.83%	25.00%	54.17%	20.83%	0.00%	79.17%
QDA	**74.50%**	other	stand-sit	sit-stand	other	stand-sit	sit-stand
RUS	**75.00%**	Predicted					

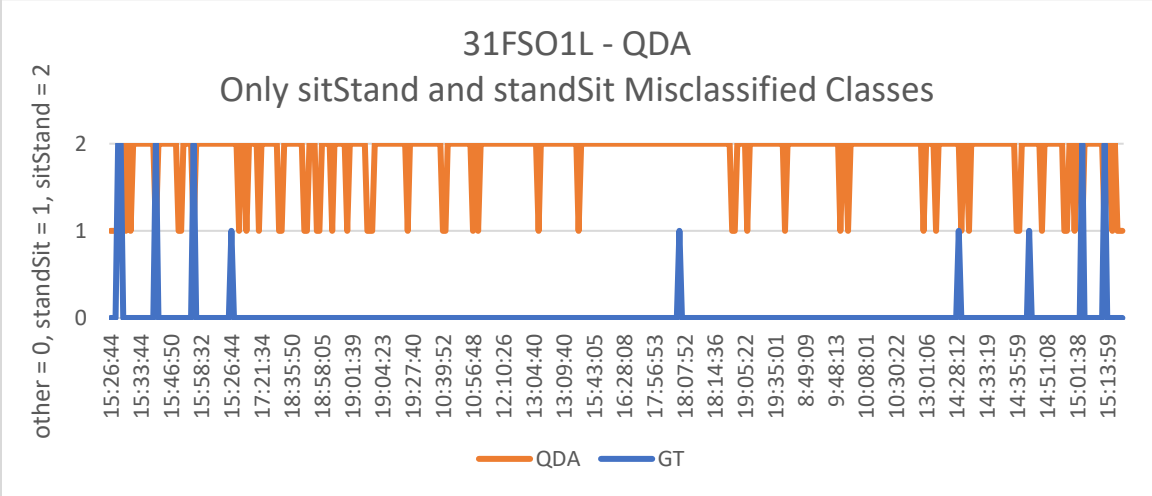

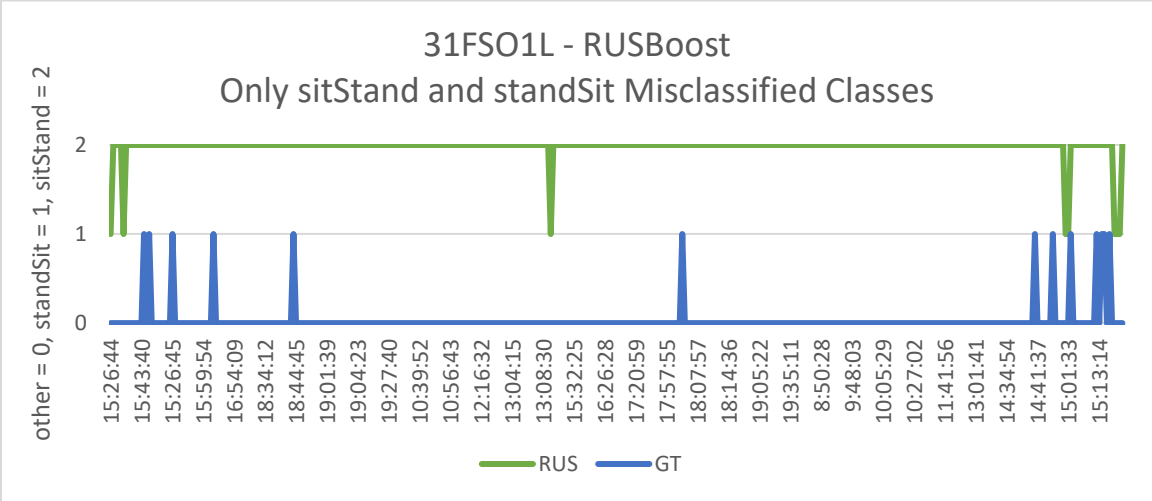

32PKO1L							
		QDA			RUS		
TRUE	other	94.04%	1.49%	4.47%	91.80%	1.74%	6.46%
	stand-sit	14.47%	48.68%	36.84%	11.84%	60.53%	27.63%
	sit-stand	28.41%	18.18%	53.41%	13.64%	29.55%	56.82%
QDA	93.76%	other	stand-sit	sit-stand	other	stand-sit	sit-stand
RUS	91.59%	Predicted					

33BEO1L							
		QDA			RUS		
TRUE	other	93.33%	1.84%	4.83%	81.54%	3.85%	14.61%
	stand-sit	21.74%	55.07%	23.19%	1.45%	62.32%	36.23%
	sit-stand	61.04%	6.49%	32.47%	9.09%	14.29%	76.62%
QDA	91.25%	other	stand-sit	sit-stand	other	stand-sit	sit-stand
RUS	81.05%	Predicted					

34REO1L							
		QDA			RUS		
TRUE	other	88.12%	3.30%	8.58%	89.24%	3.62%	7.14%
	stand-sit	3.13%	62.50%	34.38%	6.25%	56.25%	37.50%
	sit-stand	32.35%	23.53%	44.12%	17.65%	11.76%	70.59%
QDA	87.86%	other	stand-sit	sit-stand	other	stand-sit	sit-stand
RUS	89.05%	Predicted					

Appendix H. Motion Density Additional Details

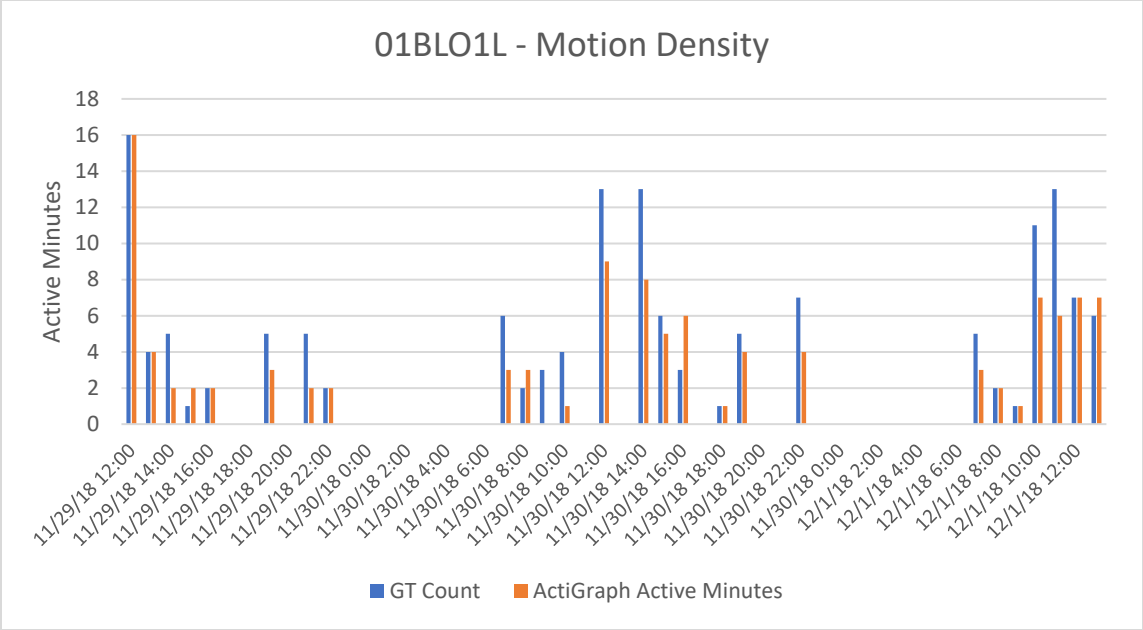
01BLO1L - Motion Density
Active Minutes
18
16
14
12
10
8
6
4
2
0
11/29/18 12:00
11/29/18 14:00
11/29/18 16:00
11/29/18 18:00
11/29/18 20:00
11/29/18 22:00
11/30/18 0:00
11/30/18 2:00
11/30/18 4:00
11/30/18 6:00
11/30/18 8:00
11/30/18 10:00
11/30/18 12:00
11/30/18 14:00
11/30/18 16:00
11/30/18 18:00
11/30/18 20:00
11/30/18 22:00
11/30/18 0:00
12/1/18 2:00
12/1/18 4:00
12/1/18 6:00
12/1/18 8:00
12/1/18 10:00
12/1/18 12:00
GT Count
ActiGraph Active Minutes

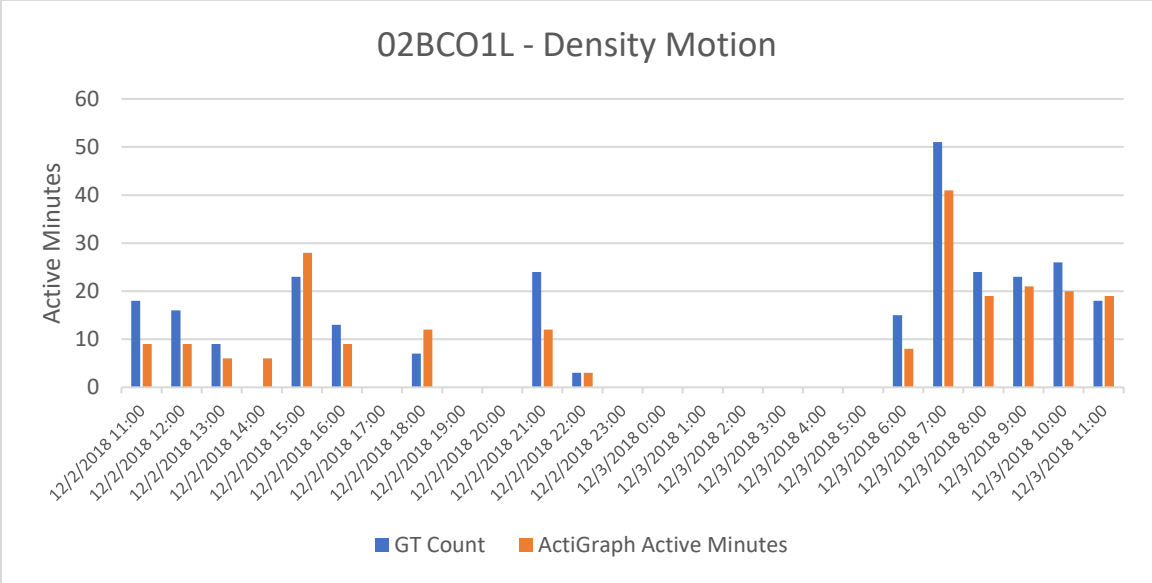
02BCO1L - Density Motion
Active Minutes
60
50
40
30
20
10
0
12/2/2018 11:00
12/2/2018 12:00
12/2/2018 13:00
12/2/2018 14:00
12/2/2018 15:00
12/2/2018 16:00
12/2/2018 17:00
12/2/2018 18:00
12/2/2018 19:00
12/2/2018 20:00
12/2/2018 21:00
12/2/2018 22:00
12/2/2018 23:00
12/3/2018 0:00
12/3/2018 1:00
12/3/2018 2:00
12/3/2018 3:00
12/3/2018 4:00
12/3/2018 5:00
12/3/2018 6:00
12/3/2018 7:00
12/3/2018 8:00
12/3/2018 9:00
12/3/2018 10:00
12/3/2018 11:00
GT Count
ActiGraph Active Minutes

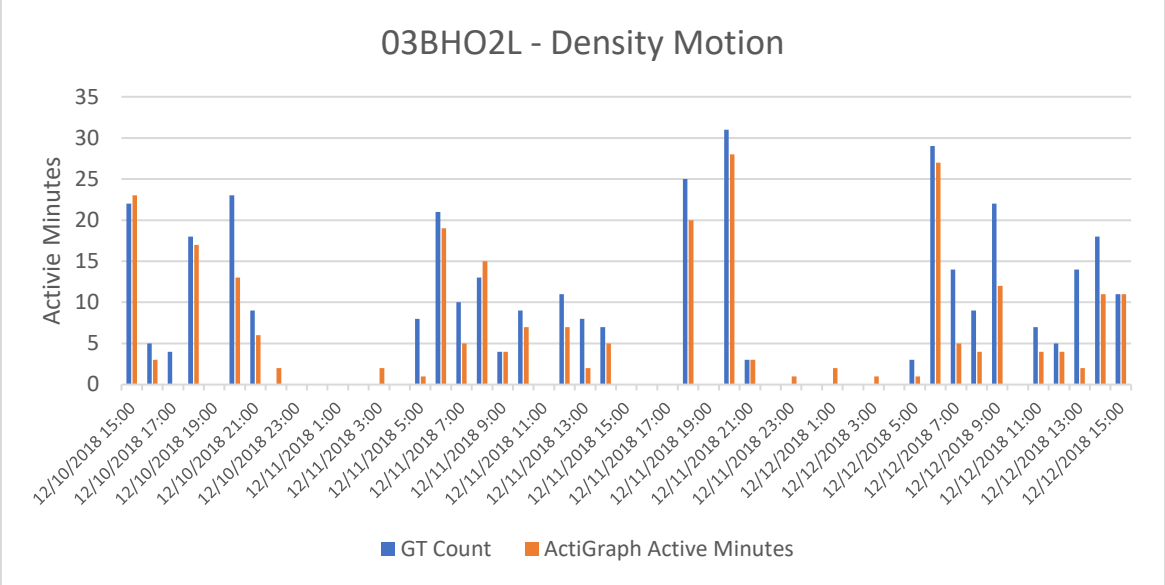
03BHO2L - Density Motion
Activie Minutes
35
30
25
20
15
10
5
0
12/10/2018 15:00
12/10/2018 17:00
12/10/2018 19:00
12/10/2018 21:00
12/10/2018 23:00
12/11/2018 1:00
12/11/2018 3:00
12/11/2018 5:00
12/11/2018 7:00
12/11/2018 9:00
12/11/2018 11:00
12/11/2018 13:00
12/11/2018 15:00
12/11/2018 17:00
12/11/2018 19:00
12/11/2018 21:00
12/11/2018 23:00
12/12/2018 1:00
12/12/2018 3:00
12/12/2018 5:00
12/12/2018 7:00
12/12/2018 9:00
12/12/2018 11:00
12/12/2018 13:00
12/12/2018 15:00
GT Count
ActiGraph Active Minutes

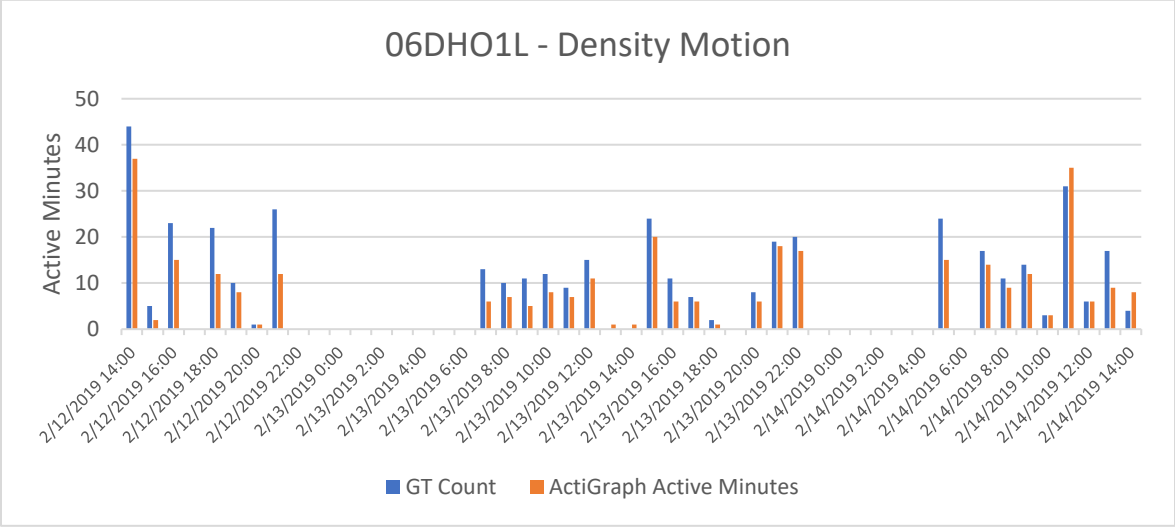
06DHO1L - Density Motion
Active Minutes
50
40
30
20
10
0
2/12/2019 14:00
2/12/2019 16:00
2/12/2019 18:00
2/12/2019 20:00
2/12/2019 22:00
2/13/2019 0:00
2/13/2019 2:00
2/13/2019 4:00
2/13/2019 6:00
2/13/2019 8:00
2/13/2019 10:00
2/13/2019 12:00
2/13/2019 14:00
2/13/2019 16:00
2/13/2019 18:00
2/13/2019 20:00
2/13/2019 22:00
2/14/2019 0:00
2/14/2019 2:00
2/14/2019 4:00
2/14/2019 6:00
2/14/2019 8:00
2/14/2019 10:00
2/14/2019 12:00
2/14/2019 14:00
GT Count
ActiGraph Active Minutes

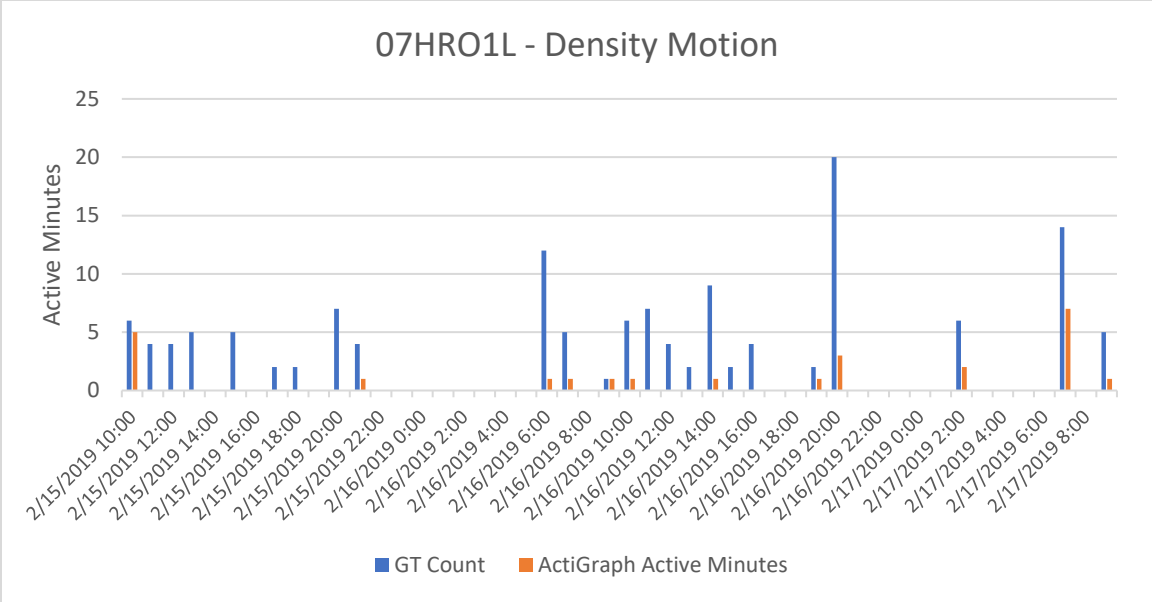
07HRO1L - Density Motion
Active Minutes
25
20
15
10
5
0
2/15/2019 10:00
2/15/2019 12:00
2/15/2019 14:00
2/15/2019 16:00
2/15/2019 18:00
2/15/2019 20:00
2/15/2019 22:00
2/16/2019 0:00
2/16/2019 2:00
2/16/2019 4:00
2/16/2019 6:00
2/16/2019 8:00
2/16/2019 10:00
2/16/2019 12:00
2/16/2019 14:00
2/16/2019 16:00
2/16/2019 18:00
2/16/2019 20:00
2/16/2019 22:00
2/17/2019 0:00
2/17/2019 2:00
2/17/2019 4:00
2/17/2019 6:00
2/17/2019 8:00
GT Count
ActiGraph Active Minutes

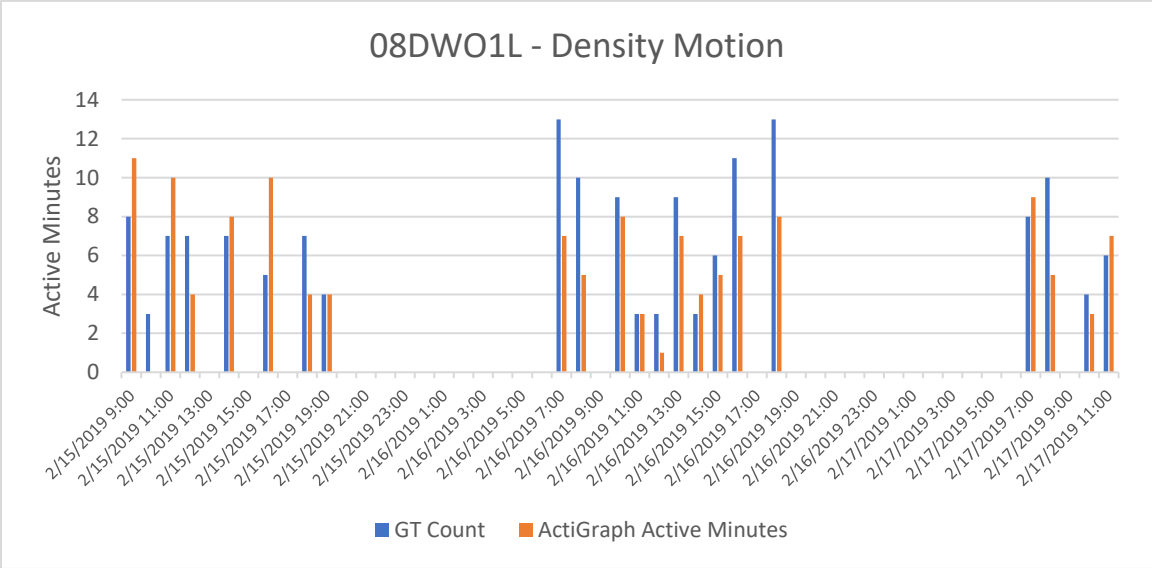
08DWO1L - Density Motion
Active Minutes
14
12
10
8
6
4
2
0
2/15/2019 9:00
2/15/2019 11:00
2/15/2019 13:00
2/15/2019 15:00
2/15/2019 17:00
2/15/2019 19:00
2/15/2019 21:00
2/15/2019 23:00
2/16/2019 1:00
2/16/2019 3:00
2/16/2019 5:00
2/16/2019 7:00
2/16/2019 9:00
2/16/2019 11:00
2/16/2019 13:00
2/16/2019 15:00
2/16/2019 17:00
2/16/2019 19:00
2/16/2019 21:00
2/16/2019 23:00
2/17/2019 1:00
2/17/2019 3:00
2/17/2019 5:00
2/17/2019 7:00
2/17/2019 9:00
2/17/2019 11:00
GT Count
ActiGraph Active Minutes

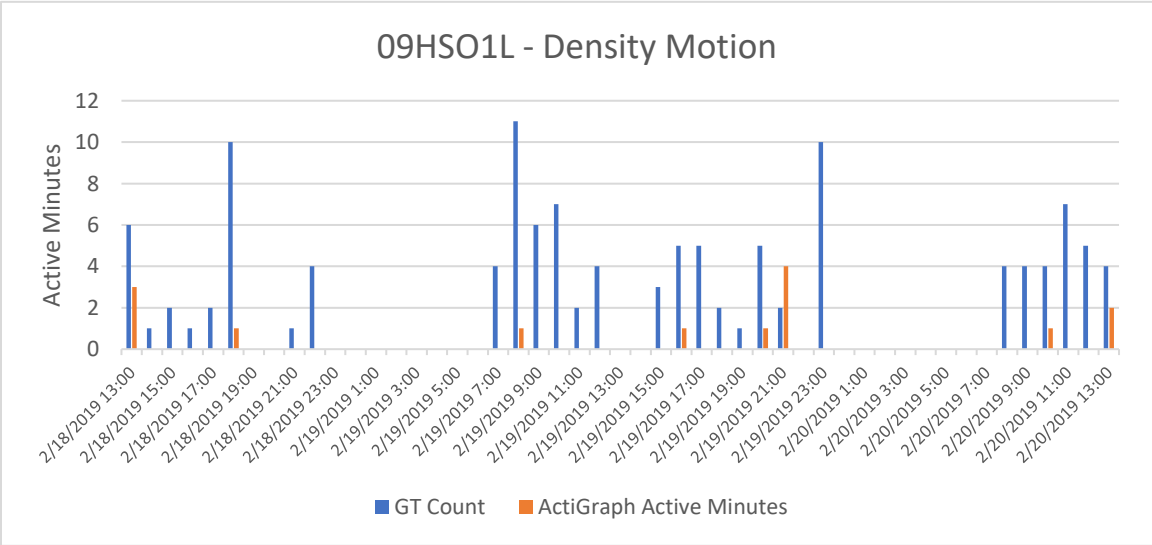
09HSO1L - Density Motion
Active Minutes
12
10
8
6
4
2
0
2/18/2019 13:00
2/18/2019 15:00
2/18/2019 17:00
2/18/2019 19:00
2/18/2019 21:00
2/18/2019 23:00
2/19/2019 1:00
2/19/2019 3:00
2/19/2019 5:00
2/19/2019 7:00
2/19/2019 9:00
2/19/2019 11:00
2/19/2019 13:00
2/19/2019 15:00
2/19/2019 17:00
2/19/2019 19:00
2/19/2019 21:00
2/19/2019 23:00
2/20/2019 1:00
2/20/2019 3:00
2/20/2019 5:00
2/20/2019 7:00
2/20/2019 9:00
2/20/2019 11:00
2/20/2019 13:00
GT Count
ActiGraph Active Minutes

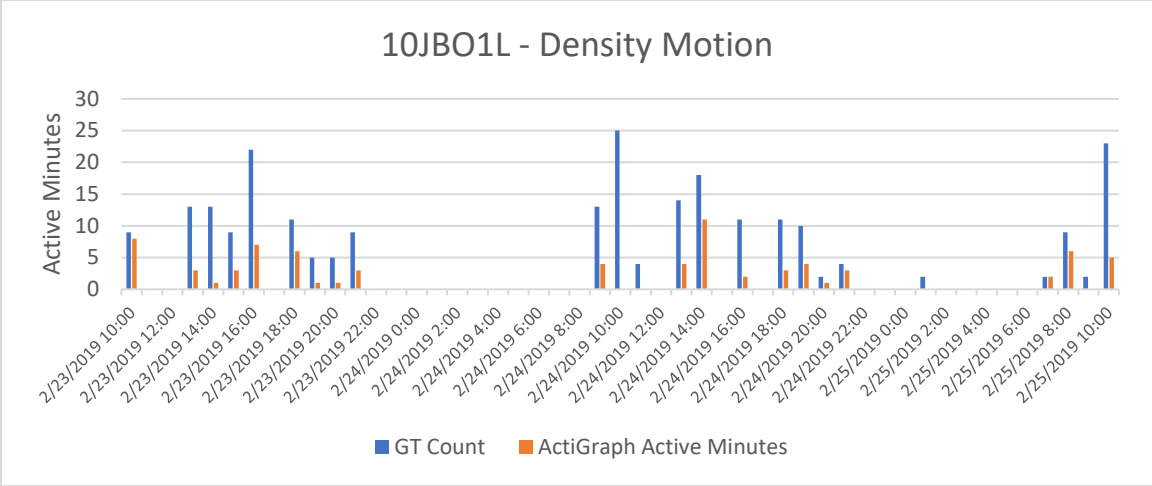

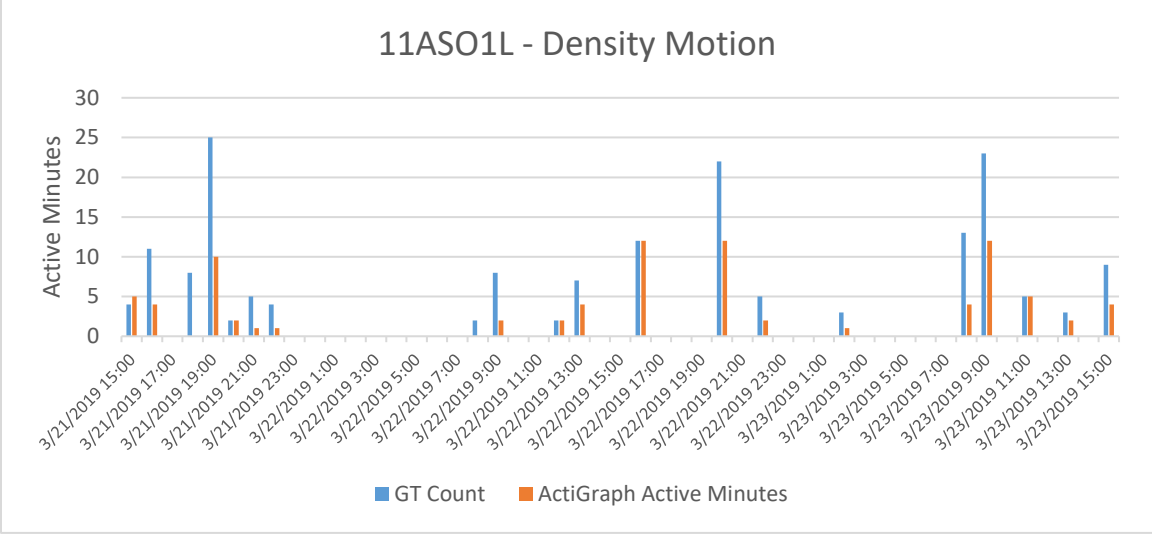

Appendix I. Vacancy Algorithm Additional Details

Appx. Table I-1 Missing motion sensor data during the data collection periods.

Subject	Last recorded time in database	First recorded time in database after missing
02BCO1L	11/5/2018 10:29:33 AM	2/8/2019 12:55:33 PM
13JAO1L/13JAO2L	4/1/2019 2:02:35 PM	7/24/2019 3:49:09 PM
15LOO1L	3/23/2019 7:24:33 PM	5/15/2019 11:47:11 AM
33BEO1L	8/27/2019 5:13:23 PM	10/2/2019 1:25:21 PM

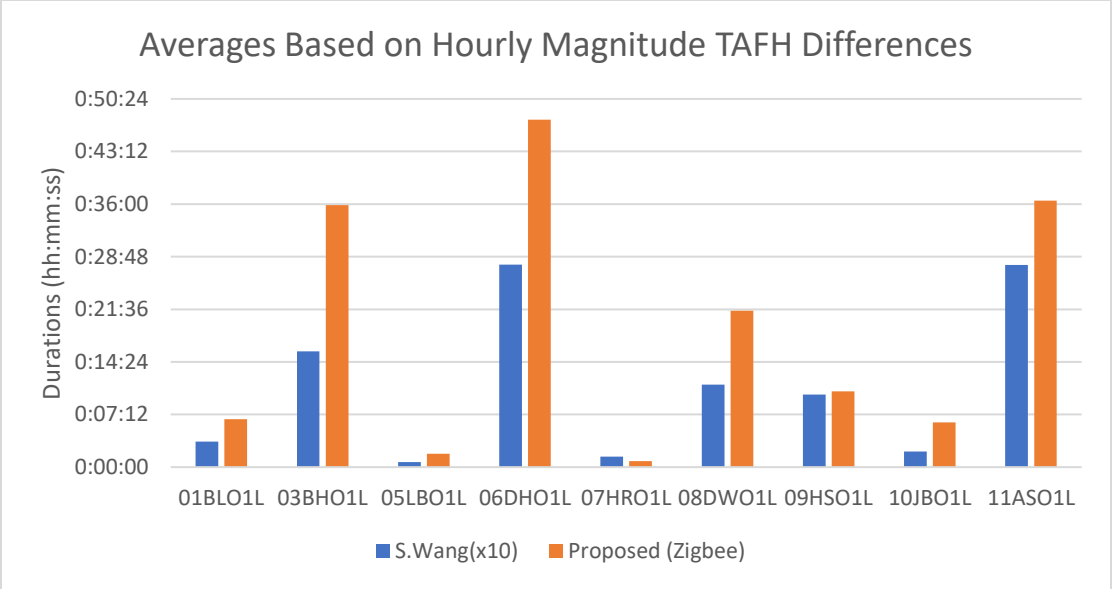
Averages Based on Hourly Magnitude TAFH Differences
Durations (hh:mm:ss)
0:50:24
0:43:12
0:36:00
0:28:48
0:21:36
0:14:24
0:07:12
0:00:00
01BLO1L
03BHO1L
05LBO1L
06DHO1L
07HRO1L
08DWO1L
09HSO1L
10JBO1L
11ASO1L
S.Wang(x10)
Proposed (Zigbee)

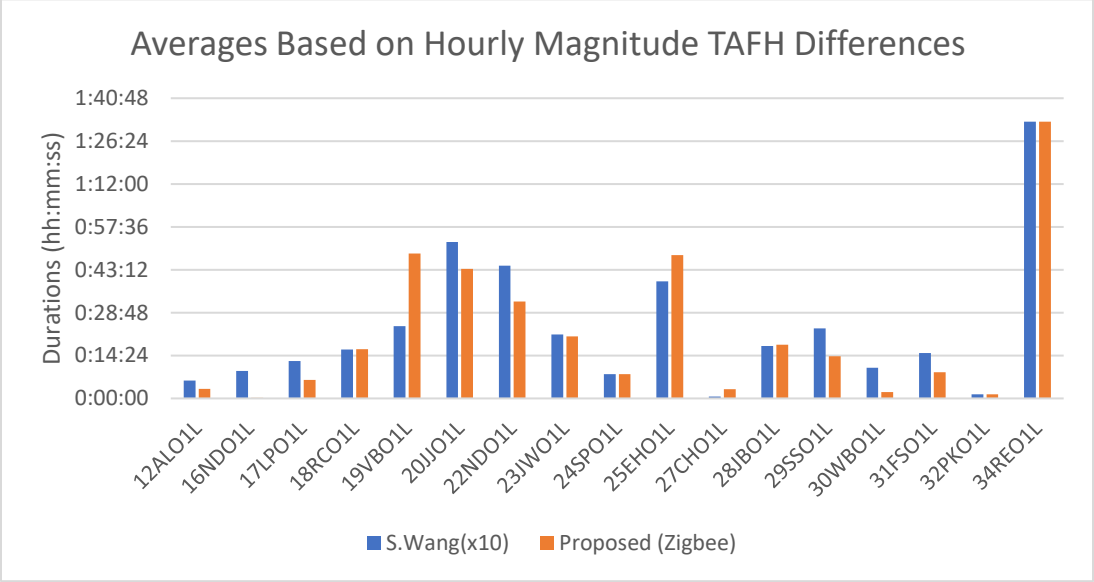
Averages Based on Hourly Magnitude TAFH Differences
Durations (hh:mm:ss)
1:40:48
1:26:24
1:12:00
0:57:36
0:43:12
0:28:48
0:14:24
0:00:00
12ALO1L
16NDO1L
17LPO1L
18RCO1L
19VBO1L
20JJO1L
22NDO1L
23IWO1L
24SPO1L
25EHO1L
27CHO1L
28JBO1L
29SSO1L
30WBO1L
31FSO1L
32PKO1L
34REO1L
S.Wang(x10)
Proposed (Zigbee)

	S.Wang(x10)		Proposed(Zigbee)	
Subject	**Accuracy**	**F1Score**	**Accuracy**	**F1Score**
01BLO1L	90.00%	92.31%	70.00%	80.00%
03BHO1L	52.63%	66.67%	47.37%	64.29%
05LBO1L	92.86%	95.24%	71.43%	83.33%
06DHO1L	52.63%	40.00%	21.05%	28.57%
07HRO1L	85.71%	92.31%	100.00%	100.00%
08DWO1L	69.23%	77.78%	53.85%	70.00%
09HSO1L	90.91%	94.12%	72.73%	84.21%
10JBO1L	83.33%	85.71%	58.33%	73.68%
11ASO1L	43.48%	55.17%	39.13%	53.33%

	S.Wang(x10)		Proposed(Zigbee)	
Subject	**Accuracy**	**F1Score**	**Accuracy**	**F1Score**
12ALO1L	77.78%	85.71%	66.67%	80.00%
16NDO1L	77.78%	87.50%	100.00%	100.00%
17LPO1L	66.67%	80.00%	91.67%	95.65%
18RCO1L	58.33%	73.68%	58.33%	73.68%
19VBO1L	34.48%	29.63%	24.14%	26.67%
20JJO1L	38.89%	56.00%	44.44%	58.33%
22NDO1L	30.77%	30.77%	23.08%	37.50%
23JWO1L	68.00%	77.78%	64.00%	76.92%
24SPO1L	57.14%	72.73%	71.43%	83.33%
25EHO1L	47.83%	53.85%	39.13%	56.25%
27CHO1L	88.89%	80.00%	22.22%	36.36%
28JBO1L	78.57%	85.71%	64.29%	78.26%
29SSO1L	53.85%	66.67%	61.54%	73.68%
30WBO1L	76.92%	86.96%	84.62%	91.67%
31FSO1L	88.89%	94.12%	94.44%	97.14%
32PKO1L	75.00%	84.21%	75.00%	85.71%
34REO1L	66.67%	80.00%	66.67%	80.00%

References

[1] N. Straiton *et al.*, “The validity and reliability of consumer-grade activity trackers in older, community-dwelling adults: A systematic review,” *Maturitas*, vol. 112, no. March, pp. 85–93, 2018, doi: 10.1016/j.maturitas.2018.03.016.

[2] J. B. Martin and J. W. Noble, “Pedometer accuracy in slow walking older adults.”

[3] S. G. B. Robyn M. Lamont, Hannah L. Daniel, Caitlyn L. Payne, “Accuracy of wearable physical activity trackers in people with Parkinson’sdisease,” *Science Direct*, vol. 63, pp. 104–108, 2018, [Online]. Available: https://doi.org/10.1016/j.gaitpost.2018.04.034.

[4] M. J. Rantz *et al.*, “Sensor technology to support aging in place,” *Journal of the American Medical Directors Association*, vol. 14, no. 6, pp. 386–391, 2013, doi: 10.1016/j.jamda.2013.02.018.

[5] J. Vespa, L. Medina, and D. Armstrong, “Demographic turning points for the United States: Population projections for 2020 to 2060. Current Population Reports, P25–1144. Washington, DC: US Census Bureau.,” *U.S. Census Bureau*, pp. 1–13, 2020, [Online]. Available: https://www.census.gov/library/publications/2020/demo/p25-1144.html.

[6] M. J. Rantz *et al.*, “Aging in Place: Adapting the Environment,” in *Using Nursing Research to Shape Health Policy*, New York, NY: Springer Publishing Company, 2017.

[7] S. Wang and M. Skubic, “Density map visualization from motion sensors for monitoring activity level,” *IET Conference Publications*, no. 541 CP, 2008, doi: 10.1049/cp:20081097.

[8] W. Pirker and R. Katzenschlager, “Gait disorders in adults and the elderly: A clinical guide,” *Wiener Klinische Wochenschrift*, vol. 129, no. 3–4, pp. 81–95, 2017, doi: 10.1007/s00508-016-1096-4.

[9] C. E. Tudor-Locke and A. M. Myers, “Challenges and Opportunities for Measuring Physical Activity in Sedentary Adults.” Accessed: Oct. 21, 2020. [Online]. Available: https://link.springer.com/article/10.2165/00007256-200131020-00002.

[10] Z. Zhou *et al.*, “A real-time system for in-home activity monitoring of elders,” *Proceedings of the 31st Annual International Conference of the IEEE Engineering in Medicine and Biology Society: Engineering the Future*

of Biomedicine, EMBC 2009, pp. 6115–6118, 2009, doi: 10.1109/IEMBS.2009.5334915.

[11] C. Soaz and K. Diepold, "Step Detection and Parameterization for Gait Assessment Using a Single Waist-Worn Accelerometer," *IEEE Transactions on Biomedical Engineering*, vol. 63, no. 5, pp. 933–942, May 2016, doi: 10.1109/TBME.2015.2480296.

[12] L. A. Uebelacker, "Mobility Device Use Among Older Adults and Incidence of Falls," *Physiology & behavior*, vol. 176, no. 1, pp. 139–148, 2017, doi: 10.1111/jgs.13393.Mobility.

[13] G. A. L. Meijer, K. R. Westerterp, F. M. H. Verhoeven, H. B. M. Koper, and F. ten Hoor, "Methods_to_Assess_Physical_Activity_with_Special_R," *IEEE Transactions on Biomedical Engineering*, vol. 38, no. 3, pp. 221–229, Mar. 1991, Accessed: Oct. 21, 2020. [Online]. Available: https://ieeexplore.ieee.org/document/133202.

[14] M. Y. Osoba, A. K. Rao, S. K. Agrawal, and A. K. Lalwani, "Balance and gait in the elderly: A contemporary review," *Laryngoscope Investigative Otolaryngology*, vol. 4, no. 1, pp. 143–153, 2019, doi: 10.1002/lio2.252.

[15] D. E. Krebs, D. Goldvasser, J. D. Lockert, L. G. Portney, and K. M. Gill-Body, "Is base of support greater in unsteady gait?," *Physical Therapy*, vol. 82, no. 2, pp. 138–147, 2002, doi: 10.1093/ptj/82.2.138.

[16] P. Johns, "Chapter 13 - Parkinson Disease," in *Clinical Neuroscience*, London: Churchill Livingstone, Elsevier Ltd., 2014, pp. 163–179.

[17] E. Stone, M. Skubic, M. Rantz, C. Abbott, and S. Miller, "Average in-home gait speed: Investigation of a new metric for mobility and fall risk assessment of elders," *Gait and Posture*, vol. 41, no. 1, pp. 57–62, 2015, doi: 10.1016/j.gaitpost.2014.08.019.

[18] E. E. Stone and M. Skubic, "Unobtrusive, continuous, in-home gait measurement using the microsoft kinect," *IEEE Transactions on Biomedical Engineering*, vol. 60, no. 10, pp. 2925–2932, 2013, doi: 10.1109/TBME.2013.2266341.

[19] F. Gu, K. Khoshelham, J. Shang, F. Yu, and Z. Wei, "Robust and accurate smartphone-based step counting for indoor localization," *IEEE Sensors Journal*, vol. 17, no. 11, pp. 3453–3460, Jun. 2017, doi: 10.1109/JSEN.2017.2685999.

[20] X. Kang, B. Huang, and G. Qi, "A novel walking detection and step counting algorithm using unconstrained smartphones," *Sensors (Switzerland)*, vol. 18, no. 1, Jan. 2018, doi: 10.3390/s18010297.

[21] "MATLAB." The MathWorks Inc., Natick, Massachusetts.

[22] M. R. Krogh, P. S. Halvorsen, O. J. Elle, J. Bergsland, and E. W. Remme, "Dynamic gravity compensation does not increase detection of myocardial ischemia in combined accelerometer and gyro sensor measurements," *Scientific Reports*, vol. 9, no. 1, pp. 1–10, 2019, doi: 10.1038/s41598-018-35630-x.

[23] D. John, A. Morton, D. Arguello, K. Lyden, and D. Bassett, ""What is a step?" Differences in how a step is detected among three popular activity monitors that have impacted physical activity research," *Sensors (Switzerland)*, vol. 18, no. 4, pp. 1–15, 2018, doi: 10.3390/s18041206.

[24] E. Fortune, V. Lugade, S. Amin, and K. R. Kaufman, "Step detection using multi- versus single tri-axial accelerometer-based systems," *Physiological Measurement*, vol. 36, no. 12, pp. 2519–2535, 2015, doi: 10.1088/0967-3334/36/12/2519.

[25] E. Fortune, V. Lugade, M. Morrow, and K. Kaufman, "Validity of using tri-axial accelerometers to measure human movement - Part II: Step counts at a wide range of gait velocities," *Medical Engineering and Physics*, vol. 36, no. 6, pp. 659–669, 2014, doi: 10.1016/j.medengphy.2014.02.006.

[26] R. C. van Lummel, S. Walgaard, A. B. Maier, E. Ainsworth, P. J. Beek, and J. H. van Dieën, "The instrumented Sit-To-Stand test (iSTS) has greater clinical relevance than the manually recorded sit-to-stand test in older adults," *PLoS ONE*, vol. 11, no. 7, pp. 1–17, 2016, doi: 10.1371/journal.pone.0157968.

[27] M. H. Pham *et al.*, "Validation of a lower back 'wearable'-based sit-to-stand and stand-to-sit algorithm for patients with Parkinson's disease and older adults in a home-like environment," *Frontiers in Neurology*, vol. 9, no. AUG, pp. 1–11, 2018, doi: 10.3389/fneur.2018.00652.

[28] T. Pozaic, U. Lindemann, A. K. Grebe, and W. Stork, "Sit-to-Stand Transition Reveals Acute Fall Risk in Activities of Daily Living," *IEEE Journal of Translational Engineering in Health and Medicine*, vol. 4, no. October, 2016, doi: 10.1109/JTEHM.2016.2620177.

[29] D. L. Marques, H. P. Neiva, I. M. Pires, D. A. Marinho, and M. C. Marques, "Accelerometer data from the performance of sit-to-stand test by elderly people," *Data in Brief*, vol. 33, p. 106328, 2020, doi: 10.1016/j.dib.2020.106328.

[30] J. Kerr, J. Carlson, S. Godbole, L. Cadmus-Bertram, J. Bellettiere, and S. Hartman, "Improving Hip-Worn Accelerometer Estimates of Sitting Using

Machine Learning Methods," *Medicine and Science in Sports and Exercise*, vol. 50, no. 7, pp. 1518–1524, 2018, doi: 10.1249/MSS.0000000000001578.

[31] K. ELLIS, J. KERR, S. GODBOLE, J. STAUDENMAYER, and G. LANCKRIET, "Hip and Wrist Accelerometer Algorithms for Free-Living Behavior Classification," *Medicine & Science in Sports & Exercise*, vol. 48, no. 5, pp. 933–940, May 2016, doi: 10.1249/MSS.0000000000000840.

[32] B. Ghojogh and M. Crowley, "Linear and Quadratic Discriminant Analysis : Tutorial," no. 4, pp. 1–16.

[33] A. Hickey, B. Galna, J. C. Mathers, L. Rochester, and A. Godfrey, "A multi-resolution investigation for postural transition detection and quantification using a single wearable," *Gait and Posture*, vol. 49, pp. 411–417, 2016, doi: 10.1016/j.gaitpost.2016.07.328.

[34] R. C. van Lummel *et al.*, "Intra-rater, inter-rater and test-retest reliability of an instrumented timed up and Go (iTUG) test in patients with Parkinson's disease," *PLoS ONE*, vol. 11, no. 3, pp. 1–11, 2016, doi: 10.1371/journal.pone.0151881.

[35] A. Atrsaei *et al.*, "Postural transitions detection and characterization in healthy and patient populations using a single waist sensor," *Journal of NeuroEngineering and Rehabilitation*, vol. 17, no. 1, pp. 1–14, 2020, doi: 10.1186/s12984-020-00692-4.

[36] W. G. M. Janssen, J. B. J. Bussmann, H. L. D. Horemans, and H. J. Stam, "Validity of accelerometry in assessing the duration of the sit-to-stand movement," *Medical and Biological Engineering and Computing*, vol. 46, no. 9, pp. 879–887, 2008, doi: 10.1007/s11517-008-0366-3.

[37] A. Godfrey, R. Conway, D. Meagher, and G. ÓLaighin, "Direct measurement of human movement by accelerometry," *Medical Engineering and Physics*, vol. 30, no. 10, pp. 1364–1386, 2008, doi: 10.1016/j.medengphy.2008.09.005.

[38] V. J. Palmer *et al.*, "What Do Older People Do When Sitting and Why? Implications for Decreasing Sedentary Behavior," *The Gerontologist*, vol. 59, no. 4, pp. 686–697, 2019, doi: 10.1093/geront/gny020.